

Development 140, 1123–1136 (2013) doi:10.1242/dev.082875
 © 2013. Published by The Company of Biologists Ltd

Functional dissection of the paired domain of Pax6 reveals molecular mechanisms of coordinating neurogenesis and proliferation

Tessa Walcher¹, Qing Xie², Jian Sun², Martin Irmler³, Johannes Beckers^{3,4}, Timucin Öztürk¹, Dierk Niessing⁵, Anastassia Stoykova⁶, Ales Cvekl², Jovica Ninkovic^{1,7} and Magdalena Götz^{1,7,8,*}

SUMMARY

To achieve adequate organ development and size, cell proliferation and differentiation have to be tightly regulated and coordinated. The transcription factor Pax6 regulates patterning, neurogenesis and proliferation in forebrain development. The molecular basis of this regulation is not well understood. As the bipartite DNA-binding paired domain of Pax6 regulates forebrain development, we examined mice with point mutations in its individual DNA-binding subdomains PAI (Pax6^{Leca4}, N50K) and RED (Pax6^{Leca2}, R128C). This revealed distinct roles in regulating proliferation in the developing cerebral cortex, with the PAI and RED subdomain mutations reducing and increasing, respectively, the number of mitoses. Conversely, neurogenesis was affected only by the PAI subdomain mutation, phenocopying the neurogenic defects observed in full Pax6 mutants. Genome-wide expression profiling identified molecularly discrete signatures of Pax6^{Leca4} and Pax6^{Leca2} mutations. Comparison to Pax6 targets identified by chromatin immunoprecipitation led to the identification and functional characterization of distinct DNA motifs in the promoters of target genes dysregulated in the Pax6^{Leca2} or Pax6^{Leca4} mutants, further supporting the distinct regulatory functions of the DNA-binding subdomains. Thus, Pax6 achieves its key roles in the developing forebrain by utilizing particular subdomains to coordinate patterning, neurogenesis and proliferation simultaneously.

KEY WORDS: Transcriptional regulator, Radial glia, Cortex development, Mouse

INTRODUCTION

During organ formation, cell proliferation and differentiation have to be tightly controlled and coordinated. This is of particular relevance in the CNS, as regulation of neuron numbers and subtypes profoundly affects functional properties of the nervous system. However, the molecular programs coordinating proliferation and neurogenesis are largely little understood. It is known that key transcriptional regulators influence both fate and patterning decisions as well as stem and progenitor cell proliferation (e.g. Zaret and Carroll, 2011), thereby acting as coordinators at the molecular level. The molecular programs by which these regulatory proteins exert their distinct functions remain poorly understood. The transcription factor Pax6 acts as a master regulator in various tissues, including the developing CNS and eye (Hanson and Van Heyningen, 1995; Dohrmann et al., 2000; Kozmik, 2008; Osumi et al., 2008). Pax6 has been established as a key regulator of patterning, fate and proliferation and is required to achieve appropriate CNS and eye development (Hanson and Van Heyningen, 1995; Stoykova et al., 1996; Stoykova et al., 1997; Götz

et al., 1998; Chapouton et al., 1999; Stoykova et al., 2000; Toresson et al., 2000; Yun et al., 2001; Estivill-Torras et al., 2002; Heins et al., 2002; Haubst et al., 2004; Quinn et al., 2007; Sansom et al., 2009; Tuoc et al., 2009). In addition, Pax6 is sufficient to elicit eye formation (Altmann et al., 1997; Chow et al., 1999) and instruct neuron formation even from non-neurogenic glial cells (Heins et al., 2002; Berninger et al., 2007). Despite recent advances in identifying Pax6-regulated genes *in vivo* (Sansom et al., 2009; Wolf et al., 2009; Xie and Cvekl, 2011), how Pax6 instructs neurogenesis or how it coordinates various developmental aspects at the molecular level remains largely elusive.

Pax6 belongs to the class IV Pax transcription factors, which possess two complete domains, namely the paired domain (PD) and paired-type homeodomain (HD) for DNA binding followed by the C-terminal transactivation domain (Mansouri et al., 1996; Chi and Epstein, 2002). As the HD and PD recognize different Pax6 consensus binding sites (Chi and Epstein, 2002), they may regulate distinct functions by controlling particular targets either separately or in a cooperative manner (Jun and Desplan, 1996; Singh et al., 2000; Mikkola et al., 2001; Mishra et al., 2002; Xie and Cvekl, 2011). Indeed, Pax6 selectively utilizes the HD in the paired-less form of the protein to regulate the survival of mature dopaminergic neurons in the adult olfactory bulb via its αA-crystalline target (Ninkovic et al., 2010). The HD has also been implicated in regulating lens formation and retinal specification during eye development (Ashery-Padan et al., 2000; Ashery-Padan and Gruss, 2001; van Heyningen and Williamson, 2002), but has surprisingly little effect in forebrain development (Haubst et al., 2004; Ninkovic et al., 2010). These data imply that the multitude of effects that Pax6 exerts on patterning, neurogenesis and proliferation in the developing brain should be largely mediated by the PD.

¹Institute of Stem Cell Research, Helmholtz Center Munich, 85764 Neuherberg-Munich, Germany. ²Departments of Ophthalmology and Visual Sciences and Genetics, Albert Einstein College of Medicine, Bronx, NY 10461, USA. ³Center of Life and Food Sciences Weihenstephan, Technical University Munich, 85354 Freising, Germany. ⁴Institute of Experimental Genetics, Helmholtz Center Munich, 85764 Neuherberg-Munich, Germany. ⁵Institute of Structural Biology, Helmholtz Center Munich, 85764 Neuherberg-Munich, Germany. ⁶Department of Molecular Cell Biology, RG Molecular Developmental Neurobiology, Max Planck Institute for Biophysical Chemistry, 37077 Goettingen, Germany. ⁷Physiological Genomics, Institute of Physiology, Munich University, 80336 Munich, Germany. ⁸Munich Cluster for Systems Neurology (SyNergy), Munich, Germany.

*Author for correspondence (magdalena.goetz@helmholtz-muenchen.de)

Interestingly, the PD itself is also structured in a modular, bipartite manner, with an N-terminal PAI subdomain and C-terminal RED subdomain, which can bind cooperatively or independently to their cognate sites (Epstein et al., 1994a; Yamaguchi et al., 1997). Alternative splicing of *Pax6* exon 5a regulates the insertion of 14 amino acids into the PAI subdomain, thereby abolishing PAI subdomain DNA binding while retaining RED subdomain activity (Epstein et al., 1994b; Kozmik et al., 1997; Anderson et al., 2002). Thus, it would be interesting to determine the function of these subdomains to see whether they regulate distinct programs in the developing CNS.

Recently, two mouse lines (*Pax6*^{Leca4} and *Pax6*^{Leca2}) were identified, each carrying a point mutation in one of the two bipartite DNA-binding subdomains of the PD (Thaung et al., 2002). These mutations (see supplementary material Fig. S1) result in the substitution of lysine for asparagine (N50K) in the PAI subdomain (*Pax6*^{Leca4}) or of cysteine for arginine (R128C) in the RED subdomain (*Pax6*^{Leca2}), a mutation that has also been observed in patients (Azuma et al., 1996). Both of these mutations would be expected to affect DNA binding of the respective subdomain (Thaung et al., 2002) (supplementary material Fig. S1) and the milder eye phenotype compared with full *Pax6* mutants (Thaung et al., 2002) would be consistent with a selective disruption of either subdomain. So far, only full mutants of *Pax6*, with either premature STOP codons that result in no protein or a truncated protein lacking the transactivation domain (Theiler et al., 1978; Hill et al., 1991; Matsuo et al., 1993; Lyon et al., 2000; Favor et al., 2001; Thaung et al., 2002; Graw et al., 2005) or the loss of a splice acceptor site resulting in the loss of exon 5a and 6 and a failure to translocate into the nucleus (Haubst et al., 2004; Graw et al., 2005; Dames et al., 2010), have been studied. Therefore, we set out to examine the extent to which the Leca2 and Leca4 mutations might affect the developing forebrain in a more distinct manner.

MATERIALS AND METHODS

Animals

All experimental procedures were performed in accordance with German and European Union guidelines. The *Pax6*^{Leca2} and *Pax6*^{Leca4} mouse lines (Thaung et al., 2002) were obtained from the GlaxoSmithKline Research & Development (UK) and maintained as previously published (Thaung et al., 2002). *Pax6*^{Sey} mice (Hill et al., 1991) were maintained on a C57BL/6J×DBA/2J (B6D2F1) background.

Immunohistochemistry and *in situ* hybridization

Whole heads and brains isolated from E12 to E17 embryos were fixed in 4% (w/v) paraformaldehyde in phosphate-buffered saline (PBS). Tissue preparation and immunostaining were performed as described (Haubst et al., 2004). Antibodies are described in supplementary material Table S1. Riboprobes for *Ngn2* (kindly provided by Francois Guillemot, NIMR, London, UK), *Rlbp1* (Holm et al., 2007) and *Id2*, *Lgals1*, *Id4*, *Hjrp* and *Zic1* (templates generated by PCR cloning from mouse cDNA; see supplementary material Table S2 for primers) were synthesized with digoxigenin-labeled NTPs (Roche) according to the manufacturer's recommendation. *In situ* hybridization was performed on cryosections as described (Pinto et al., 2008).

Chromatin immunoprecipitation-qPCR (qChIP) assay

The qChIP experiments were performed as previously described (Asami et al., 2011).

Clonal analysis

Clonal analysis was performed as described (Haubst et al., 2004). For overexpression of *Pax6* with the Leca mutations, full-length cDNA of mouse *Pax6*^{Leca4} and *Pax6*^{Leca2} were cloned into a CAG-GFP retroviral

vector, with CAG-GFP vector as negative control and CAG-*Pax6*-IRES-GFP as positive control (Berninger et al., 2007; Blum et al., 2011).

RNA isolation, microarray analysis and qRT-PCR

Total RNA was isolated from rostral cerebral cortex tissue of E14 embryos of *Pax6*^{Leca4}, *Pax6*^{Leca2}, *Pax6*^{Sey} and respective wild-type littermates and the microarray analysis was performed as described (Pinto et al., 2008). Data sets were filtered for average expression exceeding 50 in at least one group (mutant or wild type), false discovery rate (FDR) below 10% and linear ratios exceeding 1.4 \times (mutant/wild type). Array data are available at GEO under accession number GSE35260.

For RT-PCR, extracted RNA was reverse transcribed to cDNA using the SuperScript II Kit (Invitrogen) according to the manufacturer's instructions. Real-time PCR was performed using gene-specific primers (supplementary material Table S2) as described (Pinto et al., 2008).

Luciferase assay

The pGL3-based promoter plasmids containing six copies of each DNA-binding motif, the parental expression plasmid pKW10, and pKW10 expressing wild-type *Pax6* have been described previously (Xie and Cvekl, 2011). The pKW10 expression vectors containing the mutant Leca2 and Leca4 forms of *Pax6* were generated using the QuikChange mutagenesis system (Stratagene). The luciferase assay was performed as previously described (Asami et al., 2011).

Quantification and statistical analysis

All quantifications were performed on images from the dorsal telencephalon in rostral regions using level-matched sections of at least three stage-matched embryos of each genotype from at least three different litters. Statistical analysis was performed using the one-way ANOVA test.

RESULTS

Telencephalon development in *Pax6*^{Leca4} (PAI subdomain) and *Pax6*^{Leca2} (RED subdomain) mutant mice

The first gross morphological analysis of homozygous *Pax6*^{Leca4} and *Pax6*^{Leca2} mutant mouse embryos showed similar eye and craniofacial defects (supplementary material Fig. S2) to the functional null allele (*Pax6*^{Sey}; supplementary material Fig. S2) (Hill et al., 1991; Tzoulaki et al., 2005). However, in contrast to *Pax6*^{Sey} and *Pax6*^{Leca4} mutants, which both die at birth, *Pax6*^{Leca2} mutants developed to adulthood in an almost Mendelian ratio (21% instead of 25%, n=64/311; supplementary material Fig. S2). Notably, craniofacial abnormalities were no longer grossly evident in adult *Pax6*^{Leca2} mutants.

In contrast to *Pax6*^{Sey}, both subdomain mutants (Fig. 1A,B) had a detectable olfactory bulb (OB), although of reduced size (Fig. 1A',A'',B',B''; supplementary material Fig. S2, note the incomplete penetrance in *Pax6*^{Leca2} in S2B,C'''). The absence of the OB in *Pax6*^{Sey} is due to misspecification of the olfactory placode, which normally expresses *Pax6*, and the aberrant assembly of OB neurons within the ventral telencephalon forming the olfactory bulb-like structure (OBLS) (Jiménez et al., 2000; Nomura and Osumi, 2004). However, staining for reelin to detect mitral cells revealed no such aberrant OBLS in *Pax6*^{Leca4} or *Pax6*^{Leca2} brains (supplementary material Fig. S3A-C), suggesting an initially normal formation of the OB anlage, which then fails to further extend in these mice.

Next we examined the thickness of the cerebral cortex by comparing anatomically matched, DAPI-stained coronal sections of the embryonic day (E) 14 telencephalon (Fig. 1C,C',D,D'). In *Pax6*^{Leca4} homozygotes, radial cortical thickness was significantly reduced in the rostral cortex (Fig. 1C-C''), where *Pax6* is expressed at highest levels (Bishop et al., 2000). This phenotype resembles that of *Pax6*^{Sey} cortices. By contrast, no reduction in radial length

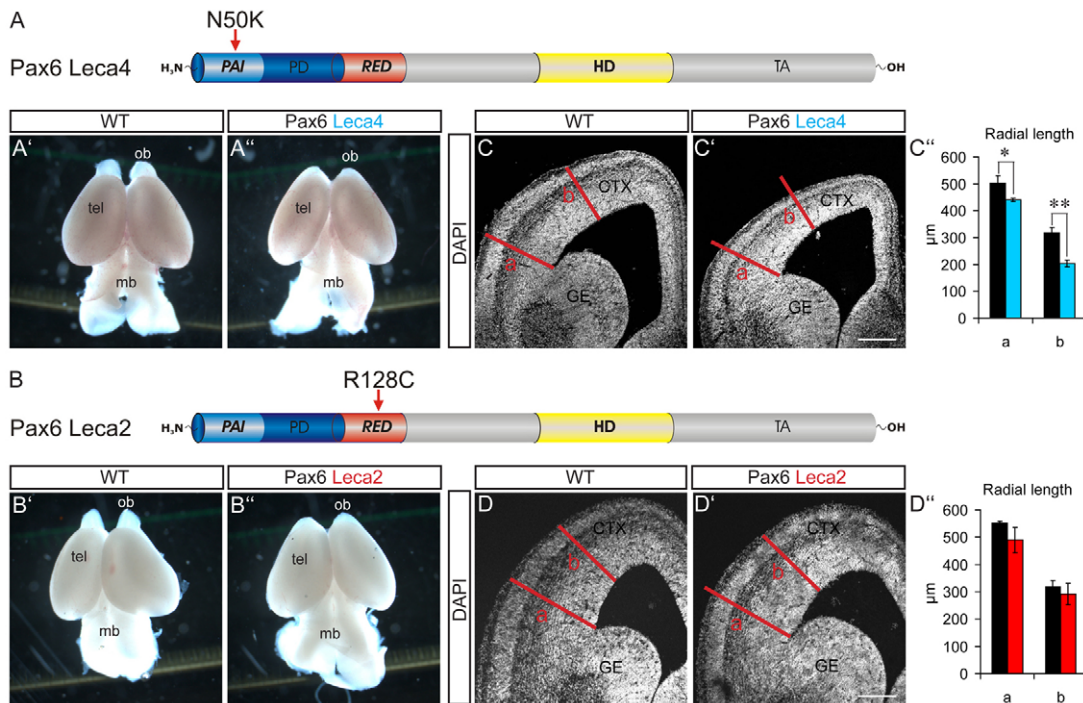


Fig. 1. A point mutation in the PAI or RED subdomain of the Pax6 DNA-binding domain impairs telencephalon development. (A,B) The domain structure of Pax6. Arrows indicate the position of the point mutations in the PAI (Pax6^{Leca4}, A) and RED (Pax6^{Leca2}, B) subdomains. (A',A'',B',B'') E14 brains of Pax6^{Leca4} (A''), Pax6^{Leca2} (B'') mice and their WT littermates (A',B'). (C,C'',D,D'') Micrographs of representative sections of the E14 telencephalon of Pax6^{Leca4} (C''), Pax6^{Leca2} (D'') and their WT littermates (C,D). (C'',D'') Radial length of the cerebral cortex at the positions (a, b) indicated by red lines in the sections. Black bars, WT; blue or red bars, Leca4 or Leca2 mutant. Data are mean \pm s.e.m.; $n \geq 3$ (embryos analyzed); * $P < 0.05$; ** $P < 0.01$. ob, olfactory bulb; tel, telencephalon; mb, midbrain; CTX, cortex; GE, ganglionic eminence. Scale bars: 150 μ m.

was detectable at comparable positions in the Pax6^{Leca2} mutant (Fig. 1D'').

Proliferation is differently affected in the cerebral cortex of Pax6^{Leca4} and Pax6^{Leca2} mice

The reduction in the radial thickness of the Pax6^{Leca4} neocortex might be the consequence of impaired proliferation, impaired neurogenesis and/or increased cell death, as Pax6 has been implicated in all these functions (Schmahl et al., 1993; Götz et al., 1998; Chapouton et al., 1999; Stoykova et al., 2000; Toresson et al., 2000; Yun et al., 2001; Estivill-Torras et al., 2002; Heins et al., 2002; Nikoletopoulou et al., 2007; Ninkovic et al., 2010). We first examined the number of proliferating cells by immunostaining for the phosphorylated form of histone H3 (PH3) present in the G2/M phase of the cell cycle (Fig. 2). This allows the discrimination of apical progenitors, which undergo cell divisions at the ventricular surface, and basal progenitors, which undergo cell division distant from the ventricle (Fig. 2A,C). The numbers of both apical and basal PH3⁺ cells were significantly decreased at E12 and E14 in the rostral cerebral cortex of Pax6^{Leca4} mutants (Fig. 2B), whereas they were almost doubled ($P < 0.05$) at E14 in the Pax6^{Leca2} cerebral cortex (Fig. 2D). Apical and basal progenitors were Pax6⁺ and Tbr2⁺ (Eomes – Mouse Genome Informatics), respectively, in both mutants (Fig. 2E-H'), and also the morphology of Pax6⁺ radial glia stained with RC2 (see supplementary material Table S1) appeared grossly normal (Fig. 2I,J'). Thus, only the number of cells in mitosis, but not the identity of these progenitors, is distinctly affected in the Pax6^{Leca4} and Pax6^{Leca2} mutants.

Dorssoventral patterning is largely normal in the telencephalon of Pax6^{Leca4} and Pax6^{Leca2} mice

Intriguingly, the proliferation phenotypes of both the Pax6^{Leca4} and Pax6^{Leca2} cerebral cortex differ from the phenotype of full Pax6 mutants, such as Pax6^{Sey} or conditional Pax6 deletion, which have normal numbers of apical, but increased numbers of basal, progenitors (Haubst et al., 2004; Tuoc et al., 2009). As a particularly high number of basal progenitors is characteristic of the ventral telencephalon, and because the transcription factors that are normally restricted there, such as Gsx1/2, Dlx1/2 and Olig2, spread into the dorsal telencephalon, i.e. the pallium, in full Pax6 mutants (Stoykova et al., 2000; Toresson et al., 2000; Yun et al., 2001), this ventralization of the cortex contributes to the aberrations in proliferation and can be partially rescued in Pax6^{Sey};Gsx2 double-mutant mice (Toresson et al., 2000). In contrast to Pax6^{Sey}, ventral telencephalic genes were not expressed in most of the dorsal telencephalon, the dorsal and medial pallium in either Leca mutant (Fig. 3A-C). However, at the pallial-subpallial (dorsal telencephalon-ventral telencephalon) boundary (PSB), scattered Gsx2⁺ and Olig2⁺ cells spread into the ventral pallium (the region ventral to the sulcus but dorsal to the boundary; see Fig. 3M) in the Pax6^{Leca4}, but not Pax6^{Leca2}, mutant (Fig. 3A',B',D',E'). Note that Olig2⁺ cells had spread within the Pax6^{Leca4} ventricular zone and hence are not oligodendrocyte progenitors migrating normally into the dorsal telencephalon at subventricular zone positions (arrowheads in Fig. 3D-F). Taken together, these data suggest that patterning of most of the dorsal telencephalon is normal in both Pax6^{Leca4} and Pax6^{Leca2} mutants, whereas the ventral pallium close to the PSB is ventralized in Pax6^{Leca4} homozygotes. Notably, the

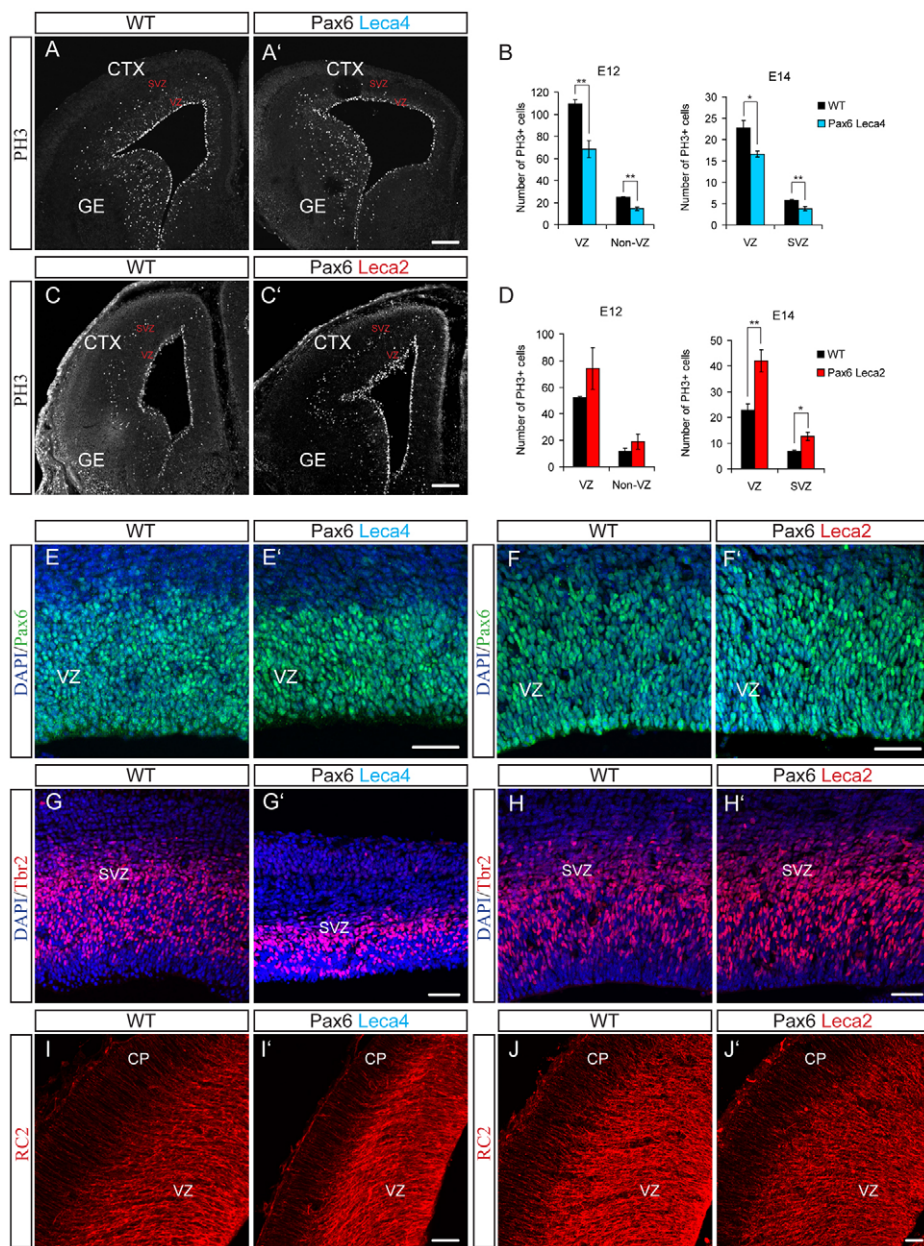


Fig. 2. Mutations in the PAI and RED subdomains of Pax6 affect the number of apical and basal mitoses in an opposing manner. (A,A',C,C') Micrographs of E14 telencephalon sections showing cells immunoreactive for phosphohistone H3 (PH3) in Pax6^{Leca4} and Pax6^{Leca2} mice and their WT littermates. (B,D) The number of PH3⁺ progenitors in Pax6^{Leca4}, Pax6^{Leca2} and their WT littermates at E12 and E14. Data are mean \pm s.e.m., $n \geq 3$ (embryos analyzed); * $P < 0.05$, ** $P < 0.01$. Note the opposite effects of the Pax6^{Leca4} and Pax6^{Leca2} mutations on cortical progenitors. (E-J') Micrographs showing immunoreactivity for Pax6 (E-F'), Tbr2 (G-H') and RC2 (I-J') on E14 dorsal telencephalon of Pax6^{Leca4}, Pax6^{Leca2} and WT littermates. CTX, cortex; GE, ganglionic eminence; VZ, ventricular zone; SVZ, subventricular zone. Scale bars: 100 μ m in A,A',C,C'; 50 μ m in E-J'.

sulcus, which constitutes the morphological dorsal border of this region, is still maintained in both Leca mutant cortices, whereas it is virtually absent in the Pax6^{Sey} cerebral cortex (Fig. 3C',F',I',L').

In contrast to Gsx2 or Olig2, however, Mash1 (Ascl1 – Mouse Genome Informatics) was upregulated in a rather widespread manner in both Pax6^{Leca2} and Pax6^{Leca4} cerebral cortices (Fig. 3G,H'), although in fewer cells than in Pax6^{Sey} (Fig. 3I,I'). As the bHLH transcription factors Neurog1/2 and Mash1 negatively regulate each other (Fode et al., 2000; Britz et al., 2006) and Neurog1/2 were downregulated in the Pax6^{Sey} cerebral cortex (Haubst et al., 2004), we examined Neurog2 as a possible cause for the increase in Mash1 expression. In pronounced contrast to the Pax6^{Sey} cerebral cortex, a strong Neurog2 mRNA signal was present throughout the cerebral cortex of both Pax6^{Leca4} and Pax6^{Leca2} mutants (Fig. 3J-L'). Thus, the function of both PD subdomains is required to restrict Mash1 expression in the cerebral cortex, whereas mutation of either subdomain is dispensable for grossly normal expression of Neurog2, Gsx2 and Olig2.

Neurogenesis is selectively impaired in the cerebral cortex of Pax6^{Leca4} but not Pax6^{Leca2} mice

The change in the number of progenitors in Leca mutants, but the normal expression of progenitor markers such as Neurog2 and Tbr2, prompted us to analyze neurogenesis in Leca mutants by immunostaining for Map2, which labels all differentiating neurons in the cortical plate (CP), and for Tbr1, which is enriched in layer VI neurons (Fig. 4). Whereas the CP was notably thinner in the Pax6^{Leca4} cerebral cortex at E14 and E17, in Pax6^{Leca2} it was comparable to that of wild-type (WT) littermates (Fig. 4; supplementary material Fig. S4). Furthermore, neurons in the deep layers of the cerebral cortex that were immunopositive for Ctip2 (Bcl11b – Mouse Genome Informatics) and Foxp2 (supplementary material Fig. S4A,B) and Cux1⁺ upper layer neurons (supplementary material Fig. S4A,B) were reduced in number in the Pax6^{Leca4} cerebral cortex, but grossly normal in number in the Pax6^{Leca2} cerebral cortex at E17 (supplementary material Fig. S4A,B) and adult (supplementary material Fig. S4C). Thus, neurons

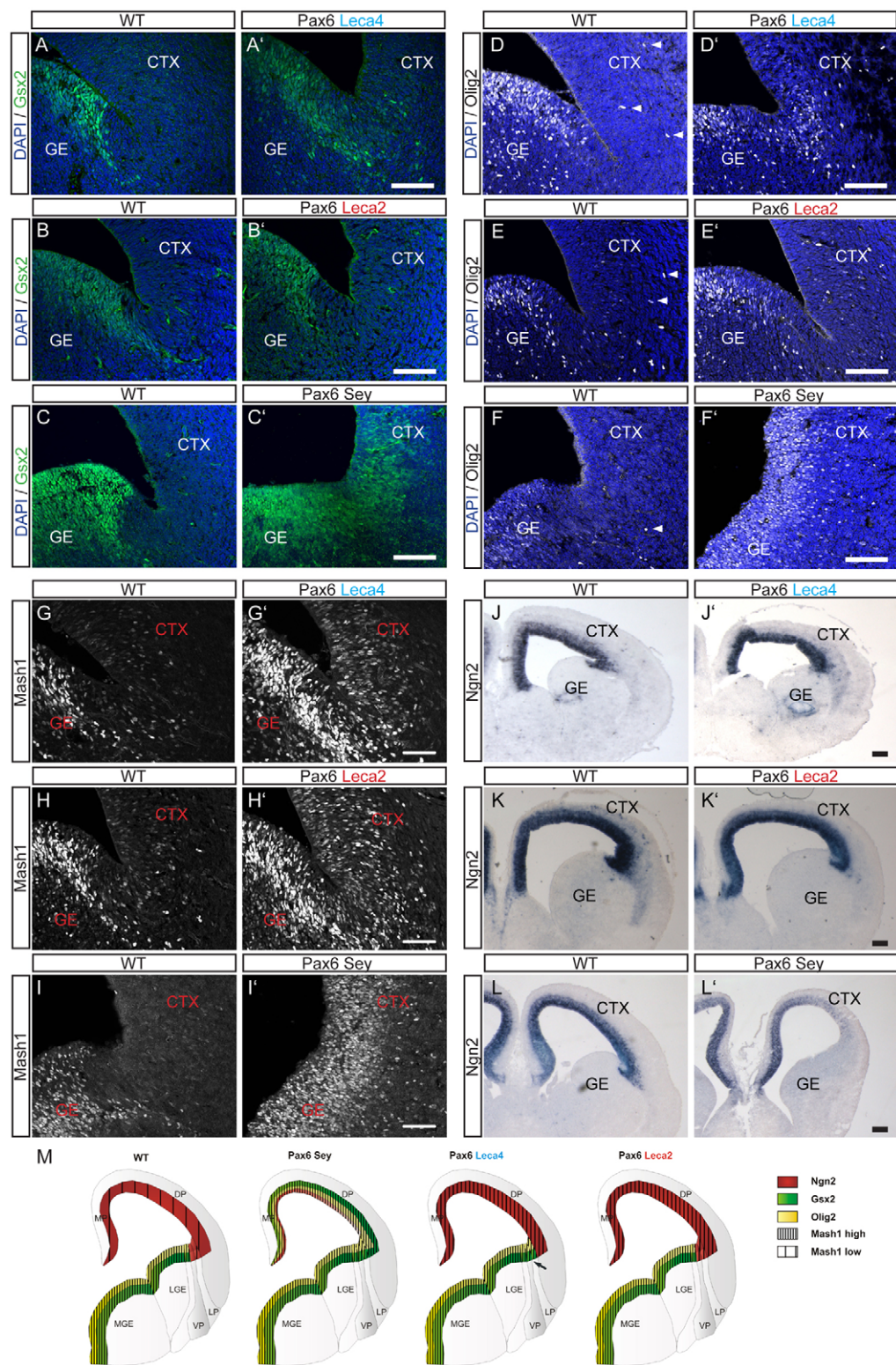


Fig. 3. PAI and RED subdomains are largely redundant in controlling dorsoventral telencephalic patterning. (A-I') Micrographs showing the expression of typical ventral markers in the E14 telencephalon of *Pax6^{Leca4}*, *Pax6^{Leca2}*, *Pax6^{Sey}* mice and their WT littermates. Note that only a few scattered *Gsx2*⁺ or *Olig2*⁺ cells are present in the *Pax6^{Leca2}* and *Pax6^{Leca4}* cerebral cortices in contrast to the overall extension in *Pax6^{Sey}*. White arrowheads (D-F) indicate migrating *Olig2*⁺ oligodendrocyte progenitors. (J-L') Micrographs showing *Ngn2* (marking dorsal telencephalon) expression in E14 dorsal telencephalon of *Pax6^{Leca4}*, *Pax6^{Leca2}*, *Pax6^{Sey}* and WT littermates. (M) Summary of the patterning in each mutant. The arrow indicates the ectopic expression in the ventral and lateral pallium in the *Pax6^{Leca4}* mutant. CTX, cortex; GE, ganglionic eminence (L and M indicate lateral and medial); P, pallium (M, D, V and L indicate medial, dorsal, ventral and lateral). Scale bars: 100 μ m.

in the CP are reduced in the PAI subdomain mutant *Pax6^{Leca4}*, but unaffected in the RED subdomain mutant *Pax6^{Leca2}*.

The latter finding is intriguing given the increase in mitotic cells in the *Pax6^{Leca2}* cerebral cortex, which might result in delayed neuronal differentiation or even an increase in neuron numbers if the increased progenitors all generate neurons. As *Pax6* has also been implicated in the regulation of neuron survival

(Nikoletopoulou et al., 2007), we investigated a possible alteration in cell death rate by quantifying cells immunoreactive for activated caspase 3 in the rostral cerebral cortex of each mutant as compared with their respective WT littermates (supplementary material Fig. S5). No change in the number of activated caspase 3⁺ cells was detected in *Pax6^{Leca4}*, but in the *Pax6^{Leca2}* cerebral cortex almost double the number of activated caspase 3⁺ cells was observed

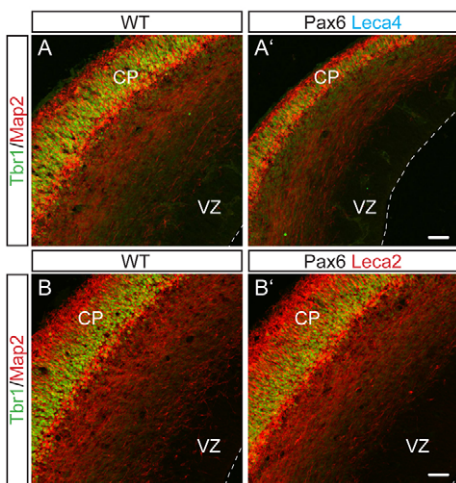


Fig. 4. Neurogenesis is impaired by the PAI subdomain mutation ($\text{Pax6}^{\text{Leca4}}$) but not the RED mutation ($\text{Pax6}^{\text{Leca2}}$). (A–B') Micrographs showing cells immunoreactive for Tbr1 marking layer VI neurons and Map2 marking cortical plate in coronal sections of E14 dorsal telencephalon of (A') $\text{Pax6}^{\text{Leca4}}$, (B') $\text{Pax6}^{\text{Leca2}}$ and (A,B) WT littermates. Note the cortical plate reduction in the $\text{Pax6}^{\text{Leca4}}$ mice. CP, cortical plate; VZ, ventricular zone. Scale bars: 100 μm .

(supplementary material Fig. S5). Interestingly, apoptotic cells were selectively increased in the progenitor layers of $\text{Pax6}^{\text{Leca2}}$ cerebral cortex (supplementary material Fig. S5), i.e. in the region of increased PH3⁺ cells.

In vitro clonal analysis demonstrates effects of $\text{Pax6}^{\text{Leca4}}$, but not $\text{Pax6}^{\text{Leca2}}$, mutation on neurogenesis and proliferation

To directly investigate the neurogenic capacity of Pax6 harboring the Leca2 and Leca4 mutations we first examined the progeny of single progenitor cells after overexpression of the Leca mutant forms in dissociated primary cultures of WT E14 cerebral cortex. Replication incompetent MLV-based retroviral vectors encoding $\text{Pax6}^{\text{Leca2}}$, $\text{Pax6}^{\text{Leca4}}$, WT Pax6 or controls expressing an eGFP reporter (Fig. 5B) were used to infect fewer than 50 cells per coverslip, and distinct clusters of infected cells were considered as clones and analyzed after 1 week *in vitro* (Heins et al., 2002; Haubst et al., 2004). Clones were classified as pure neuronal (NeuN⁺ cells), mixed (NeuN⁺ and NeuN⁻ cells) or pure non-neuronal clones (NeuN⁻ cells) (NeuN is also known as Rbfox3 – Mouse Genome Informatics) (Fig. 5A).

Forced expression of WT Pax6 increased pure neuronal clones (Fig. 5C), consistent with our previous data (Heins et al., 2002; Haubst et al., 2004). Conversely, clone composition did not differ from that with the GFP-only control vector after overexpression of the PAI mutant $\text{Pax6}^{\text{Leca4}}$, suggesting that the Leca4 mutant has lost its neurogenic capacity (Fig. 5C). In pronounced contrast, $\text{Pax6}^{\text{Leca2}}$ transduction significantly increased the number of neuronal clones, thus indicating maintenance of its neurogenic capacity (Fig. 5C). These data were further corroborated by analysis of clones infected with the GFP control virus in cultures isolated from the $\text{Pax6}^{\text{Leca4}}$ cerebral cortex at E14, which generated significantly fewer pure neuronal clones than those from their WT littermates (Fig. 5D), suggesting a defect in neuronal progenitor cells. Conversely, $\text{Pax6}^{\text{Leca2}}$ cells showed no change in clone composition (Fig. 5E) consistent with their apparently normal neurogenesis. Taken together, these data suggest a selective role of the N50 residue

within the PAI subdomain for neurogenic fate instruction in cortical progenitors, whereas the R128C mutation within the RED domain does not impair this function.

We also observed intriguing differences in clone size. Forced expression of WT Pax6 resulted in reduced clone size, as previously described (GFP control, 5.9 ± 1.4 cells per clone; Pax6-GFP, 3.6 ± 0.8) (see Haubst et al., 2004). Whereas overexpression of the PAI mutant $\text{Pax6}^{\text{Leca4}}$ was still able to reduce clone size (Leca4-GFP, 3.5 ± 0.7), clone size resembled that of the GFP control upon forced expression of the RED mutant $\text{Pax6}^{\text{Leca2}}$ (Leca2-GFP, 5.9 ± 1.5). These data further support defects in the anti-proliferative role of Pax6 by the R128C mutation within the RED domain, whereas the PAI domain mutation does not affect this function.

Distinct changes in genome-wide expression in the $\text{Pax6}^{\text{Leca4}}$ versus $\text{Pax6}^{\text{Leca2}}$ cerebral cortex

Given the notably different phenotypes in the cerebral cortex of individual PAI and RED subdomain missense mutants, we set out to determine the transcriptional alterations caused by these mutations. We analyzed genome-wide expression in rostral regions of E14 WT and mutant cerebral cortices by Affymetrix MOE430 2.0 arrays. Differences between WT and mutant littermates were determined by a stringent filter consisting of statistical significance ($\text{FDR} < 10\%$), an average expression level exceeding 50 and at least 1.4-fold difference in expression. This revealed 416 probe sets altered in the PAI domain mutant $\text{Pax6}^{\text{Leca4}}$, of which 179 (43%; supplementary material Table S3) were reduced in expression level (Fig. 6A), whereas only 94 probe sets differed from WT in the RED subdomain mutant $\text{Pax6}^{\text{Leca2}}$ (63% downregulated; supplementary material Table S4) (Fig. 6C). The reliability of this transcriptome analysis was confirmed by qRT-PCR of independent samples for 26 genes (Fig. 6B,B',D,D'). Importantly, only 17 probe sets were altered in both mutants (Fig. 6E; supplementary material Table S6), revealing largely discrete sets of gene expression differences in the PAI and RED domain mutant mice, consistent with the distinct phenotypes of these mutants.

Genes dysregulated in the $\text{Pax6}^{\text{Leca2}}$ cerebral cortex encode transcription factors promoting proliferation, such as Zic1 (Fig. 6G; Fig. 7A,B) (Pourebrahim et al., 2007; Brill et al., 2010; Watabe et al., 2011) and Zic3 (Inoue et al., 2007), or regulating the progression through the cell cycle, such as Id4 (Fig. 6G) (Yun et al., 2004). In addition, pro-apoptotic genes such as Hrk and *Bcl2l11* (Putcha et al., 2001; Ghosh et al., 2011) were upregulated in agreement with increased cell death (supplementary material Fig. S5).

Conversely, in the $\text{Pax6}^{\text{Leca4}}$ cerebral cortex, we observed significant downregulation of pro-proliferative factors such as Id2 (Fig. 6G) (Uribe and Gross, 2010) and a series of neurogenic transcription factors including Dmrt1, Meis1 (Fig. 7A,B), Tcfap2d (Tfap2d; AP-2δ), Tcfap2c (Tfap2c; AP-2γ), Pou3f4, Sall3 and Cux2 (Shimazaki et al., 1999; Cubelos et al., 2008; Pinto et al., 2009). In addition, other genes encoding factors involved in neurogenesis, such as members of the prokineticin family (Prkcb, Prkg2), components of the retinoic acid signaling pathway (Rlbp1, Rbp1, Pbx3) (Fig. 6G; Fig. 7A,B) and Wnt signaling pathway (downregulation of Wnt7a) (Hirabayashi et al., 2004) were reduced in expression in the $\text{Pax6}^{\text{Leca4}}$ cerebral cortex, and negative regulators of Wnt signaling such as Lgals1 (Fig. 6G) (Satelli and Rao, 2011) were increased. Interestingly, these genes involved in neurogenesis were also dysregulated in Pax6^{Sey} , but not in $\text{Pax6}^{\text{Leca2}}$ (Fig. 6F).

In order to identify direct targets among the differentially regulated genes, we compared those affected in the Leca mutants

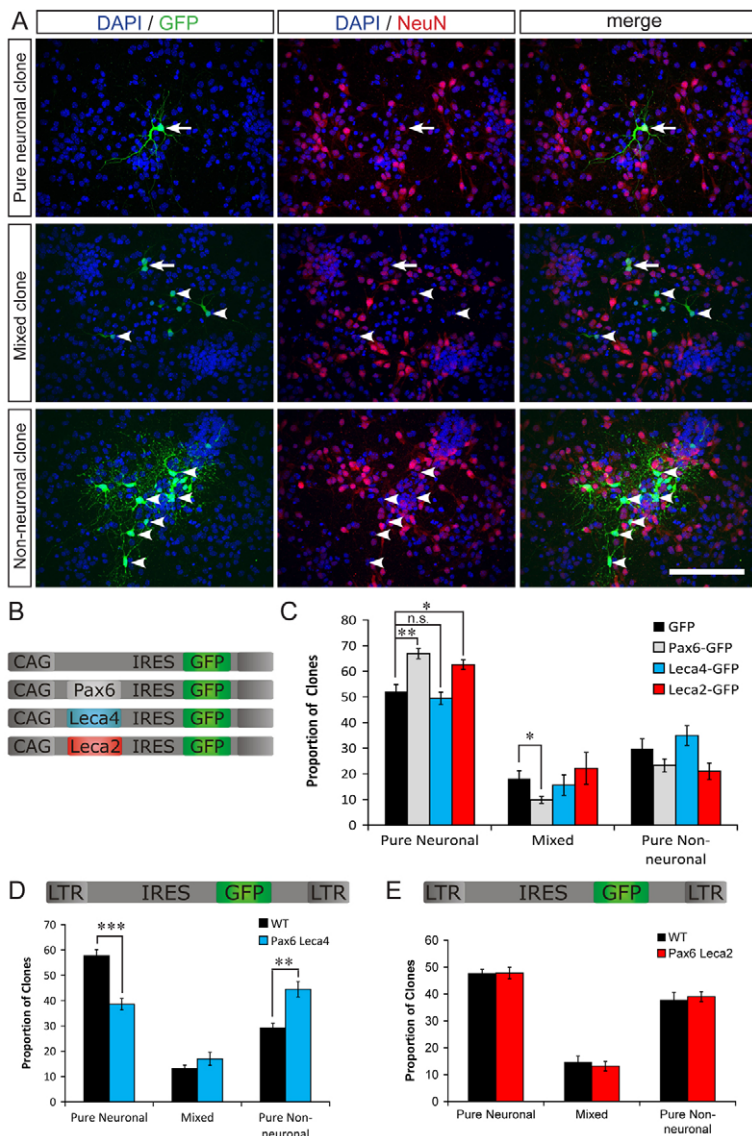


Fig. 5. The PAI subdomain mutation interferes with neuronal fate commitment. (A) Representative images of neuronal, non-neuronal and mixed clones. Arrows indicate neuronal cells and arrowheads non-neuronal cells. Scale bar: 50 μ m. (B) Summary of the retroviral constructs employed in C. (C) The clone types generated after overexpression of Pax6 or its mutated forms Pax6^{Leca4} and Pax6^{Leca2} in E14 WT mouse cortical progenitors. Note the significant increase in pure neuronal clones after overexpression of Pax6 (gray) and Pax6^{Leca2} (red) but not Pax6^{Leca4} (blue) compared with the control GFP-expressing virus. (D,E) The clone types generated from the E14 cortical progenitors isolated from the Pax6^{Leca4} mutant (D), Pax6^{Leca2} mutant (E) or WT littermates. Data are mean \pm s.e.m.; $n \geq 6$ (coverslips analyzed); ** $P < 0.01$, *** $P < 0.001$; n.s., not significant.

with Pax6 ChIP data obtained with E15 WT cerebral cortex, lens and pancreas cells (Xie and Cvekl, 2011; Xie et al., 2013). Interestingly, Pax6 was bound to the promoters of ~20% of the genes regulated in either Pax6^{Leca4} or Pax6^{Leca2} (supplementary material Tables S3, S4 and S7). To gain further insights into direct Pax6 targets, we also compared gene expression changes with the full Pax6^{Sey} mutant, isolating tissue at the same stage and from the same region. A much larger number of genes were differentially regulated in this mutant (Fig. 6F), which might result from a partially redundant function of the PAI and RED subdomains, as observed for patterning. Indeed, patterning is profoundly altered in the full Pax6 mutant, with Olig2, Gsx1/2, Mash1 and Dlx transcription factors ectopically increased in the Pax6^{Sey} cerebral cortex, which will in turn further affect gene expression, whereas only Mash1 was increased in both Leca mutants, and *Olig2* mRNA (but not the protein; see Fig. 3) was elevated in Pax6^{Leca2} (supplementary material Tables S3-S5). Moreover, comparing Pax6 ChIP data with the genes regulated in the respective Leca mutants and the full Pax6 mutant revealed an overlap of 23% (supplementary material Tables S7-S9), and 93% of these were regulated in the same manner (i.e. up- or downregulated), suggesting that they are direct targets and not indirectly affected by patterning.

Taken together, our data revealed largely distinct batteries of genes with disrupted expression in both Pax6 missense mutants versus the Pax6^{Sey} nonsense mutant, suggesting their differential regulation by the PAI or the RED subdomain.

The Leca4 and Leca2 mutations of Pax6 selectively affect transactivation of PAI- or RED domain-containing motifs

The largely discrete alterations in gene expression in the Pax6^{Leca4} and Pax6^{Leca2} cerebral cortices suggest distinct effects of the respective mutations on gene expression. Indeed, bioinformatic and crystallographic analyses also predicted a selective effect of the N50 amino acid that is mutated in the Pax6^{Leca4} line on DNA binding of the PAI subdomain. N50 is the first residue in the DNA-contacting helix (α 3) of the PAI subdomain and part of a cluster of seven amino acid residues that render Pax6 unique DNA binding specificity compared with other Pax proteins (Czerny and Busslinger, 1995). Crystallographic data established direct contact between N50 and an invariant T residue found in many Pax6 binding site motifs (Xu et al., 1999; Xie and Cvekl, 2011). Therefore, the N50K mutation is predicted to disrupt a crucial interaction between the PAI subdomain of Pax6 and DNA (supplementary material Fig. S1B) (Thaung et

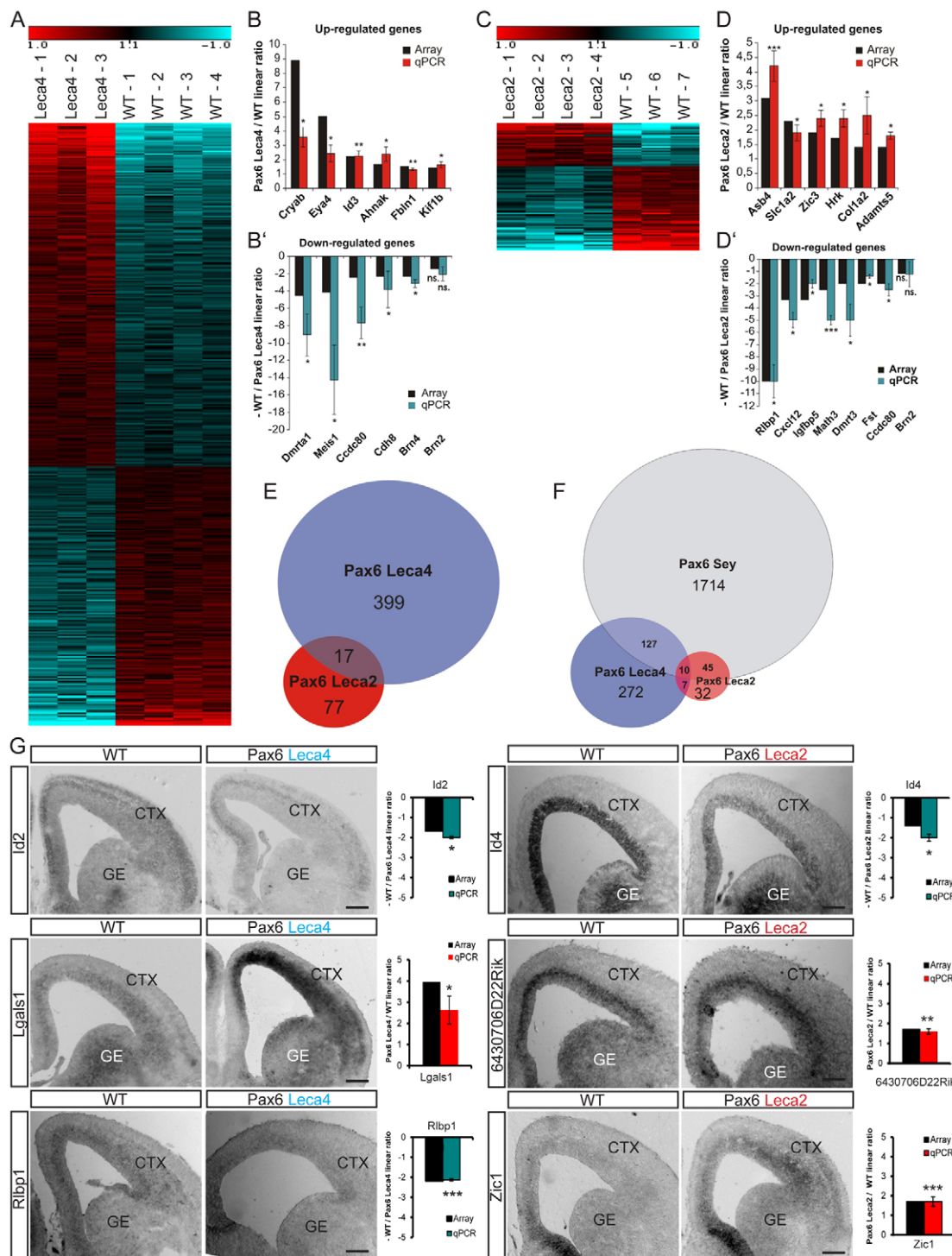
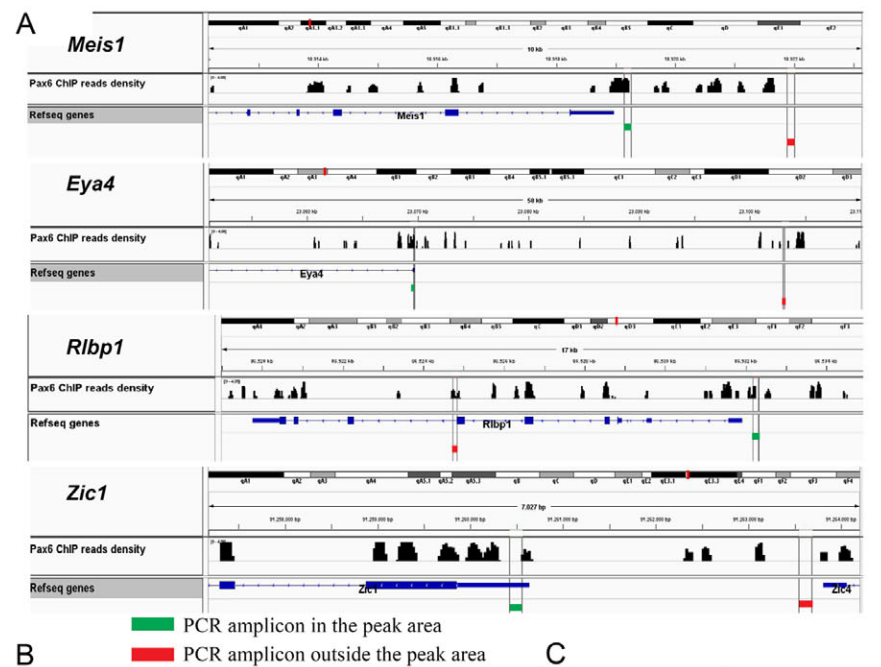


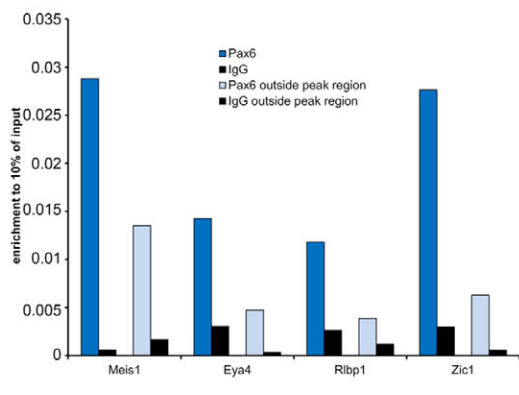
Fig. 6. PAI and RED subdomain mutations affect different gene sets. **(A,C)** Heat map representing the expression of dysregulated genes in the Pax6^{Leca4} (A) or Pax6^{Leca2} (C) E14 mouse cortex compared with WT littermates. Red/blue indicate higher/lower expression values. **(B,B',D,D')** Gene expression changes in Pax6^{Leca4} and Pax6^{Leca2} compared with WT littermates as measured by Affymetrix array analysis or qRT-PCR. **(E,F)** Venn diagrams depicting the overlap between the dysregulated probe sets in the Pax6^{Leca4} and Pax6^{Leca2} cortices (E) and in these versus the Pax6^{Sey} cortex (F). **(G)** Micrographs showing *in situ* hybridization on sections of E14 telencephalon of Pax6^{Leca4}, Pax6^{Leca2} and WT littermates for *Id2*, *Lgals1*, *Rlbp1*, *Id4*, *Hjurp* and *Zic1*. To the right is shown the expression changes detected in the microarray and by qPCR. Data are mean \pm s.e.m.; * P <0.05, ** P <0.01, *** P <0.001; ns., not significant. CTX, cortex; GE, ganglionic eminence. Scale bars: 200 μ m.

al., 2002). The R128 amino acid mutated in the Pax6^{Leca2} line is located within the sixth helix (α 6) of the PD domain and has a perfect DNA binding distance of 2.1 Å, suggesting that the R128C

mutation disrupts the DNA binding capacity of the RED subdomain (supplementary material Fig. S1C). This is in agreement with decreased or absent DNA binding as previously reported



B



C

Motif Names	Motifs
P6CON	
1-1 PAI/ β^{GC} /L (SELEX)	
1-2 PAI/ β^{GC} /L (Natural)	
1-3 PAI/ β^{GC} /L (Natural)	
2-1 HD/PAI/ β^{GC} /L (SELEX)	
2-2 HD/PAI/ β^{GC} /L (Natural)	
3-1 PAI/ β^{GC} /L/RED (SELEX)	
3-2 PAI/ β^{GC} /L/T/RED (Natural)	
3-3 PAI/ β^{GC} /L/T/RED (Natural)	
4-1 HD/L/RED (SELEX)	

D

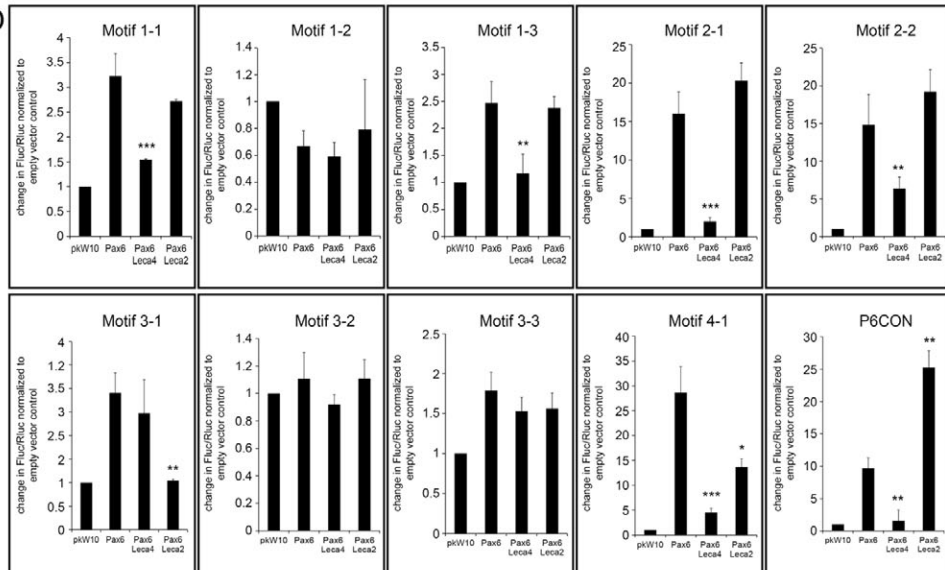


Fig. 7. Leca4 and Leca2 mutations in Pax6 affect its transactivation properties on Pax6 DNA-binding motifs. (A) Pax6 binding regions in the promoters of target genes and position of primers used for ChIP-qPCR. (B) Enrichment of Pax6 binding to target loci in the area containing the newly identified motifs (binding within the peak regions) and in the adjacent area (binding outside of the peak regions). (C) DNA-binding site variants regulated by Pax6. (D) The transactivation properties of WT Pax6, Pax6^{Leca2} and Pax6^{Leca4}. Data are shown as mean \pm s.e.m.; *P<0.05, **P<0.01, ***P<0.001.

(Yamaguchi et al., 1997; Chauhan et al., 2004). Thus, *in silico* analysis predicts selective disruption of the DNA binding activity of the respective subdomains in the mutant proteins (supplementary material Fig. S1B,C).

However, cooperative effects have also been observed between these and other subdomains of Pax6, raising the question of the extent to which these mutant forms of Pax6 disrupt binding to various Pax6 binding sites. To clarify this, we examined the transactivation properties of the mutant proteins in luciferase assays using PAI and RED binding sites (Fig. 7C) derived from *in vivo* Pax6 binding sites (Xie and Cvekl, 2011). Strikingly, 80% (four of five) of the motifs containing ‘dominant’ PAI over RED binding motifs were impaired in their regulation by the Leca4 mutant (Fig. 7D). By contrast, no defects in activation of these constructs were observed with the Leca2 mutant Pax6, supporting the contention that these mutations exclusively affect one subdomain (Fig. 7D). From these studies, we conclude that the N50C residue of Pax6 is important for Pax6 function on sites 1-1, 1-2, 1-3, 2-1, 2-2, 4-1 and P6CON, but not for motifs 3-1, 3-2 and 3-3. By contrast, the Leca2 mutant form of Pax6 (R128C) showed loss of activity with two of the four novel domains containing a RED motif (Fig. 7D), one of which (3-1) was not affected in transactivation by the Leca4 mutation in the PAI subdomain of Pax6 (Fig. 7D). One motif was affected by either Leca4 or Leca2 mutation (4-1), whereas others (1-2, 3-2 and 3-3) were not affected in regulation by any of these mutations. Thus, the Leca4 and Leca2 mutations exert largely selective effects on motifs containing PAI or RED motifs, respectively, consistent with the distinct battery of genes regulated in these mutants *in vivo*. Indeed, the observation that one motif was affected by both mutations is reminiscent of a minority of genes being dysregulated in both Pax6^{Leca2} and Pax6^{Leca4} mutants, whereas others were affected by none of the mutations, reminiscent of the absence of a severe patterning phenotype *in vivo*.

Although *in vivo* regulation is too complex to claim that these elements were one to one responsible for the altered gene expression in the mutants, it is noteworthy that 80% of the genes with Pax6 binding (ChIP⁺; see supplementary material Table S9) and significant dysregulation in the Pax6^{Leca2} cerebral cortex contained one or more of the motifs that the Leca2 mutant failed to activate normally in the reporter assay (Table 1). By contrast, only 35.5% (using the Genomatix platform) of the promoters of randomly selected cortical genes (Pinto et al., 2008) contain at least one of these binding motifs. Taken together, phenotypic and genome-wide expression analyses, ChIP and *in vitro* transactivation assays all support the distinct behaviors of these mutant proteins, with selective effects *in vitro* and *in vivo*.

DISCUSSION

Here we unravelled a molecular logic of how a single transcriptional regulator coordinates neurogenesis, proliferation and patterning. We show that Pax6 utilizes distinct subdomains to control proliferation or to exert selective effects on neurogenesis, whereas these subdomains act largely in a redundant manner for patterning. Our data underline the concept of a modular organization of Pax6 function, not only performing distinct tasks via the PD and HD, but also by assigning distinct roles to the PAI and RED subdomains.

The PAI and RED subdomains regulate dorsoventral patterning

Whereas the multitude of phenotypes observed after deletion of the entire Pax6 protein (Schmahl et al., 1993; Quinn et al., 2007; Tuoc et al., 2009) makes it difficult to dissect individual roles of Pax6, analysis of the Leca mutants not only elucidates the role of the distinct DNA-binding domains, but also helps to discriminate direct effects on neurogenesis and proliferation from indirect effects due to alterations in patterning of the cerebral cortex. In

Table 1. Dysregulated genes in Pax6^{Leca2} cortex and in Pax6 Chip analysis, including Pax6 DNA-binding motifs identified for the individual genes

Probe set	Gene symbol or ID	Leca2 significant probe sets (20/94)	Pax6 Chip binding sites*	Leca4 significant probe sets (3)	Sey significant probe sets (13)	Motifs															
						P1-2	P1-3	P4-1	P1-2	P1-1	P1-2	P2-1	P3-1	P1-1	P2-1	P1-3	P2-1	P3-1	P3-2	P4-1	
1418310_a_at	<i>Rlbp1</i> ^b	0.12	Lens	0.46	0.02	P1-2	P1-3	P4-1	P1-2												
1418054_at	<i>Neurod4</i>	0.28	Cortex		0.10	P1-1	P1-2														
1438551_at	<i>Neurog1</i>	0.38	Cortex	2.53	0.16	P2-1	P2-1	P3-1													
1424186_at	<i>Ccdc80</i>	0.51	Cortex	0.41	0.55	P1-1															
1423260_at	<i>Id4</i>	0.58	Cortex			P1-1	P2-1	P1-3	P2-1												
1420459_at	<i>Ripply3</i>	0.59	Lens		0.69	P3-1	P3-2	P4-1													
1421365_at	<i>Fst</i>	0.66	Cortex			P3-1	P3-2														
1433782_at	<i>Cldn12</i>	0.67	Cortex, pancreas			P1-3	P3-1														
1417872_at	<i>Fhl1</i>	0.67	Cortex		0.6	P1-1	P1-1	P4-1										P3-1			
1442312_at	<i>Tbl1xr1</i>	0.69	Cortex, lens			P3-3	P1-1										P1-3	P4-1			
1418172_at	<i>Hebp1</i>	0.70	Lens			P4-1															
1430798_x_at	<i>Mrpl15</i>	1.46	Pancreas			P2-2	P3-1	P1-1	P2-2	P3-1	P4-1	P4-1	P4-1								
1447628_x_at	<i>Mrps5</i>	1.50	Lens			P2-1	P3-3														
1456005_a_at	<i>Bcl2l11</i>	1.67	Lens		1.95	P1-3	P2-1	P2-1	P2-1	P3-1	P4-1										
1439854_at	<i>Hrk</i>	1.80	Cortex		2.00	P2-1	P3-1	P3-1	P3-2	P4-1											
1452526_a_at	<i>Pax6</i>	1.81	Lens, pancreas		1.52	P2-2	P3-1	P3-3		P1-2	P2-1	P4-1	P1-3	P2-1	P2-1	P3-2	P3-3	P4-1	P3-3	P3-1	P3-2
1439627_at	<i>Zic1</i>	1.87	Pancreas		2.73	P1-3	P2-2	P4-1	P1-1	P1-2	P2-1	P2-1	P2-1	P2-1	P2-2	P3-3	P4-1	P4-1	P4-1	P1-1	P3-1
1438737_at	<i>Zic3</i>	1.90	Lens		2.83	P1-3															
1438194_at	<i>Slc1a2</i>	2.66	Cortex		1.61	P1-3	P1-1	P4-1	P4-1	P3-3	P4-1	P4-1	P4-1								
1433919_at	<i>Asb4</i>	3.54	Cortex		12.29	P1-3	P3-1	P4-1	P4-1	P2-1	P3-3										

Important binding domains are highlighted. P1-1, PAI/βGC/L (Selex); P1-2, PAI/βGC/L (Natural); P1-3, PAI/β-GC/L (Natural); P2-1, HD/PAI/βGC/L (Selex); P2-2, HD/PAI/βGC/L (Natural); P3-1 (light gray shading), PAI/βGC/L/RED (Selex); P3-2, PAI/β-GC/L/T/RED (Natural); P3-3, PAI/βGC/L-TT/RED (Natural); P4-1 (dark gray shading), HD/LRED (Selex).

*(Xie et al., 2013).

^bIdentified by ChIP-seq in cortex chromatin (see Fig. 7A,B).

all Pax6 mutants, including conditional deletions in a cortex-specific manner (Tuoc et al., 2009), mouse chimera (Quinn et al., 2007) or even upon acute deletion of *Pax6* by Cre electroporation (Asami et al., 2011), the ectopic misexpression of genes characteristic of the ventral telencephalon, such as *Gsx2*, *Olig2*, *Mash1* or *Dlx* transcription factors, occurred, changing neuronal fate from glutamatergic to GABAergic (Stoykova et al., 2000; Toresson et al., 2000; Heins et al., 2002; Kroll and O'Leary, 2005). Given that proliferation differs somewhat between the ventral and dorsal telencephalon, with a faster cell cycle and a much higher number of subventricular zone progenitors in the former, it has thus far not been possible to dissect direct effects of Pax6 on proliferation and neurogenesis from indirect effects due to altered regionalization.

In pronounced contrast, none of the ventral transcription factors *Dlx1/2/5/6*, *Gsx1/2* or *Olig1/2* was misexpressed in a widespread manner in the dorsal cerebral cortex of Leca2 or Leca4 mice, with the sole exception of *Mash1*. Interestingly, despite the expanded *Mash1* expression, *Neurog2* (*Ngn2*), which is normally regulated in an opposing manner to *Mash1* in the forebrain (Fode et al., 2000; Parras et al., 2002), and *Tbr2* were both still expressed normally in the cerebral cortex of both Leca mutants. Both *Neurog2* and *Tbr2* are virtually absent in the *Pax6^{Sey}* cerebral cortex at this stage (Stoykova et al., 2000; Muzio et al., 2002; Scardigli et al., 2003). As they are involved in glutamatergic neurogenesis (Schuurmans et al., 2004; Sessa et al., 2008), this further contributes to the conversion of glutamatergic to GABAergic neurogenesis in the full Pax6 mutants (Kroll and O'Leary, 2005; Quinn et al., 2007; Tuoc et al., 2009). Accordingly, glutamatergic neurogenesis is maintained in the Leca mutants and GABAergic neurons are neither increased nor accumulate ectopically in the white matter as observed in *Pax6^{Sey}* mutants (supplementary material Fig. S4; data not shown). These phenotypes reveal that the remaining Pax6 subdomain function (PAI or RED) is still sufficient to achieve relatively normal dorsoventral patterning and therefore to allow the role of Pax6 in neurogenesis and progenitor proliferation to be determined in the absence of mispatterning.

Interestingly, the subdomain of the dorsal telencephalon closest to the boundary to the ventral telencephalon, the ventral pallium, appears most susceptible to mispatterning and ectopically expressed *Gsx2* and *Olig2* in the PAI, but not in the RED, subdomain mutant of Pax6. Thus, the PAI subdomain is crucial in the previously described antagonistic role of *Gsx2* and *Pax6* (Toresson et al., 2000) and the RED subdomain on its own is not sufficient to fully restrict *Gsx2* to its normal region of expression. Moreover, a profound upregulation of the ventral pallium-specific transcription factor *Dbx1* is observed in the genome-wide microarray expression analysis of the *Pax6^{Leca4}* cerebral cortex to an even higher extent than in the *Pax6^{Sey}* mutant, whereas no change in *Dbx1* was observed in the *Pax6^{Leca2}* cerebral cortex. This further supports abnormalities in the ventral pallium upon N50K mutation in the PAI domain, whereas the R128C mutation in the RED domain does not affect patterning.

PAI domain-specific function in neurogenesis

Despite the absence of mispatterning, the gross morphology of the cerebral cortex of *Pax6^{Leca4}* mice resembled the morphology observed in full Pax6 mutant mice, with a smaller, shorter cerebral cortex (Fig. 1) (Asami et al., 2011) and a thinner CP with reduced numbers of neurons (Schmahl et al., 1993; Heins et al., 2002). By contrast, this phenotype was not visible in mice carrying the R128C mutation in the RED domain, consistent with normal neurogenesis

in these mice. These selective effects on neurogenesis were further corroborated by clonal analysis *in vitro*. Thus, the PAI domain is essential for neuronal fate instruction, whereas the R128C mutation in the RED domain does not affect this function of Pax6.

Distinct effects of the PAI and RED subdomain mutations on cell proliferation

The numbers of mitotic cells are clearly increased by E14 in the cerebral cortex of the RED domain *Pax6^{Leca2}* mutants, whereas their number is decreased in the *Pax6^{Leca4}* cerebral cortex, supposedly contributing to the smaller size of the *Pax6^{Leca4}* cerebral cortex. Notably, the number of apical mitoses is unaffected in the full Pax6 mutant cortex, suggesting that the effects of both subdomains largely outcompete each other in these progenitors and that the selective increase in progenitors dividing at non-apical positions in the full Pax6 mutant (Götz et al., 1998; Haubst et al., 2004; Tuoc et al., 2009) might largely result from ventralization of the cortex. However, the Leca mutations affect proliferation of both apical and basal progenitors in the dorsal pallium in the absence of patterning defects, suggesting a different, indirect mechanism of how Pax6 might regulate basal progenitor divisions, as it is not expressed in basal progenitors, including in the Leca mutants.

The novel concept that the same transcription factor affects proliferation in opposing manners via its DNA-binding subdomains also has implications with regard to the diverse effects of Pax6 on region- and cell type-specific proliferation (Marquardt et al., 2001; Haubst et al., 2004; Sakurai and Osumi, 2008; Sansom et al., 2009). Loss of Pax6 can lead to a decrease in proliferation, such as in the developing diencephalon (Warren and Price, 1997), retina (Marquardt et al., 2001) and postnatal glial progenitors (Sakurai and Osumi, 2008), or to increased proliferation in the telencephalon as described above. Interestingly, even in the same cell type, i.e. the progenitors of the cerebral cortex, Pax6 has been observed to both promote and inhibit proliferation (Holm et al., 2007; Osumi et al., 2008; Sansom et al., 2009). Thus, this analysis of the specific mutations in the paired subdomains sheds new light on how Pax6 affects proliferation and cell division at multiple levels (see Asami et al., 2011).

Consistent with the distinct effects of the Leca2 and Leca4 mutations, genes promoting cell cycle exit such as *Gadd45b* are upregulated in the *Pax6^{Leca4}* cerebral cortex, whereas the pro-proliferative factors *Id2* (Uribe and Gross, 2010) and tenascin C (von Holst et al., 2007) are decreased in expression. Conversely, transcription factors that promote proliferation, such as *Zic1* and *Zic3* (Inoue et al., 2007; Pourebrahim et al., 2007; Brill et al., 2010; Watabe et al., 2011), were upregulated in the *Pax6^{Leca2}* cerebral cortex. Interestingly, genes encoding centrosome-associated proteins that were prominently affected in expression in the *Pax6^{Sey}* cerebral cortex or after acute Pax6 deletion (Asami et al., 2011), such as the direct Pax6 target *Spag5*, which regulates the orientation of cell division, are not affected in either of the Leca mutants. Instead, increased apoptosis occurs in the progenitor zone of the *Pax6^{Leca2}* cerebral cortex in agreement with the increased expression of pro-apoptotic genes such as *Bcl2l11* and *Hrk*. The extent to which this is due to aberrant events in mitosis or proliferation or reflects direct regulation of these genes by Pax6 remains to be determined. Importantly, our analysis addresses the roles of the PAI and RED subdomains within the canonical Pax6 isoform, as the alternatively spliced Pax6(5a) isoform (Epstein et al., 1994a) is less abundant in the developing cortex at the stages we analyzed (Haubst et al., 2004) and genomic deletion of exon 5a does not impair proliferation, neurogenesis or patterning of the cerebral cortex (Haubst et al., 2004).

Pax6^{Leca4} (PAI subdomain) versus Pax6^{Leca2} (RED subdomain) mutations affect Pax6 function through a series of distinct sites *in vitro* and *in vivo*

The distinct phenotypes in Pax6^{Leca4} and Pax6^{Leca2} mutants also imply that the respective point mutations do not have a deleterious effect on the Pax6 protein, as this would result in a phenocopy of the complete null mutation. As predicted by structural analysis and confirmed by gene expression reporter assays, these mutations affect DNA binding of each subdomain selectively. The Leca4 mutation in the PAI subdomain interfered only with transcriptional activation mediated by the PAI, but not RED, binding site motifs. Similarly, the Leca2 mutation in the RED subdomain largely spares activation via the PAI site motifs, even though a few motifs were affected in regulation by both of the Leca mutant forms (4-1) and the Leca2 mutation also resulted in superactivation of the P6CON motif. Cooperation between PAI and RED subdomains has been observed previously (Yamaguchi et al., 1997; Chauhan et al., 2004) and Leca mutations might affect the interaction of Pax6 with other proteins (Cvekl et al., 1999; Kamachi et al., 2001; Planque et al., 2001; Sivak et al., 2004; Tuoc and Stoykova, 2008) and thereby alter transcription. Indeed, the effects of Pax6 point mutations are complex and it is important to note that the two mutations analyzed here might also differ in their respective severities (Alibés et al., 2010).

Notwithstanding these considerations, both luciferase experiments and genome-wide expression analyses support the rather discrete and modular effects of these subdomain mutations, rather than one being a subset of the other. Moreover, comparing the ChIP data (Xie et al., 2013) with the transcriptomes of the Pax6^{Sey} and Leca mutant mice revealed an overlap of 23% (supplementary material Tables S7-S9), with almost all of these genes regulated in the same direction as in the mutants, suggesting that they are direct targets of Pax6 and not, for example, indirectly affected by mispatterning in the Pax6^{Sey} cerebral cortex. Thus, our analysis provides candidates for novel direct Pax6 targets that are regulated preferentially by distinct subdomains *in vivo*.

Beyond these individual targets, however, the concept of modular Pax6 function is of broader relevance. Pax6 not only utilizes its modular structure to perform rather distinct functions via its HD and PD (Haubst et al., 2004; Ninkovic et al., 2010), but also even individual helix-turn-helix PD subdomains seemingly exert distinct and even partially opposing functions. Our data thereby provide a molecular framework of how the same transcription factor can affect proliferation in opposing manners and regulate progenitor numbers rather precisely depending on subdomain activity, Pax6 levels and the cellular context. Thus, the co-activation of both pro- and anti-proliferative genes in the same cell population, as is the case for Pax6 (Sansom et al., 2009), might allow particularly fine-tuned regulation of proliferation, implementing the complex differences in the cell cycle progression of self-renewing or committed progenitors, a crucial aspect in the ontogeny and phylogeny of the cerebral cortex.

Acknowledgements

We thank Andrea Steiner, Angelika Waiser and Detlef Franzen for their excellent technical support and the animal caretakers of the Helmholtz Center Munich for their assistance.

Funding

Grant support was provided by the Deutsche Forschungsgemeinschaft (DFG) [including SFB 870], the German-Israeli Foundation for Scientific Research and Development (GIF), the European Transcriptome, Regulome and Cellular Commitment Consortium (EuTRACC) and the Bundesministerium für Bildung und Forschung (BMBF) to M.G.; National Institutes of Health (NIH) grants [R01

EY012200, R21 EY017296] to A.C.; and in part by the Helmholtz Alliance CoReNe to J.B. and Nationales Genomforschungsnetz (NGFN)-Plus to J.B., as well as an unrestricted grant from Research to Prevent Blindness to the Department of Ophthalmology and Visual Sciences. Deposited in PMC for release after 12 months.

Competing interests statement

The authors declare no competing financial interests.

Supplementary material

Supplementary material available online at

<http://dev.biologists.org/lookup/suppl/doi:10.1242/dev.082875/-DC1>

References

- Alibés, A., Nadra, A. D., De Masi, F., Bulyk, M. L., Serrano, L. and Stricher, F. (2010). Using protein design algorithms to understand the molecular basis of disease caused by protein-DNA interactions: the Pax6 example. *Nucleic Acids Res.* **38**, 7422-7431.
- Altmann, C. R., Chow, R. L., Lang, R. A. and Hemmati-Brivanlou, A. (1997). Lens induction by Pax-6 in Xenopus laevis. *Dev. Biol.* **185**, 119-123.
- Anderson, T. R., Hedlund, E. and Carpenter, E. M. (2002). Differential Pax6 promoter activity and transcript expression during forebrain development. *Mech. Dev.* **114**, 171-175.
- Asami, M., Pilz, G. A., Ninkovic, J., Godinho, L., Schroeder, T., Huttner, W. B. and Götz, M. (2011). The role of Pax6 in regulating the orientation and mode of cell division of progenitors in the mouse cerebral cortex. *Development* **138**, 5067-5078.
- Ashery-Padan, R. and Gruss, P. (2001). Pax6 lights-up the way for eye development. *Curr. Opin. Cell Biol.* **13**, 706-714.
- Ashery-Padan, R., Marquardt, T., Zhou, X. and Gruss, P. (2000). Pax6 activity in the lens primordium is required for lens formation and for correct placement of a single retina in the eye. *Genes Dev.* **14**, 2701-2711.
- Azuma, N., Nishina, S., Yanagisawa, H., Okuyama, T. and Yamada, M. (1996). Pax6 missense mutation in isolated foveal hypoplasia. *Nat. Genet.* **13**, 141-142.
- Berninger, B., Costa, M. R., Koch, U., Schroeder, T., Sutor, B., Grothe, B. and Götz, M. (2007). Functional properties of neurons derived from *in vitro* reprogrammed postnatal astroglia. *J. Neurosci.* **27**, 8654-8664.
- Bishop, K. M., Goudreau, G. and O'Leary, D. D. (2000). Regulation of area identity in the mammalian neocortex by Emx2 and Pax6. *Science* **288**, 344-349.
- Blum, R., Heinrich, C., Sánchez, R., Lepier, A., Gundelfinger, E. D., Berninger, B. and Götz, M. (2011). Neuronal network formation from reprogrammed early postnatal rat cortical glial cells. *Cereb. Cortex* **21**, 413-424.
- Brill, E., Gobble, R., Angeles, C., Lagos-Quintana, M., Crago, A., Laxa, B., Decarolis, P., Zhang, L., Antonescu, C., Socci, N. D. et al. (2010). ZIC1 overexpression is oncogenic in liposarcoma. *Cancer Res.* **70**, 6891-6901.
- Britz, O., Mattar, P., Nguyen, L., Langevin, L. M., Zimmer, C., Alam, S., Guillermot, F. and Schuurmans, C. (2006). A role for proneural genes in the maturation of cortical progenitor cells. *Cereb. Cortex* **16 Suppl. 1**, i138-i151.
- Chapouton, P., Gärtner, A. and Götz, M. (1999). The role of Pax6 in restricting cell migration between developing cortex and basal ganglia. *Development* **126**, 5569-5579.
- Chauhan, B. K., Yang, Y., Cvekllová, K. and Cvekl, A. (2004). Functional properties of natural human PAX6 and PAX6(5a) mutants. *Invest. Ophthalmol. Vis. Sci.* **45**, 385-392.
- Chi, N. and Epstein, J. A. (2002). Getting your Pax straight: Pax proteins in development and disease. *Trends Genet.* **18**, 41-47.
- Chow, R. L., Altmann, C. R., Lang, R. A. and Hemmati-Brivanlou, A. (1999). Pax6 induces ectopic eyes in a vertebrate. *Development* **126**, 4213-4222.
- Cubelos, B., Sebastián-Serrano, A., Kim, S., Moreno-Ortiz, C., Redondo, J. M., Walsh, C. A. and Nieto, M. (2008). Cux-2 controls the proliferation of neuronal intermediate precursors of the cortical subventricular zone. *Cereb. Cortex* **18**, 1758-1770.
- Cvekl, A., Kashanchi, F., Brady, J. N. and Piatigorsky, J. (1999). Pax-6 interactions with TATA-box-binding protein and retinoblastoma protein. *Invest. Ophthalmol. Vis. Sci.* **40**, 1343-1350.
- Czerny, T. and Busslinger, M. (1995). DNA-binding and transactivation properties of Pax-6: three amino acids in the paired domain are responsible for the different sequence recognition of Pax-6 and BSAP (Pax-5). *Mol. Cell. Biol.* **15**, 2858-2871.
- Dames, P., Puff, R., Weise, M., Parhofer, K. G., Göke, B., Götz, M., Graw, J., Favor, J. and Lechner, A. (2010). Relative roles of the different Pax6 domains for pancreatic alpha cell development. *BMC Dev. Biol.* **10**, 39.
- Dohrmann, C., Gruss, P. and Lemaire, L. (2000). Pax genes and the differentiation of hormone-producing endocrine cells in the pancreas. *Mech. Dev.* **92**, 47-54.
- Epstein, J., Cai, J., Glaser, T., Jeppe, L. and Maas, R. (1994a). Identification of a Pax paired domain recognition sequence and evidence for DNA-dependent conformational changes. *J. Biol. Chem.* **269**, 8355-8361.

- Epstein, J. A., Glaser, T., Cai, J., Japeal, L., Walton, D. S. and Maas, R. L.** (1994b). Two independent and interactive DNA-binding subdomains of the Pax6 paired domain are regulated by alternative splicing. *Genes Dev.* **8**, 2022-2034.
- Estivill-Torres, G., Pearson, H., van Heyningen, V., Price, D. J. and Rashbass, P.** (2002). Pax6 is required to regulate the cell cycle and the rate of progression from symmetrical to asymmetrical division in mammalian cortical progenitors. *Development* **129**, 455-466.
- Favor, J., Peters, H., Hermann, T., Schmahl, W., Chatterjee, B., Neuhauser-Klaus, A. and Sandulache, R.** (2001). Molecular characterization of Pax6(2Neu) through Pax6(10Neu): an extension of the Pax6 allelic series and the identification of two possible homomorph alleles in the mouse *Mus musculus*. *Genetics* **159**, 1689-1700.
- Fode, C., Ma, Q., Casarosa, S., Ang, S. L., Anderson, D. J. and Guillemot, F.** (2000). A role for neural determination genes in specifying the dorsoventral identity of telencephalic neurons. *Genes Dev.* **14**, 67-80.
- Ghosh, A. P., Cape, J. D., Klocke, B. J. and Roth, K. A.** (2011). Deficiency of pro-apoptotic Hrk attenuates programmed cell death in the developing murine nervous system but does not affect Bcl-x deficiency-induced neuron apoptosis. *J. Histochem. Cytochem.* **59**, 976-983.
- Götz, M., Stoykova, A. and Gruss, P.** (1998). Pax6 controls radial glia differentiation in the cerebral cortex. *Neuron* **21**, 1031-1044.
- Graw, J., Löster, J., Puk, O., Münster, D., Haubst, N., Soewarto, D., Fuchs, H., Meyer, B., Nürnberg, P., Pretsch, W. et al.** (2005). Three novel Pax6 alleles in the mouse leading to the same small-eye phenotype caused by different consequences at target promoters. *Invest. Ophthalmol. Vis. Sci.* **46**, 4671-4683.
- Hanson, I. and Van Heyningen, V.** (1995). Pax6: more than meets the eye. *Trends Genet.* **11**, 268-272.
- Haubst, N., Berger, J., Radjendirane, V., Graw, J., Favor, J., Saunders, G. F., Stoykova, A. and Götz, M.** (2004). Molecular dissection of Pax6 function: the specific roles of the paired domain and homeodomain in brain development. *Development* **131**, 6131-6140.
- Heins, N., Malatesta, P., Cecconi, F., Nakafuku, M., Tucker, K. L., Hack, M. A., Chapouton, P., Barde, Y. A. and Götz, M.** (2002). Glial cells generate neurons: the role of the transcription factor Pax6. *Nat. Neurosci.* **5**, 308-315.
- Hill, R. E., Favor, J., Hogan, B. L., Ton, C. C., Saunders, G. F., Hanson, I. M., Prosser, J., Jordan, T., Hastie, N. D. and van Heyningen, V.** (1991). Mouse small eye results from mutations in a paired-like homeobox-containing gene. *Nature* **354**, 522-525.
- Hirabayashi, Y., Itoh, Y., Tabata, H., Nakajima, K., Akiyama, T., Masuyama, N. and Gotoh, Y.** (2004). The Wnt/beta-catenin pathway directs neuronal differentiation of cortical neural precursor cells. *Development* **131**, 2791-2801.
- Holm, P. C., Mader, M. T., Haubst, N., Wizenmann, A., Sigvardsson, M. and Götz, M.** (2007). Loss- and gain-of-function analyses reveal targets of Pax6 in the developing mouse telencephalon. *Mol. Cell. Neurosci.* **34**, 99-119.
- Inoue, T., Ota, M., Ogawa, M., Mikoshiba, K. and Aruga, J.** (2007). Zic1 and Zic3 regulate medial forebrain development through expansion of neuronal progenitors. *J. Neurosci.* **27**, 5461-5473.
- Jiménez, D., García, C., de Castro, F., Chédotal, A., Sotelo, C., de Carlos, J. A., Valverde, F. and López-Mascaraque, L.** (2000). Evidence for intrinsic development of olfactory structures in Pax-6 mutant mice. *J. Comp. Neurol.* **428**, 511-526.
- Jun, S. and Desplan, C.** (1996). Cooperative interactions between paired domain and homeodomain. *Development* **122**, 2639-2650.
- Kamachi, Y., Uchikawa, M., Tanouchi, A., Sekido, R. and Kondoh, H.** (2001). Pax6 and SOX2 form a co-DNA-binding partner complex that regulates initiation of lens development. *Genes Dev.* **15**, 1272-1286.
- Kozmík, Z.** (2008). The role of Pax genes in eye evolution. *Brain Res. Bull.* **75**, 335-339.
- Kozmík, Z., Czerny, T. and Busslinger, M.** (1997). Alternatively spliced insertions in the paired domain restrict the DNA sequence specificity of Pax6 and Pax8. *EMBO J.* **16**, 6793-6803.
- Kroll, T. T. and O'Leary, D. D.** (2005). Ventralized dorsal telencephalic progenitors in Pax6 mutant mice generate GABA interneurons of a lateral ganglionic eminence type. *Proc. Natl. Acad. Sci. USA* **102**, 7374-7379.
- Lyon, M. F., Bogani, D., Boyd, Y., Guillot, P. and Favor, J.** (2000). Further genetic analysis of two autosomal dominant mouse eye defects, Ccw and Pax6(coop). *Mol. Vis.* **6**, 199-203.
- Mansouri, A., Hallonet, M. and Gruss, P.** (1996). Pax genes and their roles in cell differentiation and development. *Curr. Opin. Cell Biol.* **8**, 851-857.
- Marquardt, T., Ashery-Padan, R., Andrejewski, N., Scardigli, R., Guillemot, F. and Gruss, P.** (2001). Pax6 is required for the multipotent state of retinal progenitor cells. *Cell* **105**, 43-55.
- Matsuo, T., Osumi-Yamashita, N., Noji, S., Ohuchi, H., Koyama, E., Myokai, F., Matsuo, N., Taniguchi, S., Doi, H., Iseki, S. et al.** (1993). A mutation in the Pax-6 gene in rat small eye is associated with impaired migration of midbrain crest cells. *Nat. Genet.* **3**, 299-304.
- Mikkola, I., Bruun, J. A., Holm, T. and Johansen, T.** (2001). Superactivation of Pax6-mediated transactivation from paired domain-binding sites by dna-independent recruitment of different homeodomain proteins. *J. Biol. Chem.* **276**, 4109-4118.
- Mishra, R., Gorlov, I. P., Chao, L. Y., Singh, S. and Saunders, G. F.** (2002). Pax6, paired domain influences sequence recognition by the homeodomain. *J. Biol. Chem.* **277**, 49488-49494.
- Muzio, L., Di Benedetto, B., Stoykova, A., Boncinelli, E., Gruss, P. and Mallamaci, A.** (2002). Emx2 and Pax6 control regionalization of the pre-neuronogenic cortical primordium. *Cereb. Cortex* **12**, 129-139.
- Nikolopoulou, V., Plachta, N., Allen, N. D., Pinto, L., Götz, M. and Barde, Y. A.** (2007). Neurotrophin receptor-mediated death of misspecified neurons generated from embryonic stem cells lacking Pax6. *Cell Stem Cell* **1**, 529-540.
- Ninkovic, J., Pinto, L., Petricca, S., Lepier, A., Sun, J., Rieger, M. A., Schroeder, T., Cvekl, A., Favor, J. and Götz, M.** (2010). The transcription factor Pax6 regulates survival of dopaminergic olfactory bulb neurons via crystallin α A. *Neuron* **68**, 682-694.
- Nomura, T. and Osumi, N.** (2004). Misrouting of mitral cell progenitors in the Pax6/small eye rat telencephalon. *Development* **131**, 787-796.
- Osumi, N., Shinohara, H., Numayama-Tsuruta, K. and Maekawa, M.** (2008). Concise review: Pax6 transcription factor contributes to both embryonic and adult neurogenesis as a multifunctional regulator. *Stem Cells* **26**, 1663-1672.
- Parras, C. M., Schuurmans, C., Scardigli, R., Kim, J., Anderson, D. J. and Guillemot, F.** (2002). Divergent functions of the proneural genes Mash1 and Ngn2 in the specification of neuronal subtype identity. *Genes Dev.* **16**, 324-338.
- Pinto, L., Mader, M. T., Irmler, M., Gentilini, M., Santoni, F., Drechsel, D., Blum, R., Stahl, R., Bulfone, A., Malatesta, P. et al.** (2008). Prospective isolation of functionally distinct radial glial subtypes – lineage and transcriptome analysis. *Mol. Cell. Neurosci.* **38**, 15-42.
- Pinto, L., Drechsel, D., Schmid, M. T., Ninkovic, J., Irmler, M., Brill, M. S., Restani, L., Gianfranceschi, L., Cerri, C., Weber, S. N. et al.** (2009). AP2gamma regulates basal progenitor fate in a region- and layer-specific manner in the developing cortex. *Nat. Neurosci.* **12**, 1229-1237.
- Planque, N., Leconte, L., Coquelle, F. M., Benkhelifa, S., Martin, P., Felder-Schmittbuhl, M. P. and Saule, S.** (2001). Interaction of Maf transcription factors with Pax-6 results in synergistic activation of the glucagon promoter. *J. Biol. Chem.* **276**, 35751-35760.
- Pourebrahim, R., Van Dam, K., Bauters, M., De Wever, I., Sciot, R., Cassiman, J. J. and Teijpar, S.** (2007). ZIC1 gene expression is controlled by DNA and histone methylation in mesenchymal proliferations. *FEBS Lett.* **581**, 5122-5126.
- Putcha, G. V., Moulder, K. L., Golden, J. P., Bouillet, P., Adams, J. A., Strasser, A. and Johnson, E. M.** (2001). Induction of BIM, a proapoptotic BH3-only BCL-2 family member, is critical for neuronal apoptosis. *Neuron* **29**, 615-628.
- Quinn, J. C., Molinek, M., Martynoga, B. S., Zaki, P. A., Faedo, A., Bulfone, A., Hevner, R. F., West, J. D. and Price, D. J.** (2007). Pax6 controls cerebral cortical cell number by regulating exit from the cell cycle and specifies cortical cell identity by a cell autonomous mechanism. *Dev. Biol.* **302**, 50-65.
- Sakurai, K. and Osumi, N.** (2008). The neurogenesis-controlling factor, Pax6, inhibits proliferation and promotes maturation in murine astrocytes. *J. Neurosci.* **28**, 4604-4612.
- Sansom, S. N., Griffiths, D. S., Faedo, A., Kleinjan, D. J., Ruan, Y., Smith, J., van Heyningen, V., Rubenstein, J. L. and Livesey, F. J.** (2009). The level of the transcription factor Pax6 is essential for controlling the balance between neural stem cell self-renewal and neurogenesis. *PLoS Genet.* **5**, e1000511.
- Satelli, A. and Rao, U. S.** (2011). Galectin-1 is silenced by promoter hypermethylation and its re-expression induces apoptosis in human colorectal cancer cells. *Cancer Lett.* **301**, 38-46.
- Scardigli, R., Bäumer, N., Gruss, P., Guillemot, F. and Le Roux, I.** (2003). Direct and concentration-dependent regulation of the proneural gene Neurogenin2 by Pax6. *Development* **130**, 3269-3281.
- Schmahl, W., Knoedlseder, M., Favor, J. and Davidson, D.** (1993). Defects of neuronal migration and the pathogenesis of cortical malformations are associated with Small eye (Sey) in the mouse, a point mutation at the Pax-6 locus. *Acta Neuropathol.* **86**, 126-135.
- Schuurmans, C., Armant, O., Nieto, M., Stenman, J. M., Britz, O., Klenin, N., Brown, C., Langevin, L. M., Seibt, J., Tang, H. et al.** (2004). Sequential phases of cortical specification involve Neurogenin-dependent and -independent pathways. *EMBO J.* **23**, 2892-2902.
- Sessa, A., Mao, C. A., Hadjantonakis, A. K., Klein, W. H. and Broccoli, V.** (2008). Tbr2 directs conversion of radial glia into basal precursors and guides neuronal amplification by indirect neurogenesis in the developing neocortex. *Neuron* **60**, 56-69.
- Shimazaki, T., Arsenijevic, Y., Ryan, A. K., Rosenfeld, M. G. and Weiss, S.** (1999). A role for the POU-III transcription factor Brn-4 in the regulation of striatal neuron precursor differentiation. *EMBO J.* **18**, 444-456.
- Singh, S., Stellrecht, C. M., Tang, H. K. and Saunders, G. F.** (2000). Modulation of Pax6 homeodomain function by the paired domain. *J. Biol. Chem.* **275**, 17306-17313.
- Sivak, J. M., West-Mays, J. A., Yee, A., Williams, T. and Fini, M. E.** (2004). Transcription factors Pax6 and AP-2alpha interact to coordinate corneal epithelial repair by controlling expression of matrix metalloproteinase gelatinase B. *Mol. Cell. Biol.* **24**, 245-257.
- Stoykova, A., Fritsch, R., Walther, C. and Gruss, P.** (1996). Forebrain patterning defects in Small eye mutant mice. *Development* **122**, 3453-3465.

- Stoykova, A., Götz, M., Gruss, P. and Price, J.** (1997). Pax6-dependent regulation of adhesive patterning, R-cadherin expression and boundary formation in developing forebrain. *Development* **124**, 3765-3777.
- Stoykova, A., Treichel, D., Hallonet, M. and Gruss, P.** (2000). Pax6 modulates the dorsoventral patterning of the mammalian telencephalon. *J. Neurosci.* **20**, 8042-8050.
- Thaung, C., West, K., Clark, B. J., McKie, L., Morgan, J. E., Arnold, K., Nolan, P. M., Peters, J., Hunter, A. J., Brown, S. D. M. et al.** (2002). Novel ENU-induced eye mutations in the mouse: models for human eye disease. *Hum. Mol. Genet.* **11**, 755-767.
- Theiler, K., Varnum, D. S. and Stevens, L. C.** (1978). Development of Dickie's small eye, a mutation in the house mouse. *Anat. Embryol.* **155**, 81-86.
- Toresson, H., Potter, S. S. and Campbell, K.** (2000). Genetic control of dorsal-ventral identity in the telencephalon: opposing roles for Pax6 and Gsh2. *Development* **127**, 4361-4371.
- Tuoc, T. C. and Stoykova, A.** (2008). Trim11 modulates the function of neurogenic transcription factor Pax6 through ubiquitin-proteosome system. *Genes Dev.* **22**, 1972-1986.
- Tuoc, T. C., Radyushkin, K., Tonchev, A. B., Piñon, M. C., Ashery-Padan, R., Molnár, Z., Davidoff, M. S. and Stoykova, A.** (2009). Selective cortical layering abnormalities and behavioral deficits in cortex-specific Pax6 knock-out mice. *J. Neurosci.* **29**, 8335-8349.
- Tzoulaki, I., White, I. M. and Hanson, I. M.** (2005). PAX6 mutations: genotype-phenotype correlations. *BMC Genet.* **6**, 27.
- Uribe, R. A. and Gross, J. M.** (2010). Id2a influences neuron and glia formation in the zebrafish retina by modulating retinoblast cell cycle kinetics. *Development* **137**, 3763-3774.
- van Heyningen, V. and Williamson, K. A.** (2002). PAX6 in sensory development. *Hum. Mol. Genet.* **11**, 1161-1167.
- von Holst, A., Egbers, U., Prochiantz, A. and Faissner, A.** (2007). Neural stem/progenitor cells express 20 tenascin C isoforms that are differentially regulated by Pax6. *J. Biol. Chem.* **282**, 9172-9181.
- Warren, N. and Price, D. J.** (1997). Roles of Pax-6 in murine diencephalic development. *Development* **124**, 1573-1582.
- Watabe, Y., Baba, Y., Nakauchi, H., Mizota, A. and Watanabe, S.** (2011). The role of Zic family zinc finger transcription factors in the proliferation and differentiation of retinal progenitor cells. *Biochem. Biophys. Res. Commun.* **415**, 42-47.
- Wolf, L. V., Yang, Y., Wang, J., Xie, Q., Braunerger, B., Tamm, E. R., Zavadil, J. and Čvekl, A.** (2009). Identification of pax6-dependent gene regulatory networks in the mouse lens. *PLoS ONE* **4**, e4159.
- Xie, Q. and Čvekl, A.** (2011). The orchestration of mammalian tissue morphogenesis through a series of coherent feed-forward loops. *J. Biol. Chem.* **286**, 43259-43271.
- Xie, Q., Yang, Y., Huang, J., Ninkovic, J., Walcher, T., Wolf, L., Vitzenzon, A., Zheng, D., Götz, M., Beebe, D. et al.** (2013). Pax6 interactions with chromatin and identification of its novel direct target genes in lens and forebrain. *PLoS ONE* **8**, e54507.
- Xu, H. E., Rould, M. A., Xu, W., Epstein, J. A., Maas, R. L. and Pabo, C. O.** (1999). Crystal structure of the human Pax6 paired domain-DNA complex reveals specific roles for the linker region and carboxy-terminal subdomain in DNA binding. *Genes Dev.* **13**, 1263-1275.
- Yamaguchi, Y., Sawada, J., Yamada, M., Handa, H. and Azuma, N.** (1997). Autoregulation of Pax6 transcriptional activation by two distinct DNA-binding subdomains of the paired domain. *Genes Cells* **2**, 255-261.
- Yun, K., Potter, S. and Rubenstein, J. L.** (2001). Gsh2 and Pax6 play complementary roles in dorsoventral patterning of the mammalian telencephalon. *Development* **128**, 193-205.
- Yun, K., Mantani, A., Garel, S., Rubenstein, J. and Israel, M. A.** (2004). Id4 regulates neural progenitor proliferation and differentiation in vivo. *Development* **131**, 5441-5448.
- Zaret, K. S. and Carroll, J. S.** (2011). Pioneer transcription factors: establishing competence for gene expression. *Genes Dev.* **25**, 2227-2241.

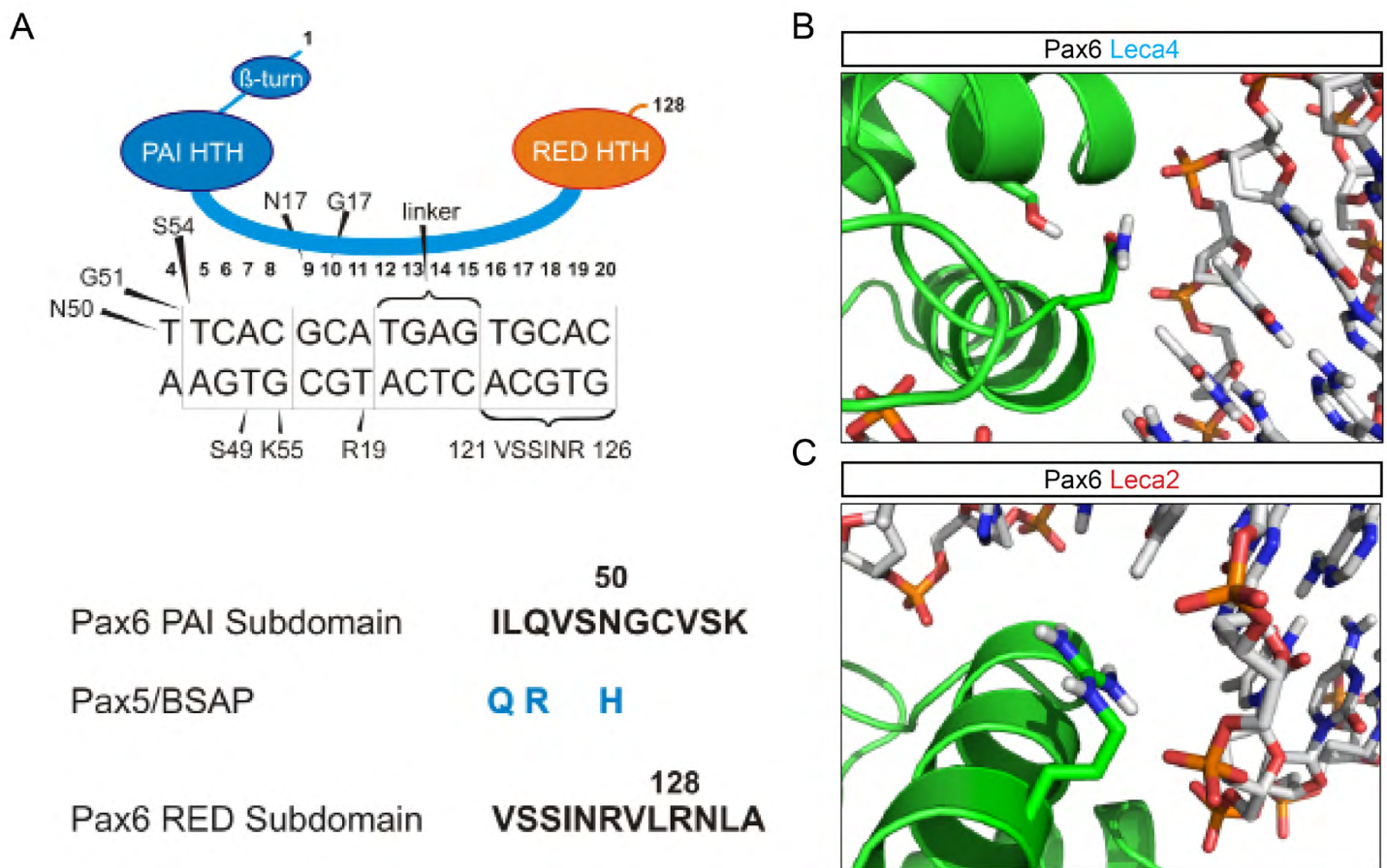


Fig. S1. Influence of Leca4 and Leca2 mutations on their respective subdomain binding properties. (A) The subdomain structure of Pax6 PD (Xu et al. 1999). N50 makes a direct contact with invariant T found in many Pax6 binding sites (Qie and Cvekl, 2011). R128 is a part of the RED subdomain (helix-turn-helix). The direct contacts between RED and DNA remain to be established (Xu et al. 1999). (B,C) Ribbon diagram depicting the 3D structure of the DNA-bound Pax6 paired domain (PDB-ID: 6PAX) with the amino acid affected by the Leca4 (B) or Leca2 (C) mutation shown with their side chains. *In silico* mutation and analysis of these residues suggest that Pax6^{Leca4} and Pax6^{Leca2} both have altered DNA-binding properties. Cartoon was made with the program Pymol (DeLano Scientific) and mutations were generated using the program Coot with standard rotamer library.

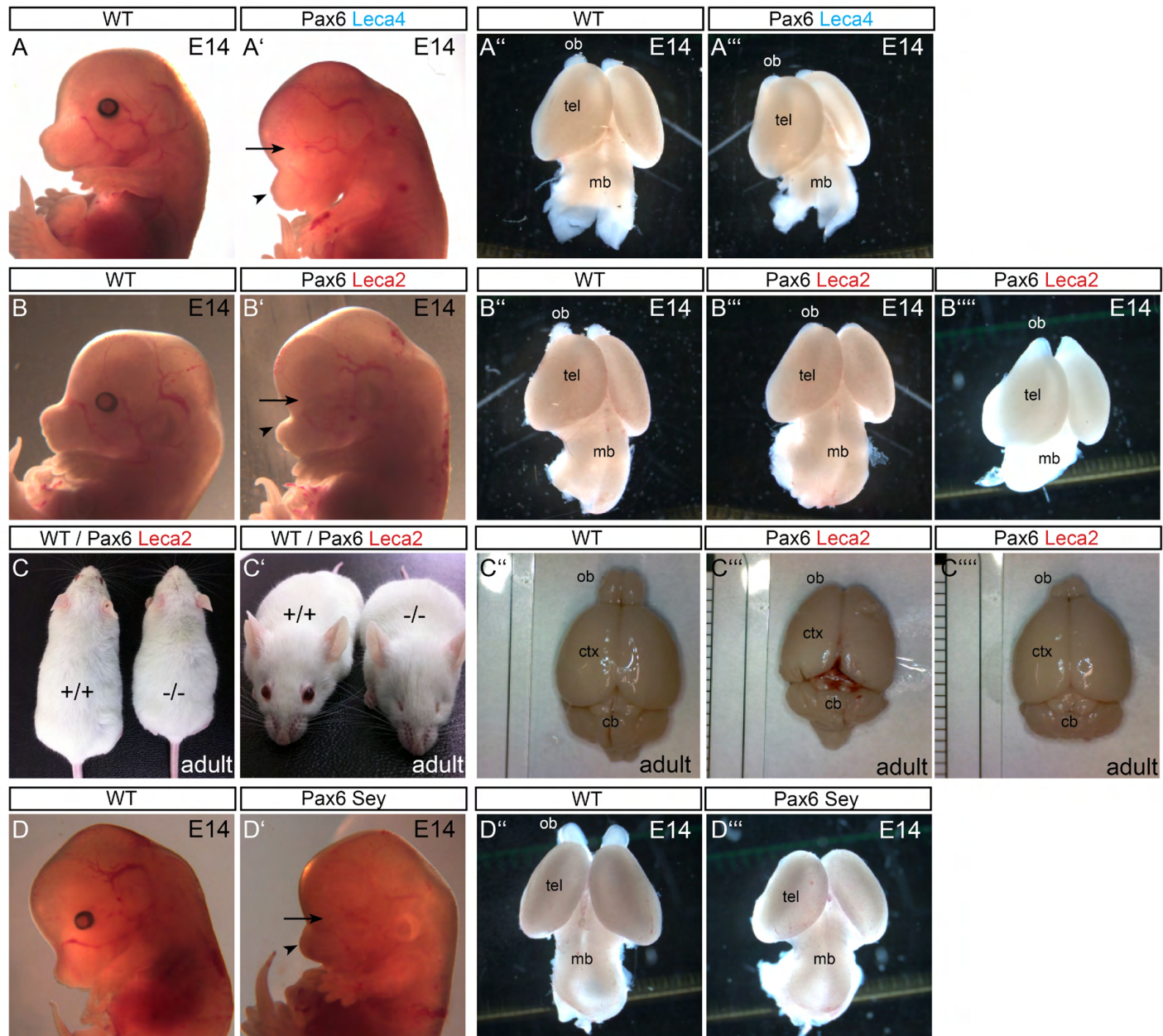


Fig. S2. Mice harboring a mutation in the PAI subdomain or in the RED subdomain of the paired DNA-binding domain of Pax6 display cross morphological defects in forebrain development. (A,A',B,B',D,D') E14 embryos of Pax6^{Leca4}, Pax6^{Leca2}, Pax6^{Sey} and control mice. Note the missing eye (arrow) and craniofacial abnormalities (arrowheads) in all three mutants. (A'',A''', B'',B''', B''''', D'',D''') E14 brains of Pax6^{Leca4}, Pax6^{Leca2}, Pax6^{Sey} and control mice. Note the reduction in olfactory bulb size in both Leca mutant mice and the complete absence in the Pax6^{Sey} mutant. Also note the different penetrance in the Pax6^{Leca2} mutant. Ob, olfactory bulb; tel, telencephalon; mb, midbrain. (C-C''') Eight-week-old adult Pax6^{Leca2} and control mice and brains. Again note the variable penetrance of olfactory bulb size in the Pax6^{Leca2} mutant.

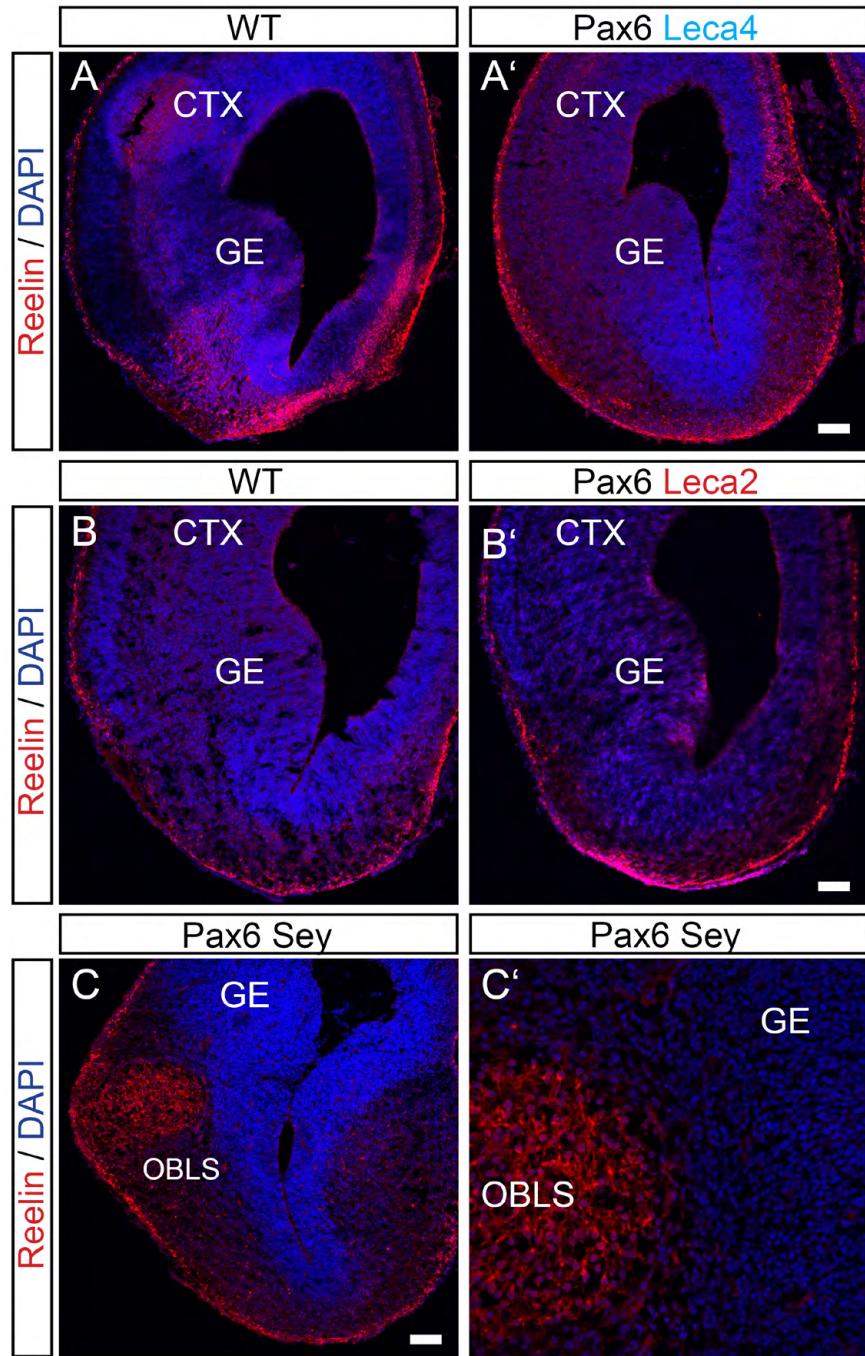


Fig. S3. Mice harboring a mutation in the PAI subdomain or in the RED subdomain of the Paired DNA-binding domain of Pax6 do not develop an OBLS. Immunofluorescence for reelin (red) combined with DAPI staining (blue) on coronal sections of E14 dorsal telencephalon of $\text{Pax6}^{\text{Leca4}}$ (A'), $\text{Pax6}^{\text{Leca2}}$ (B') and control mice (A,B). Note that no aberrant accumulation of reelin-positive cells is found in the ventral-lateral telencephalon of either of the Leca mutant mice, in contrast to the full Pax6 mutant (C,C'). CTX, cortex; GE, ganglionic eminence. Scale bars: 50 μm .

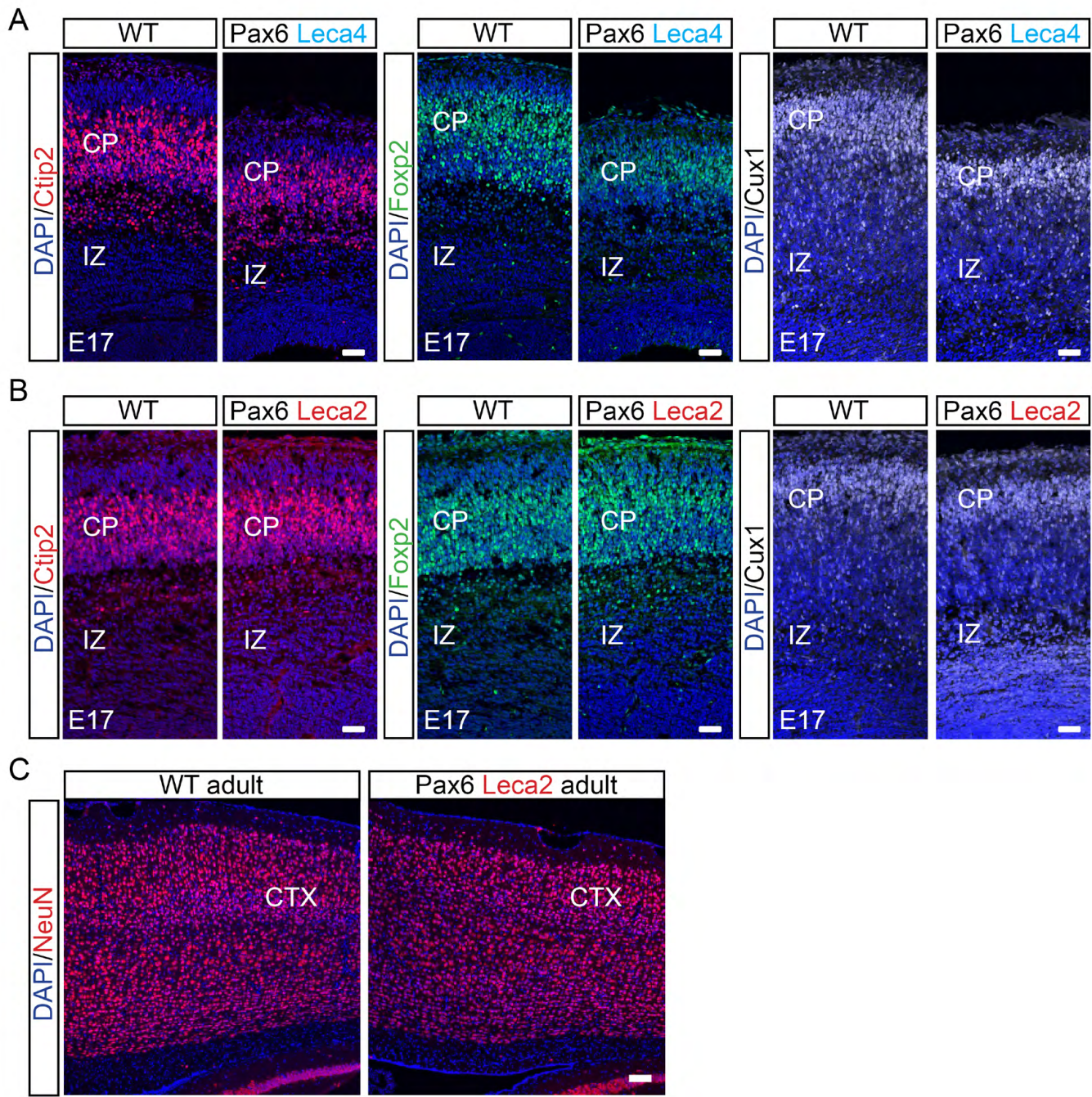


Fig. S4. Impaired neurogenesis in $\text{Pax6}^{\text{Leca4}}$ mice (PAI subdomain) but not in $\text{Pax6}^{\text{Leca2}}$ mice (RED subdomain).
(A,B) Immunofluorescence for Ctip2 (red), Foxp2 (green) or Cux1 (white) combined with DAPI staining (blue) on coronal sections of E17 dorsal telencephalon of $\text{Pax6}^{\text{Leca4}}$, $\text{Pax6}^{\text{Leca2}}$ and control mice. Note the reduced expression of all three neuronal laminar genes in the cortical plate of $\text{Pax6}^{\text{Leca4}}$ but not $\text{Pax6}^{\text{Leca2}}$ mice. **(C)** Immunofluorescence for NeuN (red) combined with DAPI staining (blue) on sagittal sections of the cortex of 8-week-old $\text{Pax6}^{\text{Leca2}}$ and control mice. CTX, cortex. Scale bars: 100 μm .

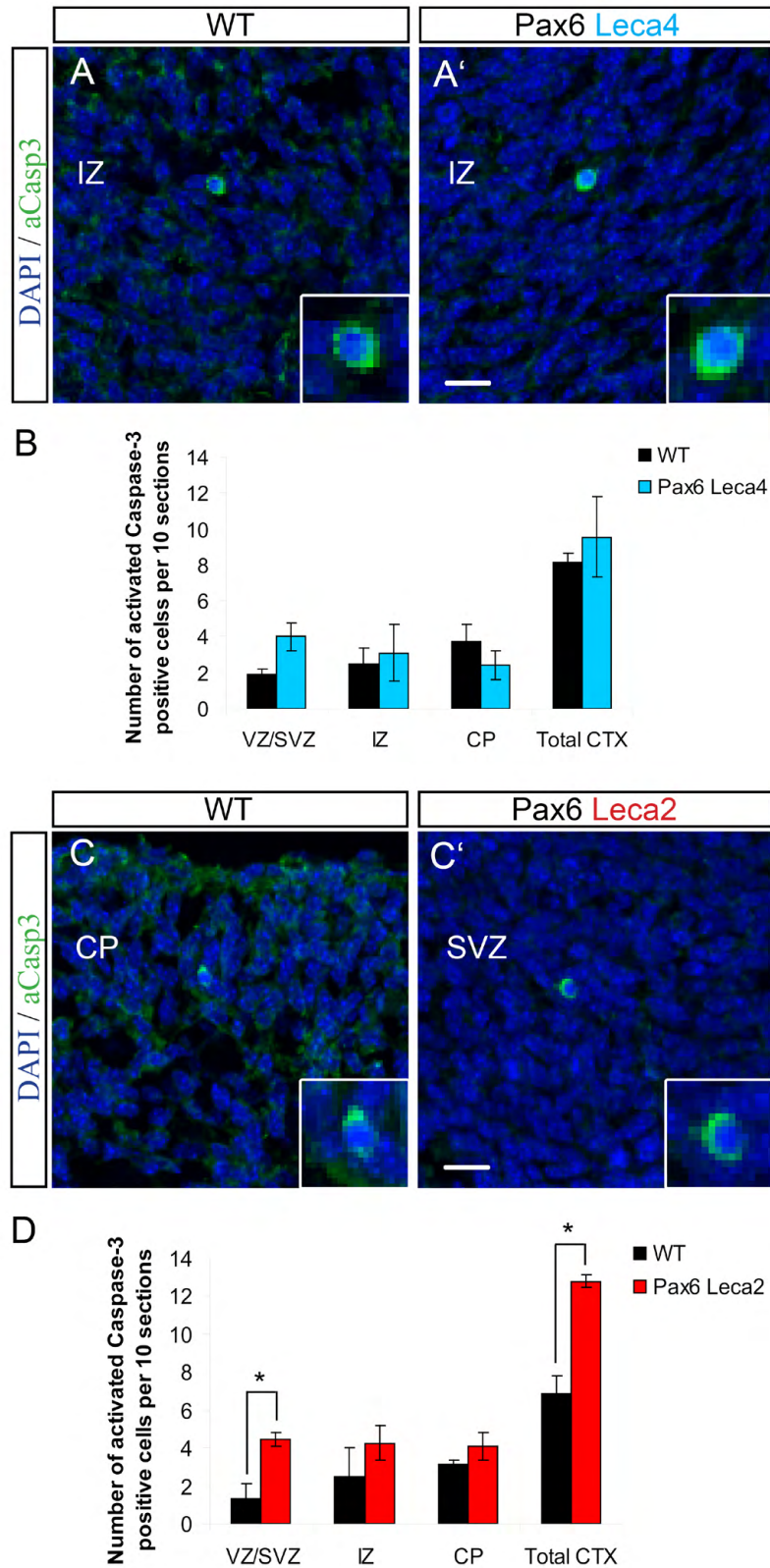


Fig. S5. Increased cell death in Pax6^{Leca2} mice (RED subdomain) but not in Pax6^{Leca4} mice (PAI subdomain). (A,A',C,C') Micrographs of E14 coronal telencephalic sections depicting cells immunoreactive for activated caspase 3 (green) in Pax6^{Leca4}, Pax6^{Leca2} and their WT littermates. (B,D) Histograms showing the number of activated caspase 3-positive cells per ten dorsal sections in Pax6^{Leca4}, Pax6^{Leca2} and their WT littermates at E14. Data are shown as total numbers per ten sections ± s.e.m.; n≥3 (embryos analyzed), average 15 sections per embryo; *P<0.05. Note the increase in apoptotic cells in the Pax6^{Leca2} but not Pax6^{Leca4} mutant. SVZ, subventricular zone; IZ, intermediate zone; CP, cortical plate. Scale bars: 10 µm.

Table S1. Antibodies for immunohistochemistry and immunocytochemistry analysis

Antibody	Species	Company	Dilution
Activated caspase 3	Rabbit	Millipore	1:100
Ctip2	Rat	Abcam	1:200
Cux1	Rabbit	Santa Cruz	1:200
Foxp2	Rabbit	Abcam	1:200
GFP	Chick	Aves Labs	1:1000
Gsx2 (Gsh2)	Rabbit	Kindly provided by K. Campbell, Division of Developmental Biology, Cincinnati Children's Hospital Medical Center, University of Cincinnati College of Medicine, Cincinnati, OH45229, USA	1:1000
Map2	Mouse IgG1	Sigma	1:200
Mash1	Mouse IgG1	Kindly provided by O. Raineteau, Brain Research Institute, University of Zürich/ETHZ, Zürich, Switzerland	1:150
NeuN	Mouse IgG1	Millipore	1:100
Olig2	Rabbit	Millipore	1:200
Pax6	Rabbit	Millipore	1:500
Pax6	Mouse IgG1	Developmental Studies Hybridoma Bank	1:50
Phosphohistone H3 (PH3)	Rabbit	Millipore	1:500
RC2 monoclonal antibody 'radial cell 2' (RC2, recognizing post- translational modifications of nestin in radial glia)	Mouse IgGM	Kindly provided by P. Leprince, Center for Cellular and Molecular Neuroscience, University of Liege, Liege, Belgium	1:200
Reelin E4	Mouse IgGM	Kindly provided by A. M. Goffinet, Universite Catholique de Louvain, Center for Neuroscience, DENE 7382, B1200 Brussels, Belgium	1:200
Tbr1	Rabbit	Abcam	1:200
Tbr2	Rabbit	Abcam	1:500

Table S2. Primer sets for RT-PCR analysis, qChIP-PCR analysis and in situ hybridization probe cloning

Gene	Forward primer	Reverse primer
RT-PCR		
<i>Adamts5</i>	AGTCATTGGGTCAAGCCCTGGC	AGCTGCAGTCATAGTCACACCC
<i>Ahnak</i>	GCTCTGAAGTGGTTCTGAGCGGG	CACTGTGATGGTGCAGCTCTGG
<i>Asb4</i>	CTGAGATCTGCTACCAGCT	CCATCGAATGTGTTCATAGGC
<i>Brn4</i> (<i>Pou3f4</i>)	GCAGGGAGTTCCCAGCAATGGG	GCCCAGTTGCAGATCTCGCGT
<i>Ccdc80</i>	AAGACTCCTCCTGATCACCACTCCC	CCACAGAGATCCTCCTGGTGGC
<i>Cdh8</i>	TCGCTACGACGACGAAGGAGGAG	TGGCAATCCCCACCGGGGTAAAA
<i>Col1a2</i>	GCTGCCACCATTGATAGTCT	CCAGAGTGGAACAGCGATT
<i>Cryab</i>	GGCACCCAGCTGGATTGACACC	TGAAGCCATGTTCGTCCTGGCG
<i>Cxcl12</i>	TGTGCCCTTCAGATTGTTGCACGGC	ACTGCCCTGCATCTCCCACGG
<i>Dmrt3</i>	AGACTAGAGCGGACTGAGCAGGC	GTGTCGCTTCGCGATACGCC
<i>Dmrt1</i>	ACTAGCTTCAGCCCAGTGCGC	TGCTTGCTAGGGAGGTGGGACG
<i>Eya4</i>	CCTACAGCCTGCCTGCCTACGA	GGTGCAAAGCTGGAACCTGGCA
<i>Fbln1</i>	GACGGCATGACTGTGGGTGTCG	CGTTCCGGTGGAAACTACGCC
<i>Fst</i>	TTCCAAGGTTGGCAGAGGTCGC	AGCAGGCAGCTCCTTCATGGC
<i>GLT-1</i> (<i>Slc1a2</i>)	ATGCTCATCCTCCCTTTATCATC	CTTTCTTGTCACTGTCTGAATCTG
<i>Hrk</i>	CCTTATTGGGGACACTTGAGGGC	GGGGTAGACAGACTCCCAGAGCC
<i>Id3</i>	TCCGCATCTCCCGATCCAGACAG	TCCCAGAGTCCCAGGGTCCCAA
<i>Id4</i>	GTTCACGAGCATTACCGTA	AAGGTTGGATTACGATTGC
<i>Igfbp5</i>	AAGAAGCTGACCCAGTCCAA	GAATCCTTGCAGGTACAGT
<i>Kif1b</i>	CAGCAGAGACTGGACGCCGGATT	ACTGCTGGGGAGGCCACACTTT
<i>Lgals1</i>	TCGGACGCCAAGAGCTTGTGC	GAAGGCAGGTTCCCGGTGTTCG
<i>Math3</i> (<i>NeuroD4</i>)	TTGAAGGAAAGGGATTGTAGAGA	GGGAGCCCTGGAGACTGATAG
<i>Meis1</i>	GGCATCAGAGCGCCAGGACCTA	CGGGCTACATACTCCCTGGCA

<i>Rlbp1</i> (<i>CRALBP</i>)	CCAAGAAAGAGCTGTCAGGGACGG	TTTGCTCTGCCCTGGTCTCTCCG
<i>Zic1</i>	CAACAGCAGCGACCGCAAGA	GGTGGGTGGCGTGGACGAC
<i>Zic3</i>	AGCGAGCAGTGAGGTTCGAGCC	ACTCAAGAGCGCGGAACCACGG
qChIP-PCR		
<i>Meis1</i>	AGGGCACATGCACACAAATA	TGCCTGCCCTACGTTATT
Outside peak region	ACTCTGCGCAAAGGTTCAT	GCCACCTAGACCGGTAACAA
<i>Eya4</i>	TCGCTTCCCTCCAGTGTCT	TCTCCCCACTTGTGTAAGC
Outside peak region	GGATGTGCAAGGTTGGTCTT	TCTCCTCCCCAATGTTCAAG
<i>Rlbp1</i>	TCCGACTTCTGTCCTGCT	AAGCCCCTGAAGTGGGTACT
Outside peak region	TAGGAATTCCCTCCATGCTG	CCGGGCTCTCTCCTAACT
<i>Zic1</i>	TCTCCTCCTCGATCCTCAA	CCAGGAAGATAAACCGCAAA
Outside peak region	ATTGAACCCACCTGACTGC	CGGTGGATTTCCACAGACT
Cloning of in situ hybridization probes		
<i>Hjurp</i>	TGGAGTCTATGGGTGGCAGGA	TTTCCCAGGCTCTGAGCAGGAC
<i>Id2</i>	CCCTCCCGGTCTCCTCCTACG	ACGCTCCACCTTGTGAAAAGGCA
<i>Id4</i>	CTCACCGCGCTAACACTGACC	AGCAAAAGCTCTGCAAGGGAGC
<i>Lgals1</i>	ATGGCCTGTGGTCTGGCGCC	AGTGGGACACTGGCTCACCC
<i>Zic1</i>	AAGCTCAACCCCAGTCGCACG	AGCTGGTGGTGGGTTGTCTGT

Table S3. Probe sets differentially expressed between WT and Pax6^{Leca4} cortices

Probe_set	Gene symbol or ID	Ratio, significant FDR<10%, ratio>1.4x, Av>50 (416)	Av Pax6 Leca4	Av WT	Pax6 Chip binding sites (Qing Xie, unpublished)
Upregulated probe sets (237)					
1434369_a_at	Cryab	8.89	255	29	cortex
1441778_at	Adcyap1	8.27	447	54	
1460412_at	Fbln7	7.47	348	47	lens
1457012_at	Dbx1	6.76	342	51	
1448326_a_at	Crabp1	6.19	796	129	
1434376_at	Cd44	6.04	243	40	cortex
1416455_a_at	Cryab	5.62	154	27	
1416953_at	Ctgf	5.41	430	79	lens
1423427_at	Adcyap1	5.28	1015	192	
1424131_at	Col6a3	5.15	490	95	
1442542_at	Eya4	5.03	776	154	lens
1445897_s_at	Ifi35	5.00	181	36	lens
1455931_at	Chrna3	4.98	333	67	
1452106_at	Nppt	4.23	347	82	
1418424_at	Tnfaip6	4.10	120	29	
1449393_at	LOC100046930	3.97	51	13	
1455439_a_at	Lgals1	3.96	1346	340	cortex, lens, pancreas
1452010_at	Chrna3	3.86	470	122	
1419573_a_at	Lgals1	3.84	1262	328	cortex, lens, pancreas
1456238_at	LOC668917	3.78	82	22	
1456665_at	Eya4	3.70	181	49	lens
1430700_a_at	Pla2g7	3.64	499	137	
1457008_at	Chrnb4	3.49	176	50	
1457048_at	Qrfpr	3.38	202	60	
1452107_s_at	Nppt	3.36	92	27	
1439795_at	Gpr64	3.27	88	27	lens
1451776_s_at	Hopx	3.26	2595	797	
1423760_at	Cd44	3.19	96	30	
1428662_a_at	Hopx	3.16	5099	1615	
1428891_at	Parm1	2.88	279	97	
1455451_at	Kctd14	2.86	153	54	

1460044_at	Onecut2	2.83	118	42	
1419633_at	Uncx	2.82	93	33	
1424404_at	0610040J01Rik	2.78	302	109	
1451415_at	1810011O10Rik	2.65	722	273	
1444980_at	Onecut2	2.59	70	27	
1424214_at	Parm1	2.57	111	43	
1449357_at	2310030G06Rik	2.55	130	51	
1438551_at	Neurog1	2.53	1491	590	cortex
1435595_at	1810011O10Rik	2.52	378	150	
1440564_at	Prokr2	2.50	399	160	
1453006_at	Fgfbp3	2.47	4461	1808	cortex
1454772_at	Snrnp200	2.43	402	166	
1436642_x_at	AW047730	2.40	1334	556	
1426622_a_a_t	Qpct	2.36	139	59	
1424127_at	Eya2	2.30	77	34	
1448713_at	Stat4	2.30	183	80	
1448162_at	Vcam1	2.28	1231	539	
1419215_at	Aox4	2.28	94	41	cortex
1424596_s_at	Lmcd1	2.25	584	259	
1451191_at	Crabp2	2.23	525	236	cortex
1423516_a_a_t	Nid2	2.23	256	115	
1417090_at	Rcn1	2.20	2041	927	pancreas, cortex
1416630_at	Id3	2.20	812	370	
1456509_at	1110032F04Rik	2.18	623	285	
1440374_at	Pde1c	2.14	554	258	cortex
1434449_at	Aqp4	2.13	77	36	
1437695_at	Prokr2	2.11	310	147	
1448390_a_a_t	Dhrs3	2.11	102	48	
1439774_at	Prrx1	2.08	156	75	
1415897_a_a_t	Mgst1	2.08	799	384	pancreas
1443998_at	Rassf2	2.06	65	32	cortex
1416776_at	Crym	2.04	489	239	
1432331_a_a_t	Prrx2	2.03	301	149	
1429856_at	Tspan18	2.01	102	51	
1448392_at	Sparc	1.99	1619	812	cortex
1440005_at	Onecut2	1.94	62	32	
1434572_at	Hdac9	1.93	570	295	
1436791_at	Wnt5a	1.93	414	215	lens
1425528_at	Prrx1	1.92	396	207	
1441499_at	Grid1	1.91	128	67	cortex

1420884_at	Sln	1.91	145	76	
1439483_at	Al506816	1.88	1170	621	
1450117_at	Tcf7l1	1.88	820	436	
1435363_at	Plekhg1	1.88	532	283	
1438571_at	Bub1	1.86	195	105	
1454985_at	Ambra1	1.85	956	516	lens
1437743_at	Aebp2	1.85	218	117	
1434070_at	Jag1	1.85	564	305	
1457587_at	Kcnq5	1.84	290	157	
1440323_at	Syt2	1.84	54	29	
1423306_at	2010002N04Rik	1.84	182	99	
1420418_at	Syt2	1.83	52	28	
1416589_at	Sparc	1.82	2095	1151	cortex
1424617_at	Ifi35	1.81	91	50	lens
1429896_at	5830408B19Rik	1.79	196	110	
1424176_a_a_t	Anxa4	1.79	85	48	
1439019_at	Fras1	1.79	228	127	
1428990_at	2310047K21Rik	1.77	262	148	
1425811_a_a_t	Csrp1	1.77	415	235	
1429284_at	Mobkl2b	1.76	564	320	lens
1424695_at	2010011I20Rik	1.76	1906	1082	
1437930_at	Glt25d2	1.74	153	88	lens
1421141_a_a_t	Foxp1	1.73	786	454	
1452065_at	Vstm2a	1.73	253	146	
1435622_at	Hs3st3a1	1.73	129	74	
1420919_at	Sgk3	1.72	187	109	pancreas, lens
1449145_a_a_t	Cav1	1.72	541	314	
1459151_x_at	Ifi35	1.71	112	65	lens
1417649_at	Cdkn1c	1.71	4180	2445	
1424659_at	Slit2	1.71	481	281	
1455123_at	St18	1.71	1481	867	
1449084_s_at	Sh3d19	1.71	423	248	
1423718_at	Ak3	1.70	730	429	
1440290_at	Gm10010	1.70	74	43	
1436590_at	Ppp1r3b	1.70	87	51	
1460248_at	Cpxm2	1.69	86	51	
1455512_at	Shisa6	1.69	172	102	
1421223_a_a_t	Anxa4	1.69	177	105	
1442434_at	D8Ert82e	1.68	1705	1012	
1426642_at	Fn1	1.68	1058	631	
1454728_s_at	Atp8a1	1.67	660	394	cortex

1447992_s_at	Pcsk2	1.67	123	74	
1435828_at	Maf	1.67	295	177	
1440445_at	Pax6os1	1.67	95	57	
1422824_s_at	Eps8	1.66	260	156	
1427256_at	Vcan	1.66	2012	1212	
1435092_at	Arl4a	1.66	171	103	
1422823_at	Eps8	1.66	228	137	
1452217_at	Ahnak	1.66	153	92	cortex
1435208_at	Dtx3l	1.66	308	186	
1423717_at	Ak3	1.65	2128	1287	
1416897_at	Parp9	1.65	235	143	
1451450_at	2010011I20Rik	1.65	3520	2133	
1424694_at	2010011I20Rik	1.65	2445	1484	
1454984_at	Lifr	1.65	246	149	pancreas
1459702_at	1459702_at	1.64	86	52	
1447849_s_at	Maf	1.64	502	306	
1435222_at	Foxp1	1.64	1892	1155	
1421597_a_a_t	Msx3	1.64	130	80	
1424097_at	Elovl7	1.63	76	47	
1433827_at	Atp8a1	1.62	664	409	cortex
1434141_at	Gucy1a3	1.61	1145	711	
1455500_at	Rnf213	1.61	205	127	
1435070_at	Aebp2	1.61	471	292	
1417195_at	Wwc2	1.61	228	142	
1421694_a_a_t	Vcan	1.60	285	178	
1421142_s_at	Foxp1	1.60	636	398	
1451321_a_a_t	Rbm43	1.59	213	134	
1425526_a_a_t	Prrx1	1.59	130	82	
1426774_at	Parp12	1.58	113	71	
1427912_at	Cbr3	1.58	91	58	
1436346_at	Cd109	1.57	98	62	
1434666_at	LOC100048247	1.57	787	500	
1433617_s_at	B4galt5	1.57	1496	954	
1452008_at	Ttc39b	1.57	734	468	
1451440_at	Chodl	1.57	123	78	
1416498_at	Ppic	1.57	547	349	
1417196_s_at	Wwc2	1.56	198	127	
1420918_at	Sgk3	1.56	118	76	pancreas, lens
1450673_at	Col9a2	1.56	52	34	
1417694_at	Gab1	1.56	2388	1534	pancreas
1429830_a_a_t	Cd59a	1.56	121	78	

1437782_at	Cntnap2	1.55	457	294	
1429270_a_at	Syce2	1.55	1868	1207	
1429987_at	9930013L23Rik	1.55	298	193	
1449314_at	Zfpm2	1.55	2060	1332	
1440691_at	Cyp2j6	1.54	80	52	
1441972_at	6230424C14Rik	1.54	175	114	
1428804_at	Mfap3l	1.54	219	142	
1425810_a_at	Csrp1	1.53	214	140	
1451119_a_at	Fbln1	1.53	867	566	cortex
1435297_at	Gjd2	1.53	220	143	
1439874_at	9330102E08Rik	1.53	146	96	
1449773_s_at	Gadd45b	1.53	93	61	
1437927_at	Dlg2	1.53	544	356	
1460409_at	Cpt1a	1.52	830	544	
1452331_s_at	Qser1	1.52	1012	665	
1440192_at	Ttc39b	1.52	327	215	
1441657_at	1441657_at	1.52	328	216	
1456060_at	Maf	1.51	1066	706	
1417932_at	Il18	1.51	609	404	
1421811_at	LOC640441	1.50	485	322	
1420534_at	Gucy1a3	1.50	69	46	
1434866_x_at	Cpt1a	1.50	141	94	
1420500_at	Dnajc1	1.49	542	363	
1425974_a_at	Trim25	1.49	172	115	
1450971_at	Gadd45b	1.49	164	110	
1420984_at	Pctp	1.48	85	57	
1439825_at	Dtx3l	1.48	235	158	
1440355_at	Kctd12b	1.48	169	114	
1457157_at	Plch1	1.48	313	212	
1449933_a_at	Tsen15	1.48	1418	959	cortex
1453070_at	Pcdh17	1.47	415	282	
1431429_a_at	Arl4a	1.47	382	260	
1453795_at	Fahd2a	1.47	605	411	
1446179_at	1446179_at	1.47	411	280	
1417693_a_at	Gab1	1.46	1375	941	pancreas
1424191_a_at	Tmem41a	1.46	1837	1257	
1441053_at	ENSMUSG00000037740	1.46	155	106	
1416579_a_at	Epcam	1.46	82	56	

1437404_at	Mast4	1.46	170	117	
1451693_a_at	Fgf12	1.46	398	274	cortex
1433942_at	Myo6	1.45	261	179	
1438796_at	Nr4a3	1.45	1925	1324	
1435262_at	Pign	1.45	386	266	
1435596_at	Pion	1.45	264	182	
1455242_at	Foxp1	1.45	1448	1002	
1450036_at	Sgk3	1.44	278	192	pancreas, lens
1440454_at	Pion	1.44	87	60	
1450716_at	Adamts1	1.44	354	245	lens
1419367_at	Decr1	1.44	803	557	
1419493_a_at	Tpd52	1.44	715	497	
1427369_at	Nlrp6	1.44	69	48	cortex
1419093_at	Tdo2	1.44	53	37	pancreas
1455182_at	Kif1b	1.43	1194	832	pancreas, lens
1449401_at	C1qc	1.43	165	115	
1423258_at	Syt9	1.43	244	170	cortex
1455324_at	Plcx2d2	1.43	4521	3156	
1450241_a_at	Evi2a	1.43	80	56	
1417381_at	C1qa	1.43	253	177	
1435751_at	Abcc9	1.43	89	62	
1437442_at	Pcdh7	1.43	363	254	cortex
1420831_at	Qsox1	1.43	197	138	
1426440_at	Dhrs7	1.43	273	191	
1451046_at	LOC100047651	1.43	117	82	
1433501_at	Ctso	1.43	259	182	cortex
1449167_at	Epb4.1l4a	1.43	189	133	lens
1433643_at	Cacna2d1	1.43	2754	1932	lens
1449876_at	Prkg1	1.42	51	36	
1417130_s_at	Angptl4	1.42	166	116	cortex
1423596_at	Nek6	1.42	1593	1120	
1440527_at	1440527_at	1.42	461	325	
1418135_at	Aff1	1.42	250	176	
1417625_s_at	Cxcr7	1.42	1968	1388	
1416441_at	Pgcp	1.42	66	46	
1435285_at	Mpped2	1.42	4871	3438	
1429089_s_at	2900026A02Rik	1.42	1140	805	
1434775_at	Pard3	1.41	1011	715	lens
1435841_s_at	Suclg2	1.41	1065	753	
1417667_a_at	Pter	1.41	230	162	pancreas
1454656_at	Spata13	1.41	888	629	
1420981_a_a	Lmo4	1.41	2916	2065	lens

t						
1425669_at	Mobkl2b	1.41	103	73	lens	
1426581_at	Ptpmt1	1.41	836	594		
1436404_at	Tlcd1	1.41	108	76		
1457651_x_at	Rem2	1.41	217	154		
Down-regulated probe sets (179)						
1426037_a_a_t	Rgs16	0.70	372	528		
1428729_at	Krit1	0.70	108	154		
1449374_at	Pipox	0.70	102	144		
1438769_a_a_t	Thyn1	0.70	364	519		
1450936_a_a_t	Dnase1l2	0.70	54	77		
1455748_at	Dynlt1d	0.70	119	170		
1449420_at	Pde1b	0.70	1305	1861		
1427535_s_at	Obsl1	0.70	285	407	cortex	
1451657_a_a_t	Enox2	0.70	46	66		
1421262_at	Lipg	0.70	308	440		
1425766_x_at	Gm6354	0.70	39	55		
1437650_at	C730026J16	0.70	224	321		
1420764_at	Scrg1	0.70	91	131		
1457243_at	Tmem219	0.70	58	83		
1423367_at	Wnt7a	0.70	515	739		
1448406_at	Eid1	0.69	2078	2990		
1456759_at	Lrrc4c	0.69	196	282	cortex	
1450188_s_at	Lipg	0.69	166	239		
1436913_at	Cdc14a	0.69	133	192		
1453060_at	Rgs8	0.69	238	344		
1427293_a_a_t	Auts2	0.69	494	715		
1442353_at	Itpa	0.69	38	55		
1442800_x_at	Fam181b	0.69	96	140		
1429653_at	Gse1	0.69	90	132		
1439248_at	Rmi1	0.69	39	57	cortex	
1451991_at	Epha7	0.69	362	528		
1455557_at	LOC553095	0.69	833	1215		
1421835_at	Mtap7	0.68	40	58		
1441690_at	Cdh8	0.68	54	79	lens	
1416934_at	Mtm1	0.68	70	102		
1440443_at	E030016H06Rik	0.68	59	87		
1440108_at	Foxp2	0.68	268	395		
1426641_at	Trib2	0.68	41	61		
1422596_at	Nkain4	0.68	451	667		

1427271_at	Zbtb44	0.68	199	294	
1438231_at	Foxp2	0.67	338	502	
1458704_at	1458704_at	0.67	47	70	
1418495_at	Zc3h8	0.67	236	351	cortex
1420838_at	Ntrk2	0.67	413	615	lens
1440996_at	1440996_at	0.67	70	104	
1448943_at	Nrp1	0.67	1369	2046	
1457836_at	Mfsd11	0.67	71	106	pancreas
1418153_at	Lama1	0.67	62	93	lens
1444679_at	Phf21a	0.67	126	189	
1440770_at	Bcl2	0.67	36	54	cortex, lens
1428571_at	Col9a1	0.66	111	167	
1438232_at	Foxp2	0.66	544	826	
1425574_at	Epha3	0.66	280	427	
1450650_at	Myo10	0.65	272	417	
1453787_at	Tmx4	0.65	84	130	
1429360_at	Klf3	0.65	519	799	
1445443_at	1445443_at	0.65	79	122	
1436371_at	Recql	0.65	73	112	
1444424_at	1444424_at	0.65	40	61	
1450181_at	Cux2	0.65	249	385	cortex
1426340_at	Slc1a3	0.65	256	396	
1452114_s_at	Igfbp5	0.64	414	643	
1452731_x_at	100041874	0.64	841	1308	
1446321_at	B230208B08Rik	0.64	99	154	
1436854_at	Trpc2	0.64	94	147	
1458023_at	Gpkow	0.64	58	91	cortex
1456533_at	Dpy19l1	0.64	769	1200	
1444510_at	1444510_at	0.64	73	114	
1429345_at	Tubgcp4	0.64	67	105	
1436578_at	Ermn	0.64	37	59	
1421970_a_at	Gria2	0.64	2067	3247	cortex
1448977_at	Tcfap2c	0.63	326	514	
1448944_at	Nrp1	0.63	846	1337	
1450930_at	Hpca	0.63	290	458	cortex
1456901_at	Adamts20	0.63	142	225	lens
1428301_at	100041874	0.63	2313	3678	
1419291_x_at	Gas5	0.62	4712	7550	
1458408_at	Samd8	0.62	103	165	
1455044_at	Tmem44	0.62	387	625	
1456397_at	Cdh4	0.62	1096	1770	
1454720_at	Apba3	0.62	59	95	
1421836_at	Mtap7	0.62	151	244	

1437677_at	ENSMUSG00000030316	0.62	101	164	
1420799_at	Ntsr1	0.61	142	232	
1421604_a_at	Klf3	0.61	185	303	
1444104_at	1444104_at	0.61	31	51	
1426526_s_at	Ovgp1	0.61	89	147	
1457318_at	A330008L17Rik	0.61	84	138	
1435770_at	Tmx4	0.61	69	113	
1456138_at	Lypd6	0.61	105	173	
1450047_at	Hs6st2	0.60	1038	1716	cortex, lens
1417133_at	Pmp22	0.60	144	238	cortex, lens
1435494_s_at	Dsp	0.60	62	103	lens
1454768_at	Kcnf1	0.60	42	70	
1438296_at	Gm14462	0.60	144	239	
1421999_at	Tshr	0.60	38	63	
1439200_x_at	1439200_x_at	0.60	1521	2543	
1441136_at	1441136_at	0.60	41	69	
1450512_at	Ntn4	0.60	49	82	lens
1416846_a_at	Pdzrn3	0.59	989	1666	
1426341_at	Slc1a3	0.59	149	254	
1454969_at	Lypd6	0.59	458	779	lens
1425833_a_at	Hpca	0.59	59	101	cortex
1420660_at	Lrrc6	0.59	42	72	
1442019_at	1442019_at	0.59	106	180	
1419034_at	Csnk2a1	0.58	722	1235	
1444500_at	Ahsa1	0.58	85	146	
1452031_at	Slc1a3	0.58	351	604	
1456495_s_at	Osbpl6	0.58	53	91	
1431056_a_at	Lpl	0.58	172	297	
1449422_at	Cdh4	0.58	758	1309	
1452386_at	Sall3	0.58	237	411	
1415904_at	Lpl	0.57	1694	2951	
1457843_at	Lypd6	0.57	97	169	lens
1422164_at	Pou3f4	0.57	115	201	
1436010_at	Lrrc16b	0.57	546	966	
1456903_at	Ptx3	0.56	30	53	
1455636_at	Lsamp	0.56	74	131	cortex
1431057_a_at	Prss23	0.56	32	57	cortex
1453596_at	Id2	0.56	67	120	pancreas, lens
1418984_at	Inadl	0.56	125	224	
1416448_at	Itpa	0.56	672	1205	

1452728_at	Kirrel3	0.56	141	254
1422428_at	Acsbg1	0.55	119	215
1449865_at	Sema3a	0.55	100	182
1442300_at	Tshr	0.55	47	84
1449848_at	Gna14	0.55	76	138
1422573_at	Ampd3	0.54	36	66 cortex
1450990_at	Gpc3	0.54	80	147
1417520_at	Nfe2l3	0.53	267	499
1415824_at	Scd2	0.53	852	1602 pancreas
1448754_at	Rbp1	0.53	934	1766 lens
1420938_at	Hs6st2	0.53	50	95 cortex, lens
1435196_at	Ntrk2	0.53	91	173 lens
1418983_at	Inadl	0.52	87	166
1453595_at	2900064B18Rik	0.52	48	93
1440273_at	1440273_at	0.50	167	332
1421937_at	Dapp1	0.50	91	182
1458112_at	Adarb2	0.50	29	57
1417312_at	Dkk3	0.50	51	103
1433989_at	Slc6a11	0.50	53	107
1444543_at	1444543_at	0.49	350	713
1429621_at	Cand2	0.49	289	592
1448842_at	Cdo1	0.48	502	1043 cortex
1456970_at	1456970_at	0.48	73	152
1455056_at	Lmo7	0.47	179	377
1453245_at	9130024F11Rik	0.47	140	298
1418376_at	Fgf15	0.46	32	69
1438842_at	Mtch2	0.46	77	167 cortex, lens
1426584_a_at	Sord	0.46	105	229
1418310_a_at	Rlbp1	0.46	665	1447 cortex
1455271_at	Gm13889	0.45	513	1127
1415964_at	Scd1	0.45	123	273
1449859_at	Golt1b	0.44	337	757 cortex, lens
1439870_at	A330008L17Rik	0.44	28	65
1457151_at	ENSMUSG00000086495	0.44	30	69
1419033_at	2610018G03Rik	0.44	71	162
1441648_at	C1qtnf4	0.44	120	276
1455365_at	Cdh8	0.43	58	133 lens
1422052_at	Cdh8	0.43	106	244 lens
1423478_at	Prkcb	0.43	88	203
1449444_a_at	LOC100048499	0.43	436	1007
1422165_at	Pou3f4	0.43	81	191
1460419_a_a	Prkcb	0.42	443	1046

t					
1453465_x_at	Gm14057	0.42	70	166	
1424186_at	Ccdc80	0.41	110	267	cortex
1438824_at	Slc20a1	0.41	67	161	
1426063_a_a_t	Gem	0.41	43	106	
1416342_at	Tnc	0.40	182	452	cortex
1447640_s_at	Pbx3	0.39	329	839	
1439794_at	Ntn4	0.39	191	495	lens
1431491_at	9430087N24Rik	0.37	132	355	
1460045_at	Cdh7	0.36	30	84	
1425443_at	Tcfap2d	0.33	30	90	
1436222_at	Gas5	0.32	269	834	
1424843_a_a_t	Gas5	0.32	314	975	
1424400_a_a_t	Aldh1l1	0.30	73	239	
1418666_at	Ptx3	0.27	265	993	
1450992_a_a_t	Meis1	0.24	50	209	
1441579_at	Dmrt1	0.22	49	220	
1432088_at	Veph1	0.19	23	124	
1449445_x_at	Mfap1a	0.12	216	1747	
1428114_at	Slc14a1	0.12	14	116	
1419370_a_a_t	Mfap1a	0.03	31	908	

Table S4. Probe sets differentially expressed between WT and Pax6^{Leca2} cortices

Probe_set	Gene symbol or ID	Significant FDR<10% ratio>1.4 (0.71)x (94)	Av Pax6 Leca2	Av WT	Pax6 Chip binding sites (Qing Xie, unpublished)
Upregulated probe sets (35)					
1433919_at	Asb4	3.54	255	72	cortex
1423422_at	Asb4	3.19	158	50	cortex
1440049_at	1440049_at	2.77	55	20	
1438194_at	Slc1a2	2.66	827	312	cortex
1438571_at	Bub1	2.53	185	73	
1454112_a_at	Haus2	2.41	291	121	
1454772_at	Snrnp200	2.25	533	237	
1434278_at	Mtm1	2.24	1804	806	
1428077_at	LOC100047091	1.95	490	251	
1419271_at	Pax6	1.90	4536	2386	cortex
1438737_at	Zic3	1.90	414	218	lens
1439627_at	Zic1	1.87	1758	941	pancreas
1452526_a_at	Pax6	1.81	506	279	cortex
1439854_at	Hrk	1.80	382	212	cortex
1428990_at	2310047K21Rik	1.74	226	130	
1433707_at	Gabra4	1.74	239	137	
1444139_at	Ddit4l	1.73	210	122	
1433685_a_at	6430706D22Rik	1.71	1914	1118	
1449571_at	Trhr	1.68	162	96	
1456005_a_at	Bcl2l11	1.67	912	546	lens
1437086_at	Ascl1	1.63	680	417	
1419719_at	Gabrb1	1.61	195	121	
1456006_at	Bcl2l11	1.61	121	75	lens
1439332_at	Ddit4l	1.61	189	117	
1416232_at	Olig2	1.59	156	98	
1458076_at	1458076_at	1.57	106	68	
1435449_at	Bcl2l11	1.56	135	87	lens
1432509_at	5033430I15Rik	1.54	210	136	
1457260_at	5730409E04Rik	1.54	54	35	
1419123_a_at	Pdgfc	1.52	637	419	
1450857_a_at	Col1a2	1.51	112	74	
1447628_x_at	Mrps5	1.50	143	95	lens
1448194_a_at	H19	1.48	1115	754	
1430798_x_at	Mrpl15	1.46	377	258	pancreas
1434327_at	2610020H08Rik	1.40	62	44	

Down-regulated probe sets (59)					
1423478_at	Prkcb	0.71	152	213	
1421836_at	Mtap7	0.71	132	186	
1453372_at	Dnajc1	0.70	121	171	
1435292_at	Tbc1d4	0.70	167	238	
1422243_at	Fgf7	0.70	37	52	
1418172_at	Hebp1	0.70	123	177	lens
1435246_at	Paqr8	0.69	173	251	
1442312_at	Tbl1xr1	0.69	49	71	cortex, lens
1417986_at	Nrarp	0.68	532	779	
1423259_at	Id4	0.68	6594	9739	cortex
1428580_at	Blvra	0.67	275	408	
1420501_at	Dnajc1	0.67	217	322	
1417574_at	Cxcl12	0.67	58	87	
1417872_at	Fhl1	0.67	1617	2423	cortex
1429273_at	Bmper	0.67	286	429	
1433782_at	Cldn12	0.67	212	319	cortex, pancreas
1421365_at	Fst	0.66	97	147	cortex
1450928_at	LOC100045546	0.66	3797	5732	
1448507_at	Efh1	0.66	35	53	
1425474_a_at	Vps39	0.65	132	202	
1456543_at	Prokr1	0.65	90	138	
1434025_at	1434025_at	0.65	73	113	
1451461_a_at	Aldoc	0.64	5210	8093	
1439661_at	Slc16a14	0.64	254	397	
1437774_at	ENSMUSG0000008543 8	0.63	312	493	
1420500_at	Dnajc1	0.63	253	403	
1452398_at	Plce1	0.62	417	670	
1430629_at	Slc16a14	0.62	170	276	
1455298_at	1455298_at	0.60	485	810	
1428958_at	Paqr8	0.60	435	728	
1418157_at	LOC100046044	0.60	1197	2006	
1420459_at	Ripply3	0.59	65	110	lens
1421999_at	Tshr	0.59	45	76	
1423260_at	Id4	0.58	1352	2312	cortex
1438428_at	Jph1	0.58	124	214	
1426501_a_at	Tifa	0.57	179	317	
1444468_at	Paqr8	0.56	203	365	
1460607_at	Igsf11	0.55	113	205	
1450990_at	Gpc3	0.53	69	130	
1437872_at	Napepld	0.53	109	204	
1424186_at	Ccdc80	0.51	127	252	cortex

1453465_x_at	Gm14057	0.50	70	141	
1421937_at	Dapp1	0.49	81	165	
1449581_at	Emid1	0.49	215	443	
1429308_at	Prdm16	0.47	67	143	
1437095_at	Tspan18	0.44	81	185	
1440707_at	Dmrt3	0.42	190	449	
1452114_s_at	Igfbp5	0.41	278	671	
1438405_at	Fgf7	0.41	25	61	
1455056_at	Lmo7	0.39	130	338	
1438551_at	Neurog1	0.38	202	539	
1448823_at	Cxcl12	0.37	227	610	
1436694_s_at	Neurod4	0.36	99	277	cortex
1420385_at	Gna14	0.36	20	56	
1418054_at	Neurod4	0.28	64	225	cortex
1449848_at	Gna14	0.26	39	146	
1428114_at	Slc14a1	0.25	12	46	
1434202_a_at	Fam107a	0.24	24	102	
1418310_a_at	Rlbp1	0.12	122	1059	cortex

Table S5. Probe sets differentially expressed between WT and Pax6^{Sey} cortices

Probe_set	Gene symbol or ID	Ratio, significant FDR<10%, Av>50. ratio>1.4x (1898)	Av Pax6 Sey	Av WT
Upregulated probe sets (1032)				
1427263_at	Xist	79.91	2389	30
1427262_at	Xist	45.04	521	12
1438799_at	Dlx6os1	23.27	1830	79
1449470_at	Dlx1	14.58	5498	377
1448877_at	Dlx2	13.85	3110	225
1449863_a_at	Dlx5	13.58	1397	103
1437079_at	Slc18a2	12.92	253	20
1433919_at	Asb4	12.29	579	47
1421601_at	Gsx2	8.99	500	56
1452507_at	Dlx6	8.06	282	35
1423824_at	Wls	7.96	419	53
1423422_at	Asb4	7.94	324	41
1419633_at	Uncx	7.74	147	19
1440519_at	Sp8	7.38	1225	166
1457396_at	LOC100045013	6.60	553	84
1416232_at	Olig2	6.47	286	44
1425425_a_at	Wif1	6.45	68	11
1448326_a_at	Crabp1	5.69	527	93
1450164_at	Ascl1	5.54	1199	216
1437086_at	Ascl1	5.40	2015	373
1423825_at	Wls	5.35	373	70
1437434_a_at	Wls	5.34	251	47
1439066_at	Angpt1	5.29	323	61
1433578_at	Gm5868	5.16	70	14
1420337_at	Gbx2	5.05	98	20
1447640_s_at	Pbx3	5.03	3010	599
1421193_a_at	Pbx3	4.99	1042	209
1437894_at	Prox1	4.76	111	23
1421978_at	Gad2	4.73	359	76
1450684_at	Etv1	4.69	747	159
1445314_at	Etv1	4.66	77	17
1452892_at	Stk33	4.63	105	23
1416561_at	Gad1	4.17	1605	385
1422165_at	Pou3f4	4.08	636	156
1422164_at	Pou3f4	4.06	1051	259
1424303_at	Depdc7	4.05	221	55

1431915_at	4930442E04Rik	3.94	165	42
1422607_at	Etv1	3.92	2221	566
1419424_at	Ptf1a	3.86	157	41
1440049_at	1440049_at	3.77	93	25
1433788_at	Nrxn3	3.74	838	224
1441313_x_at	Lhx9	3.69	134	36
1451972_at	Glcci1	3.61	1509	419
1456781_at	1456781_at	3.59	129	36
1422756_at	Slc32a1	3.56	379	106
1438193_at	Nrxn3	3.48	267	77
1429589_at	Gad2	3.46	539	156
1451191_at	Crabp2	3.40	424	125
1440902_at	Ermn	3.40	71	21
1460587_at	Sox2ot	3.39	768	227
1416630_at	Id3	3.36	1148	341
1427233_at	Tshz1	3.34	3207	960
1418743_a_at	LOC100047138	3.32	272	82
1419324_at	Lhx9	3.29	625	190
1444510_at	1444510_at	3.28	224	68
1424127_at	Eya2	3.28	89	27
1421597_a_at	Msx3	3.26	245	75
1449885_at	Tmem47	3.26	168	51
1436279_at	Slc26a7	3.24	114	35
1439906_at	1439906_at	3.23	840	260
1456137_at	Nrxn3	3.20	346	108
1441316_at	Wnt8b	3.17	576	182
1427232_at	Tshz1	3.16	1404	444
1420720_at	LOC100044234	3.14	194	62
1426218_at	Glcci1	3.10	1937	625
1419845_at	Dlx1as	3.10	2138	690
1449939_s_at	Dlk1	2.99	225	75
1455790_at	E2f2	2.98	163	55
1440000_at	E330013P04Rik	2.97	405	136
1445681_at	Cdca7	2.95	124	42
1428692_at	Hddc3	2.95	493	167
1450723_at	Isl1	2.92	56	19
1429905_at	Lhx9	2.91	545	187
1434432_at	Rffl	2.85	929	327
1428069_at	Cdca7	2.84	2743	966
1438737_at	Zic3	2.83	464	164
1424214_at	Parm1	2.83	115	41
1439774_at	Prrx1	2.82	96	34
1460006_at	Zfhx3	2.82	99	35
1450194_a_at	Myb	2.80	256	91

1428891_at	Parm1	2.76	241	88
1425528_at	Prrx1	2.75	296	107
1420514_at	Tmem47	2.75	802	292
1437029_at	Tacr3	2.73	79	29
1439627_at	Zic1	2.73	2226	816
1418744_s_at	LOC100047138	2.72	580	213
1458112_at	Adarb2	2.72	78	29
1423424_at	Zic3	2.70	1331	493
1441203_at	ENSMUSG00000086496	2.67	301	112
1425926_a_at	Otx2	2.66	100	37
1452142_at	Slc6a1	2.65	659	248
1449319_at	Rspo1	2.64	140	53
1440797_at	Dlx6os2	2.62	360	137
1436434_at	E2f2	2.62	398	152
1455267_at	Esrrg	2.61	251	96
1447669_s_at	Gng4	2.60	648	249
1436634_at	Robo3	2.59	107	41
1454974_at	Ntn1	2.57	226	88
1423640_at	Synpr	2.56	350	137
1416562_at	Gad1	2.55	126	50
1435029_at	B230120H23Rik	2.55	420	165
1421317_x_at	Myb	2.54	536	211
1415975_at	Carhsp1	2.52	1581	627
1416658_at	Frzb	2.49	161	65
1450042_at	Arx	2.49	6281	2527
1448626_at	Cdk5rap1	2.46	409	166
1457030_at	Mirg	2.45	267	109
1436221_at	Ildr2	2.44	341	140
1417943_at	Gng4	2.44	130	53
1452650_at	Trim62	2.43	122	50
1451306_at	Cdca7l	2.42	737	304
1420926_at	Arx	2.37	221	93
1438729_at	Sox1	2.37	2024	855
1434252_at	Tmcc3	2.36	80	34
1433762_at	C630043F03Rik	2.36	497	210
1423214_at	Plxnc1	2.36	74	31
1424767_at	Cdh22	2.36	188	80
1456364_at	C230057M02Rik	2.35	172	73
1451129_at	Calb2	2.35	850	361
1456417_at	Zic4	2.34	386	165
1417656_at	Mybl2	2.33	214	92
1423477_at	Zic1	2.31	5889	2545
1417013_at	Hspb8	2.31	97	42
1436791_at	Wnt5a	2.31	555	240

1448818_at	Wnt5a	2.30	255	111
1417019_a_at	Cdc6	2.27	642	282
1429945_at	Klhl35	2.27	116	51
1435554_at	Tmcc3	2.26	194	86
1418943_at	B230120H23Rik	2.25	65	29
1437673_at	Wnt5a	2.24	156	70
1444443_at	1444443_at	2.24	103	46
1422734_a_at	Myb	2.23	65	29
1425895_a_at	Id1	2.23	517	232
1420348_at	Lhx5	2.23	149	67
1436578_at	Ermn	2.22	85	38
1424822_at	Slain1	2.22	881	398
1437635_at	Dcbld2	2.20	1283	583
1416120_at	Rrm2	2.20	1157	527
1438571_at	Bub1	2.19	251	115
1455271_at	Gm13889	2.18	1339	614
1423123_at	Rad54l	2.18	281	129
1424850_at	Map3k1	2.18	122	56
1423124_x_at	Rad54l	2.18	294	135
1431004_at	Loxl2	2.18	267	123
1421439_at	Wnt8b	2.17	184	85
1424823_s_at	Slain1	2.17	242	111
1433862_at	Espl1	2.17	713	328
1418250_at	Arl4d	2.17	618	285
1451119_a_at	Fbln1	2.17	599	276
1449947_s_at	Zfhx3	2.16	224	103
1436293_x_at	Ildr2	2.16	376	174
1428077_at	LOC100047091	2.15	457	212
1450862_at	Rad54l	2.15	611	284
1460666_a_at	Ebf3	2.15	83	39
1455123_at	St18	2.14	891	417
1451277_at	Zadh2	2.13	485	228
1426725_s_at	Ets1	2.13	459	215
1426758_s_at	Meg3	2.12	2078	981
1437418_at	Gm3515	2.12	579	274
1455542_at	C630043F03Rik	2.11	160	76
1416749_at	Htra1	2.10	684	326
1424824_at	Slain1	2.10	1830	872
1436931_at	Rfx4	2.10	378	180
1416666_at	Serpine2	2.09	396	189
1416124_at	Ccnd2	2.09	618	296
1452183_a_at	Meg3	2.09	2858	1366
1442180_at	Dleu7	2.09	848	406
1418937_at	Dio2	2.08	119	57

1438239_at	Mid1	2.07	119	57
1452354_at	2810459M11Rik	2.07	433	209
1430058_at	Slbp	2.07	109	53
1431094_at	1110006E14Rik	2.07	86	41
1436713_s_at	Meg3	2.06	418	203
1422751_at	Tle1	2.05	2881	1404
1459253_at	1700023H06Rik	2.05	179	87
1452163_at	Ets1	2.05	344	168
1425526_a_at	Prrx1	2.05	192	94
1424143_a_at	Cdt1	2.04	3063	1500
1449481_at	Slc25a13	2.04	457	224
1442434_at	D8Ertd82e	2.03	1727	851
1455645_at	Mybpc1	2.02	97	48
1424144_at	Cdt1	2.02	808	400
1437631_at	Kcnip4	2.01	72	36
1433892_at	Spag5	2.00	381	190
1416123_at	Ccnd2	2.00	2902	1450
1436793_at	St18	2.00	477	238
1418494_at	Ebf2	2.00	158	79
1439854_at	Hrk	2.00	283	142
1456652_at	Dtl	2.00	57	29
1417587_at	Timeless	1.99	498	251
1456163_at	Fam72a	1.99	241	121
1456250_x_at	Tgfb1	1.98	134	67
1456326_at	Fndc3c1	1.98	73	37
1416575_at	Cdc45	1.98	375	189
1452905_at	Meg3	1.98	1786	902
1427707_a_at	Stil	1.98	587	297
1455956_x_at	Ccnd2	1.97	9556	4842
1449877_s_at	Kifc1	1.97	656	333
1423524_at	Mastl	1.97	129	65
1442316_x_at	Trp53bp1	1.96	55	28
1450905_at	Plxnc1	1.96	242	124
1438251_x_at	Htra1	1.95	560	286
1420649_at	Zfhx3	1.95	187	96
1423530_at	Stk32c	1.95	98	50
1435449_at	Bcl2l11	1.95	120	62
1430127_a_at	Ccnd2	1.95	9722	4987
1437263_at	A730089K16Rik	1.94	280	144
1435575_at	Kntc1	1.94	589	303
1452751_at	Ebf3	1.94	198	102
1453107_s_at	4933413G19Rik	1.94	708	365
1457424_at	Eya1	1.93	462	239
1434785_at	Cacng5	1.93	160	83

1452393_at	Akna	1.93	455	236
1422286_a_at	Tgif1	1.93	308	160
1418966_a_at	Dcbld1	1.92	313	163
1449291_a_at	Dcbld1	1.92	543	283
1428061_at	Hat1	1.92	1673	873
1427325_s_at	Akna	1.92	585	305
1456280_at	Clspn	1.91	660	345
1452912_at	Dscc1	1.91	501	262
1415976_a_at	Carhsp1	1.91	429	225
1421425_a_at	Rcan2	1.91	718	376
1424849_at	Wdr62	1.91	122	64
1450677_at	Chek1	1.91	397	209
1448083_at	LOC675405	1.90	88	46
1429268_at	2610318N02Rik	1.90	545	287
1419719_at	Gabrb1	1.90	190	100
1456005_a_at	Bcl2l11	1.88	668	355
1415945_at	Mcm5	1.88	1672	888
1454694_a_at	Top2a	1.88	4302	2288
1425601_a_at	Rtkn	1.88	213	113
1417938_at	Rad51ap1	1.88	797	424
1453851_a_at	Gadd45g	1.87	2293	1225
1434033_at	Tle1	1.87	861	461
1435727_s_at	Lima1	1.86	957	514
1451128_s_at	Kif22	1.86	1067	573
1450754_at	Cacna2d2	1.86	1004	539
1436692_at	E130308A19Rik	1.86	105	57
1452459_at	Aspm	1.86	584	314
1457423_at	LOC675405	1.86	183	98
1448535_at	Elp4	1.86	625	336
1438231_at	Foxp2	1.86	711	383
1422540_at	Fbln1	1.85	215	116
1420688_a_at	Sgce	1.85	587	317
1416701_at	Rnd3	1.85	510	276
1448899_s_at	Rad51ap1	1.85	634	343
1415810_at	Uhrf1	1.85	2786	1509
1452227_at	Sel1l3	1.84	1478	802
1425669_at	Mobkl2b	1.84	139	75
1433855_at	Abat	1.84	389	212
1426243_at	Cth	1.84	230	125
1439380_x_at	Meg3	1.83	3503	1910
1416554_at	LOC100048338	1.83	526	287
1428349_s_at	Ebf3	1.83	180	98
1417586_at	Timeless	1.83	1177	643
1434734_at	Rad54b	1.83	125	68

1421014_a_at	Clybl	1.83	134	73
1423365_at	Cacna1g	1.83	258	141
1439040_at	Cenpe	1.83	629	344
1449708_s_at	Chek1	1.83	793	434
1448194_a_at	H19	1.82	1784	980
1450629_at	Lima1	1.82	1342	738
1438232_at	Foxp2	1.82	1018	560
1450984_at	Tjp2	1.82	359	198
1415811_at	Uhrf1	1.82	496	273
1454946_at	Mybl2	1.81	332	183
1452899_at	Rian	1.81	2324	1284
1449236_at	Dll3	1.81	969	536
1422814_at	Aspm	1.81	1075	594
1419152_at	2810417H13Rik	1.81	1536	851
1417748_x_at	Foxm1	1.80	388	215
1448229_s_at	Ccnd2	1.80	8021	4451
1422499_at	Lima1	1.80	493	274
1440924_at	Kif20b	1.80	111	61
1438307_at	Hmgb2	1.80	435	242
1449207_a_at	Kif20a	1.80	775	431
1441899_x_at	Bcan	1.79	995	555
1442454_at	Top2a	1.79	248	138
1416718_at	Bcan	1.79	292	163
1429499_at	Fbxo5	1.79	1442	804
1436725_at	E130306D19Rik	1.79	250	139
1435931_at	1435931_at	1.79	224	125
1421539_at	Zic4	1.79	98	55
1448834_at	Foxm1	1.79	287	160
1448269_a_at	Klhl13	1.79	1298	725
1444416_at	Cenpa	1.79	219	123
1456006_at	Bcl2l11	1.79	95	53
1438833_at	Casc5	1.79	102	57
1437130_at	Gm5465	1.78	123	69
1458130_at	1458130_at	1.78	466	261
1437781_at	Insm2	1.78	65	37
1448650_a_at	Pole	1.78	590	331
1429809_at	Tmtc2	1.78	412	232
1450496_a_at	Ska1	1.78	404	227
1442101_at	Elfn1	1.78	165	93
1435114_at	Wdhd1	1.78	658	370
1435005_at	Cenpe	1.77	753	424
1416251_at	Mcm6	1.77	2579	1455
1418026_at	Exo1	1.77	400	226
1449171_at	Ttk	1.77	971	548

1456778_at	1456778_at	1.77	391	221
1450428_at	Lhx1	1.77	198	111
1433707_at	Gabra4	1.77	261	148
1422528_a_at	Zfp36l1	1.77	1360	768
1441984_at	Clspn	1.77	157	89
1450886_at	Gsg2	1.77	289	163
1415958_at	Slc2a4	1.77	216	122
1422462_at	Ube2t	1.77	579	328
1448777_at	Mcm2	1.77	1305	739
1420707_a_at	Traip	1.76	327	186
1423813_at	Kif22	1.76	421	238
1448123_s_at	Tgfb1	1.76	103	58
1421774_at	Vax1	1.76	115	65
1453769_at	Ckap2l	1.76	581	330
1417939_at	Rad51ap1	1.76	174	99
1438024_at	1438024_at	1.76	876	497
1425314_at	Gpr98	1.76	235	133
1438295_at	1438295_at	1.76	258	146
1455852_at	Nsl1	1.76	188	106
1438183_x_at	Sord	1.76	61	35
1424759_at	Arrdc4	1.76	253	144
1416321_s_at	Prelp	1.76	90	51
1435349_at	Nrp2	1.76	781	444
1449061_a_at	Prim1	1.76	1855	1056
1426817_at	Mki67	1.76	2553	1454
1453748_a_at	Kif23	1.75	100	57
1448226_at	Rrm2	1.75	3072	1752
1422016_a_at	Cenph	1.75	438	250
1451246_s_at	Aurkb	1.75	662	378
1424971_at	Ccdc99	1.75	646	369
1452314_at	Kif11	1.75	783	447
1439036_a_at	Atp1b1	1.75	888	508
1440007_at	D930003E18Rik	1.75	209	120
1434695_at	Dtl	1.75	759	434
1433893_s_at	Spag5	1.75	1000	572
1424278_a_at	Birc5	1.75	2264	1297
1437580_s_at	Nek2	1.74	873	501
1423516_a_at	Nid2	1.74	109	63
1439227_at	1439227_at	1.74	223	128
1433623_at	Zfp367	1.74	617	355
1421917_at	Pdgfra	1.74	133	77
1442018_at	Btg1	1.74	155	89
1439208_at	Chek1	1.74	153	88
1434096_at	Slc4a4	1.73	124	71

1435497_at	5730590G19Rik	1.73	307	177
1424659_at	Slit2	1.73	407	235
1426980_s_at	E130012A19Rik	1.73	121	70
1454889_x_at	Tmcc3	1.73	120	69
1439309_at	1439309_at	1.73	100	58
1452656_at	Zdhhc2	1.73	338	195
1441757_at	1190002F15Rik	1.73	190	110
1434428_at	D330028D13Rik	1.73	72	41
1440108_at	Foxp2	1.73	466	270
1417299_at	Nek2	1.73	301	174
1417323_at	Psrc1	1.73	1649	954
1433408_a_at	Mcm10	1.73	546	316
1421738_at	Gabra2	1.73	205	119
1435773_at	4930547N16Rik	1.73	116	67
1416122_at	Ccnd2	1.72	13035	7558
1416543_at	Nfe2l2	1.72	483	280
1425301_at	Ncam2	1.72	64	37
1455730_at	Dlgap5	1.72	533	309
1452305_s_at	Cenpn	1.72	456	265
1434767_at	C79407	1.72	895	520
1424292_at	Depdc1a	1.72	361	210
1445298_at	ENSMUSG00000048922	1.72	257	149
1436174_at	Atad2	1.72	1402	816
1458374_at	C79407	1.72	1305	760
1436685_at	Fam181a	1.71	81	47
1452715_at	Haus5	1.71	254	148
1453045_at	Ccdc41	1.71	848	495
1428834_at	Dusp4	1.71	2262	1320
1455674_at	Wdr76	1.71	313	183
1454904_at	Mtm1	1.71	348	204
1428304_at	Esco2	1.71	360	210
1421694_a_at	Vcan	1.71	582	341
1456559_at	Emx2os	1.71	153	90
1426938_at	Nova1	1.71	518	303
1418264_at	Cenpk	1.71	1292	756
1429734_at	4632434I11Rik	1.71	289	169
1417649_at	Cdkn1c	1.71	3393	1986
1418453_a_at	Atp1b1	1.71	585	343
1423213_at	Plxnc1	1.71	544	319
1418027_at	Exo1	1.71	150	88
1428104_at	Tpx2	1.71	1185	694
1437187_at	E2f7	1.71	706	414
1423428_at	Ror2	1.71	197	116
1449060_at	Kif2c	1.70	397	233

1452098_at	Chtf18	1.70	189	111
1450842_a_at	Cenpa	1.70	2653	1560
1457118_at	Shc4	1.70	93	55
1439695_a_at	Kif20b	1.70	693	407
1427580_a_at	Rian	1.70	280	165
1437251_at	Cdca2	1.70	647	381
1428105_at	Tpx2	1.70	835	491
1427062_at	Rbbp8	1.70	561	330
1417940_s_at	Rad51ap1	1.70	211	124
1421301_at	Zic2	1.70	358	211
1444583_at	Nasp	1.70	115	68
1455983_at	Cdca2	1.70	526	310
1433434_at	AW551984	1.70	62	37
1427161_at	Cenpf	1.70	1437	846
1423635_at	Bmp2	1.70	56	33
1436738_at	Pif1	1.70	326	192
1448878_at	Mxd3	1.69	849	501
1419397_at	Pola1	1.69	755	446
1450692_at	Kif4	1.69	678	401
1416802_a_at	Cdca5	1.69	1544	914
1417445_at	Ndc80	1.69	407	241
1446621_at	1446621_at	1.69	54	32
1452115_a_at	Plk4	1.69	369	219
1458447_at	Cenpf	1.69	164	97
1428480_at	Cdca8	1.69	826	490
1448833_at	Foxm1	1.68	471	280
1433532_a_at	Mbp	1.68	77	46
1431339_a_at	Efh2	1.68	1353	803
1439252_at	1439252_at	1.68	97	58
1424128_x_at	Aurkb	1.68	808	480
1450993_at	Pask	1.68	155	92
1449522_at	Unc5c	1.68	232	138
1416997_a_at	Hap1	1.68	308	183
1429440_at	1810041L15Rik	1.68	454	270
1416076_at	Ccnb1	1.68	874	520
1428481_s_at	Cdca8	1.68	3281	1954
1451928_a_at	Rad18	1.68	261	156
1432179_x_at	Ska1	1.68	54	32
1425603_at	Tmem176a	1.68	78	47
1415698_at	Golm1	1.68	3271	1950
1421963_a_at	Cdc25b	1.67	726	433
1426580_at	Plk4	1.67	738	441
1418090_at	Plvap	1.67	202	121
1422028_a_at	Ets1	1.67	108	64

1417849_at	Zfp704	1.67	465	278
1442542_at	Eya4	1.67	155	93
1455834_x_at	Tacc3	1.67	308	184
1427094_at	Pole2	1.67	718	429
1422835_at	Kcnd2	1.67	342	204
1422205_at	Sox1	1.67	78	46
1451053_a_at	Mdm1	1.67	350	209
1449109_at	Socs2	1.67	3311	1981
1438852_x_at	Mcm6	1.67	1791	1072
1437626_at	Zfp36l2	1.67	627	376
1436723_at	Cenpi	1.67	364	218
1446755_at	1446755_at	1.67	313	187
1442235_at	Plagl2	1.67	68	41
1417971_at	Nrm	1.67	433	259
1423714_at	Asf1b	1.67	684	410
1460045_at	Cdh7	1.67	101	60
1458076_at	1458076_at	1.67	84	50
1440091_at	Meis2	1.67	166	100
1416043_at	Nasp	1.67	252	151
1448623_at	Tmem123	1.67	618	371
1437370_at	Sgol2	1.67	1053	632
1416558_at	Melk	1.67	994	597
1427256_at	Vcan	1.67	1520	913
1422027_a_at	Ets1	1.66	90	54
1421225_a_at	Slc4a4	1.66	80	48
1435970_at	Nlk	1.66	3886	2337
1419943_s_at	Ccnb1	1.66	1280	770
1458984_at	1458984_at	1.66	325	196
1455488_at	Haus6	1.66	304	183
1416700_at	Rnd3	1.66	2597	1563
1438214_at	Trps1	1.66	262	158
1435796_at	Wscd2	1.66	103	62
1454744_at	F630043A04Rik	1.66	254	153
1416664_at	Cdc20	1.66	2500	1508
1456258_at	Emx2	1.66	1321	798
1423835_at	Zfp503	1.65	153	92
1429068_at	2810488G03Rik	1.65	95	58
1415800_at	Gja1	1.65	762	462
1452378_at	Malat1	1.65	727	441
1416258_at	Tk1	1.65	1083	657
1437745_at	Chd7	1.65	812	493
1416299_at	Shcbp1	1.65	1435	871
1434748_at	Ckap2	1.65	1323	804
1438470_at	Socs2	1.65	162	98

1429653_at	Gse1	1.64	310	188
1448187_at	Pold1	1.64	709	431
1456136_at	Kifc1	1.64	68	42
1424046_at	Bub1	1.64	1894	1154
1452204_at	Anks1	1.64	629	384
1439510_at	Sgol1	1.64	496	302
1427061_at	Rbbp8	1.64	1195	729
1417450_a_at	Tacc3	1.64	799	488
1441677_at	1441677_at	1.64	143	87
1433943_at	Itprip	1.64	219	134
1419112_at	Nlk	1.64	2341	1429
1429050_at	Chic2	1.64	1033	631
1423809_at	Tcf19	1.64	1324	809
1435938_at	Ckap2l	1.64	771	471
1418919_at	Sgol1	1.64	937	573
1455990_at	Kif23	1.64	1003	614
1436808_x_at	Mcm5	1.63	3868	2366
1458873_at	Aspm	1.63	104	64
1417911_at	Ccna2	1.63	1928	1180
1417506_at	Gmnn	1.63	2108	1290
1437992_x_at	Gja1	1.63	1773	1085
1429404_at	2010317E24Rik	1.63	245	150
1419153_at	2810417H13Rik	1.63	7126	4363
1423318_at	Rad18	1.63	225	138
1418281_at	Rad51	1.63	1012	620
1448953_at	Blm	1.63	426	261
1437186_at	BC055324	1.63	299	183
1425416_s_at	Psrc1	1.63	630	386
1419027_s_at	Gltp	1.63	851	522
1418108_at	Rtkn2	1.63	129	79
1454862_at	Phldb2	1.63	327	201
1432361_a_at	Cenpp	1.63	465	286
1459320_at	1459320_at	1.63	202	124
1422834_at	Kcnd2	1.63	257	158
1447363_s_at	Bub1b	1.63	1442	887
1456145_at	Dleu2	1.63	156	96
1458427_at	Brip1	1.63	69	42
1425264_s_at	Mbp	1.63	530	326
1423064_at	Dnmt3a	1.62	540	332
1436922_at	Pgil5	1.62	115	71
1448127_at	Rrm1	1.62	614	378
1443978_at	Ankle1	1.62	280	173
1443354_at	1443354_at	1.62	164	101
1450156_a_at	Hmmr	1.62	363	224

1456434_x_at	Hspb8	1.62	188	116
1436186_at	E2f8	1.62	590	364
1441447_at	Nol4	1.62	88	54
1418470_at	Yes1	1.62	79	49
1431087_at	Spc24	1.62	1433	885
1435458_at	Pim1	1.62	686	424
1429444_at	Rasl11a	1.62	133	82
1448700_at	G0s2	1.62	118	73
1416640_at	Kcne1l	1.62	271	168
1439436_x_at	Incenp	1.62	3115	1928
1426955_at	Col18a1	1.62	533	330
1452458_s_at	Ppil5	1.62	864	535
1422460_at	Mad2l1	1.61	2379	1474
1455980_a_at	Gas2l3	1.61	591	366
1427141_at	2700099C18Rik	1.61	101	63
1438811_at	Dlgap5	1.61	138	86
1429171_a_at	Ncapg	1.61	446	276
1429095_at	Cenpp	1.61	541	336
1423092_at	Incenp	1.61	1115	692
1434437_x_at	Rrm2	1.61	6722	4171
1445682_at	2700099C18Rik	1.61	80	50
1449283_a_at	Mapk12	1.61	224	139
1427252_at	Dmrtb1	1.61	103	64
1438194_at	Slc1a2	1.61	516	321
1457523_at	9530056K15Rik	1.61	76	47
1423877_at	Chaf1b	1.61	470	292
1434911_s_at	Arhgap19	1.61	377	235
1436614_at	1436614_at	1.61	69	43
1418856_a_at	Fanca	1.61	301	187
1444851_at	1444851_at	1.61	118	74
1416641_at	Lig1	1.61	1905	1187
1427541_x_at	Hmmr	1.60	378	235
1448026_at	Chd7	1.60	1000	623
1436872_at	Tacc3	1.60	279	174
1429019_s_at	Pon2	1.60	322	201
1434745_at	Ccnd2	1.60	14797	9235
1417848_at	Zfp704	1.60	903	564
1418369_at	Prim1	1.60	2516	1573
1434936_at	Hirip3	1.60	2240	1401
1446571_at	1446571_at	1.60	86	54
1452210_at	Dna2	1.60	593	371
1452954_at	Ube2c	1.60	8407	5263
1444257_at	Prr11	1.60	82	51
1455609_at	Cit	1.60	546	342

1435597_at	Atad5	1.60	442	277
1452073_at	Fam64a	1.60	866	543
1426652_at	LOC100045677	1.60	825	517
1453600_at	Ccdc18	1.60	126	79
1456914_at	Slc16a4	1.59	74	46
1437695_at	Prokr2	1.59	161	101
1448191_at	Plk1	1.59	785	493
1439520_at	Dtl	1.59	73	46
1455325_at	1455325_at	1.59	4167	2620
1453370_at	Troap	1.59	85	53
1455863_at	Spata5l1	1.59	63	40
1452242_at	Cep55	1.59	1364	858
1450761_s_at	Rims2	1.59	297	187
1415878_at	Rrm1	1.59	2676	1684
1418507_s_at	Socs2	1.59	2275	1432
1419838_s_at	Plk4	1.59	1991	1253
1417217_at	Magel2	1.59	273	172
1448466_at	Cdca5	1.59	419	264
1439394_x_at	Cdc20	1.59	566	357
1430193_at	Casc5	1.59	364	230
1435092_at	Arl4a	1.59	126	79
1435448_at	Bcl2l11	1.59	488	308
1426584_a_at	Sord	1.58	217	137
1416431_at	Tubb6	1.58	296	187
1435306_a_at	Kif11	1.58	1278	807
1432013_a_at	Fam54a	1.58	141	89
1438945_x_at	Gja1	1.58	641	405
1418237_s_at	Col18a1	1.58	256	162
1452655_at	Zdhhc2	1.58	100	63
1422773_at	Myt1	1.58	1306	825
1440294_at	1440294_at	1.58	79	50
1455439_a_at	Lgals1	1.58	513	324
1417541_at	Hells	1.58	1192	753
1455654_at	Hjurp	1.58	227	144
1450157_a_at	Hmmr	1.58	148	94
1416030_a_at	Mcm7	1.58	2789	1764
1437244_at	Gas2l3	1.58	669	424
1422513_at	Ccnf	1.58	376	238
1420032_at	Chek1	1.58	121	76
1416242_at	Klh13	1.58	189	120
1456161_at	0610040B10Rik	1.58	63	40
1458579_at	1458579_at	1.58	55	35
1420526_at	Dcbld2	1.57	176	112
1422922_at	Recql4	1.57	179	114

1425734_a_at	Ccdc77	1.57	241	153
1417626_at	Pde4dip	1.57	330	210
1452160_at	Tiparp	1.57	506	322
1419998_at	1419998_at	1.57	221	141
1438453_at	Rad51c	1.57	383	244
1449107_at	Nudt4	1.57	773	492
1451483_s_at	1700054N08Rik	1.57	306	195
1419573_a_at	Lgals1	1.57	368	235
1418541_at	Cenpo	1.57	100	64
1451832_at	Cklf	1.57	112	71
1449167_at	Epb4.1l4a	1.57	175	112
1431429_a_at	Arl4a	1.57	288	184
1439126_at	1110007A13Rik	1.56	87	55
1455840_at	Rapgef5	1.56	505	323
1430618_at	2610020C07Rik	1.56	88	56
1452924_at	Fam83d	1.56	285	182
1448369_at	Pola2	1.56	496	317
1436707_x_at	Ncaph	1.56	1635	1046
1417926_at	Ncapg2	1.56	423	271
1428976_at	Tmpo	1.56	1218	780
1453226_at	Kif18b	1.56	710	454
1424156_at	Rbl1	1.56	1035	662
1453416_at	Gas2l3	1.56	619	396
1435054_at	Eme1	1.56	424	271
1416433_at	Rpa2	1.56	1268	812
1456055_x_at	Pold1	1.56	850	545
1434365_a_at	BC055324	1.56	313	201
1452598_at	Gins1	1.56	1690	1084
1428661_at	Nfkbil2	1.56	316	203
1457260_at	5730409E04Rik	1.56	86	55
1437611_x_at	Kif2c	1.56	1182	758
1448205_at	Ccnb1	1.56	3538	2269
1433543_at	Anln	1.56	652	418
1429172_a_at	Ncapg	1.56	392	251
1425815_a_at	Hmmr	1.56	1080	694
1445602_at	A630055G03Rik	1.56	105	67
1450773_at	Kcnd2	1.56	228	147
1438434_at	Arhgap11a	1.56	1381	888
1457390_at	1457390_at	1.56	51	33
1436654_at	Gen1	1.56	220	141
1436866_at	Efna5	1.56	327	210
1431751_a_at	Mpped2	1.56	5994	3853
1424991_s_at	Tyms	1.56	1651	1062
1420028_s_at	LOC100045677	1.56	1668	1073

1428483_a_at	2610039C10Rik	1.55	667	429
1450686_at	Pon2	1.55	370	238
1455603_at	1455603_at	1.55	179	115
1448954_at	Nrip3	1.55	113	73
1452654_at	Zdhhc2	1.55	728	469
1421951_at	Lhx1	1.55	86	55
1438049_at	A430108E01Rik	1.55	266	171
1438272_at	Csmd3	1.55	79	51
1438161_s_at	Rfc4	1.55	1012	653
1429049_at	Nuak2	1.55	632	408
1431598_a_at	Lhx9	1.55	100	64
1418268_at	Htr3a	1.55	163	105
1423463_a_at	D2Ertd750e	1.55	399	258
1424766_at	Erc6l	1.55	430	278
1425043_s_at	Ccdc163	1.55	160	104
1427246_at	Magi1	1.55	261	169
1424010_at	Mfap4	1.54	739	479
1448314_at	Cdk1	1.54	3102	2008
1416101_a_at	Hist1h1c	1.54	778	504
1436854_at	Trpc2	1.54	103	66
1429658_a_at	Smc2	1.54	1275	826
1427498_a_at	Spag5	1.54	154	100
1417822_at	D17H6S56E-5	1.54	1023	663
1430228_at	Dtl	1.54	53	34
1437463_x_at	Tgfb1	1.54	183	119
1416031_s_at	Mcm7	1.54	3018	1959
1417896_at	Tjp3	1.54	98	64
1419659_s_at	Chic2	1.54	2227	1446
1427205_x_at	Ccdc46	1.54	274	178
1426528_at	Nrp2	1.54	258	168
1458480_at	Topbp1	1.54	81	53
1427375_at	Rg9mtd2	1.54	178	116
1420191_s_at	Tmem191c	1.54	94	61
1449699_s_at	C330027C09Rik	1.54	697	454
1430811_a_at	Nuf2	1.54	1249	813
1436472_at	Sifn9	1.54	276	180
1417821_at	D17H6S56E-5	1.54	575	375
1439079_a_at	Erbb2ip	1.53	76	50
1441266_at	Strn3	1.53	63	41
1422628_at	Fam111a	1.53	494	322
1416757_at	Zwilch	1.53	526	343
1449129_a_at	Kcnip3	1.53	154	101
1426774_at	Parp12	1.53	56	37
1449130_at	Cd1d1	1.53	1160	757

1457012_at	Dbx1	1.53	73	48
1448893_at	Ncor2	1.53	760	497
1416910_at	Dnajc15	1.53	1386	906
1417139_at	Dsn1	1.53	360	235
1444397_at	Spef1	1.53	67	44
1421045_at	Mrc2	1.53	207	135
1423774_a_at	Prc1	1.53	1324	866
1453361_at	Hells	1.53	63	41
1437295_at	Pkn2	1.53	734	481
1416961_at	Bub1b	1.53	1105	724
1448428_at	Nbl1	1.53	140	91
1421731_a_at	Fen1	1.52	1033	677
1421546_a_at	Racgap1	1.52	1342	880
1424471_at	Rapgef3	1.52	70	46
1452526_a_at	Pax6	1.52	356	233
1428384_at	D4Bwg0951e	1.52	102	67
1420081_s_at	D2Ertd750e	1.52	1267	832
1429812_at	2610002D18Rik	1.52	195	128
1447992_s_at	Pcsk2	1.52	85	56
1427020_at	Scara3	1.52	265	174
1422430_at	Fignl1	1.52	1118	735
1455444_at	Gabra2	1.52	151	99
1423026_at	Rad51c	1.52	125	82
1423920_at	Ncaph	1.52	742	488
1451776_s_at	Hopx	1.52	834	549
1417923_at	Pak3	1.52	499	329
1434600_at	Tjp2	1.52	515	339
1448312_at	Pcsk2	1.52	102	67
1448688_at	Podxl	1.52	337	222
1426349_s_at	Tmpo	1.52	2082	1373
1429330_at	Gabra4	1.52	114	75
1429326_at	Cenpl	1.52	233	154
1424511_at	Aurka	1.52	812	536
1427425_at	9130208E07Rik	1.52	311	205
1448713_at	Stat4	1.52	89	59
1418649_at	Egln3	1.51	283	187
1416326_at	Crip1	1.51	507	335
1451358_a_at	Racgap1	1.51	724	478
1427105_at	Cenpn	1.51	893	590
1441969_at	Trim36	1.51	365	241
1449374_at	Pipox	1.51	142	94
1440771_at	Zkscan1	1.51	98	65
1417777_at	Ptgr1	1.51	278	184
1419225_at	Cacna2d3	1.51	224	148

1426653_at	LOC100045677	1.51	185	122
1423775_s_at	Prc1	1.51	1910	1264
1450448_at	Stc1	1.51	148	98
1455721_at	Gspt2	1.51	99	66
1458240_at	Magi1	1.51	58	39
1452917_at	Rfc5	1.51	848	562
1429169_at	Rbm3	1.51	456	303
1448812_at	Hpcal1	1.51	1150	764
1444736_at	Cdh7	1.51	98	65
1434286_at	Trps1	1.51	164	109
1427193_at	Brd8	1.51	127	84
1434837_at	Mdc1	1.50	495	329
1441888_x_at	Zw10	1.50	84	56
1429028_at	Dock11	1.50	1575	1048
1448321_at	Smoc1	1.50	440	293
1429569_a_at	Ccdc46	1.50	54	36
1442484_at	D9Ertd306e	1.50	69	46
1456219_at	LOC100045988	1.50	438	291
1447122_at	Psmd1	1.50	72	48
1459658_at	Mcm5	1.50	133	89
1428518_at	Mlf1ip	1.50	393	262
1444459_at	1444459_at	1.50	205	136
1458813_at	Scn5a	1.50	250	167
1455553_at	Tmem194b	1.50	249	166
1428922_at	1200009O22Rik	1.50	93	62
1437318_at	Pak3	1.50	1097	731
1420146_at	Tiam2	1.50	248	165
1457683_at	Grik2	1.50	255	170
1424596_s_at	Lmcd1	1.50	289	193
1428662_a_at	Hopx	1.50	2169	1450
1457651_x_at	Rem2	1.50	164	110
1419513_a_at	Ect2	1.50	1860	1243
1418184_at	Cenpm	1.50	575	385
1437744_at	Slitrk4	1.50	313	209
1425179_at	Shmt1	1.50	265	177
1452717_at	Slc25a24	1.49	218	146
1456950_at	Alms1	1.49	118	79
1428942_at	Mt2	1.49	1260	843
1447357_at	ENSMUSG00000086193	1.49	96	65
1423919_at	Haus3	1.49	459	307
1422979_at	Suv39h2	1.49	468	314
1438410_at	Prtg	1.49	85	57
1428429_at	Rgmb	1.49	435	292
1434711_at	BC030867	1.49	219	147

1453038_at	4930422G04Rik	1.49	250	167
1460353_at	Tmem48	1.49	127	85
1442192_at	Tyms	1.49	69	46
1428392_at	Rassf2	1.49	474	318
1419944_at	Ccnb1	1.49	164	110
1426767_at	Wdr90	1.49	401	270
1416746_at	H2afx	1.49	4855	3264
1451163_at	Tinf2	1.49	559	376
1455851_at	Bmp5	1.49	91	61
1421940_at	LOC100045442	1.49	101	68
1416967_at	Sox2	1.49	6103	4107
1449073_at	FlnC	1.49	61	41
1416987_at	Elp4	1.49	62	41
1438325_at	Mecom	1.49	89	60
1423066_at	Dnmt3a	1.48	1367	921
1418505_at	Nudt4	1.48	2348	1581
1436200_at	Lonrf3	1.48	197	133
1416309_at	Nusap1	1.48	2431	1639
1436517_at	H1fx	1.48	2002	1350
1444029_at	Parp11	1.48	117	79
1417164_at	Dusp10	1.48	163	110
1424817_at	Spef1	1.48	639	431
1454011_a_at	Rpa2	1.48	328	222
1456342_at	Pax6	1.48	122	82
1439250_at	Slitrk3	1.48	68	46
1427216_at	Ifnz	1.48	167	113
1418542_s_at	Cenpo	1.48	329	222
1419271_at	Pax6	1.48	2292	1549
1439651_at	1439651_at	1.48	81	55
1429478_at	6720463M24Rik	1.48	132	89
1449131_s_at	Cd1d1	1.48	989	669
1460227_at	Timp1	1.48	74	50
1421939_a_at	LOC100045442	1.48	164	111
1438515_at	Zfp207	1.48	114	77
1424107_at	Kif18a	1.48	437	296
1443171_at	1443171_at	1.48	78	53
1457673_at	2610005L07Rik	1.48	102	69
1456884_at	6820445E23Rik	1.48	356	241
1435122_x_at	Dnmt1	1.48	1968	1333
1437543_at	Fubp1	1.48	399	270
1460168_at	Slbp	1.48	2474	1677
1428222_at	Dclk2	1.48	1014	687
1418334_at	Dbf4	1.47	1220	827
1455117_at	Mcm9	1.47	102	69

1453573_at	Hist1h3d	1.47	72	49
1434599_a_at	Tjp2	1.47	405	275
1456811_at	Cxxc4	1.47	70	48
1438690_at	Tyms	1.47	69	47
1434079_s_at	Mcm2	1.47	1834	1244
1452226_at	LOC100047340	1.47	2992	2031
1423525_at	Mastl	1.47	241	163
1435557_at	Fhod1	1.47	142	96
1432538_a_at	Rfc3	1.47	1312	891
1454424_at	Odz2	1.47	119	81
1434850_at	Iqgap3	1.47	384	261
1418257_at	Slc12a7	1.47	709	482
1419249_at	Cdk14	1.47	918	624
1439377_x_at	Cdc20	1.47	5381	3660
1455818_at	4930427A07Rik	1.47	313	213
1448635_at	Smc2	1.47	2132	1452
1450920_at	Ccnb2	1.47	1345	916
1450172_at	Pknox1	1.47	312	212
1424060_at	Neil3	1.47	333	227
1439269_x_at	Mcm7	1.47	2437	1661
1430311_at	Marcks	1.47	394	269
1429659_at	Smc2	1.47	230	157
1418634_at	Notch1	1.47	1995	1360
1450985_a_at	Tjp2	1.47	554	378
1451334_at	Fam58b	1.47	723	493
1453314_x_at	2610039C10Rik	1.47	1690	1153
1429284_at	Mobkl2b	1.47	322	220
1422970_at	Mxd3	1.47	365	249
1452197_at	Smc4	1.47	4433	3026
1439629_at	Nrxn3	1.46	749	511
1440868_at	Gabpb2	1.46	161	110
1423440_at	Fam33a	1.46	1735	1186
1434808_at	Palb2	1.46	290	198
1423186_at	Tiam2	1.46	1132	774
1430889_a_at	Tpmt	1.46	353	242
1419254_at	Mthfd2	1.46	388	265
1439091_at	Fancd2	1.46	112	77
1452263_at	Slc35f4	1.46	67	46
1419076_a_at	Brca2	1.46	351	240
1416149_at	Olig1	1.46	153	105
1456752_at	1456752_at	1.46	727	498
1421233_at	Pknox1	1.46	138	94
1419449_a_at	Gnai2	1.46	2863	1962
1418481_at	Pkmyt1	1.46	470	323

1435722_at	Gria4	1.46	347	238
1424629_at	Brca1	1.46	643	441
1450044_at	Fzd7	1.46	179	123
1441476_at	Socs2	1.46	80	55
1426839_at	Pold3	1.46	251	172
1417924_at	Pak3	1.46	158	109
1431873_a_at	Tube1	1.45	108	74
1440564_at	Prokr2	1.45	252	173
1448441_at	Cks1b	1.45	2530	1739
1448582_at	Ctnnbl1	1.45	2043	1405
1456706_at	4833441D16Rik	1.45	61	42
1422014_at	Foxp2	1.45	153	106
1416969_at	Gtse1	1.45	293	202
1431231_at	Hist1h3f	1.45	55	38
1458440_at	Cytsb	1.45	134	92
1442226_at	Sema3e	1.45	63	43
1436347_a_at	5530601H04Rik	1.45	249	171
1429228_at	4930534B04Rik	1.45	88	60
1425753_a_at	Ung	1.45	567	391
1441505_at	1441505_at	1.45	98	68
1456970_at	1456970_at	1.45	143	99
1440854_at	2810403A07Rik	1.45	54	37
1433891_at	Lgr4	1.45	149	103
1439396_x_at	Gpd1	1.45	86	60
1423006_at	Pim1	1.45	239	164
1455515_at	1810041L15Rik	1.45	1226	845
1417311_at	Crip2	1.45	3506	2419
1426721_s_at	Tiparp	1.45	977	675
1432059_x_at	5031425E22Rik	1.45	215	149
1453181_x_at	Plscr1	1.45	113	78
1433577_at	A730017C20Rik	1.45	601	415
1421592_at	Ncam2	1.45	79	55
1423700_at	Rfc3	1.45	764	528
1453067_at	Apitd1	1.45	442	305
1448147_at	Tnfrsf19	1.45	1522	1052
1453247_at	Zfp618	1.45	292	202
1431469_a_at	Cxxc5	1.45	689	477
1422252_a_at	Cdc25c	1.45	314	217
1436464_at	1436464_at	1.45	62	43
1446609_at	1446609_at	1.44	178	123
1441823_at	Zmiz1	1.44	68	47
1445226_at	BC023969	1.44	313	216
1415864_at	Bpgm	1.44	367	254
1456843_at	Yes1	1.44	52	36

1437528_x_at	A730017C20Rik	1.44	1305	904
1448860_at	Rem2	1.44	397	275
1428765_at	Meg3	1.44	212	147
1416214_at	Mcm4	1.44	2030	1407
1435779_at	Cep110	1.44	267	185
1448627_s_at	Pbk	1.44	3758	2606
1429242_at	1110054O05Rik	1.44	400	278
1441910_x_at	Ccne1	1.44	443	307
1439562_at	F730047E07Rik	1.44	702	487
1420082_at	D2Ertd750e	1.44	162	112
1429295_s_at	Trip13	1.44	1125	781
1455741_a_at	Ece1	1.44	199	138
1448316_at	Cmtm3	1.44	220	153
1418648_at	Egln3	1.44	153	107
1427695_a_at	Pou2f1	1.44	169	117
1437549_at	2810408I11Rik	1.44	208	145
1436449_at	Pcdh11x	1.44	115	80
1436852_at	E130308A19Rik	1.44	185	128
1425338_at	Plcb4	1.44	92	64
1419270_a_at	Dut	1.44	2981	2074
1456077_x_at	Cdc25c	1.44	389	270
1437470_at	Pknox1	1.44	716	498
1439839_at	D130051D11Rik	1.44	70	49
1435486_at	Pak3	1.44	1682	1172
1437638_at	Srrm2	1.44	199	139
1458574_at	1458574_at	1.44	64	44
1429149_at	Gins3	1.43	317	221
1434528_at	Aard	1.43	65	45
1418004_a_at	Tmem176b	1.43	2156	1504
1447781_s_at	Rg9mtd2	1.43	123	86
1438050_x_at	Gm9222	1.43	134	94
1426083_a_at	Btg1	1.43	4526	3156
1429660_s_at	Smc2	1.43	617	430
1416868_at	Cdkn2c	1.43	1169	815
1436548_at	1810012P15Rik	1.43	186	130
1422103_a_at	Stat5b	1.43	163	114
1458560_at	Aspm	1.43	58	40
1420981_a_at	Lmo4	1.43	2023	1412
1434789_at	Depdc1b	1.43	444	310
1423624_at	Fancl	1.43	483	337
1454086_a_at	Lmo2	1.43	367	256
1442406_at	9230104K21Rik	1.43	102	71
1427672_a_at	Kdm6a	1.43	594	415
1423620_at	Cenpq	1.43	1259	880

1417878_at	E2f1	1.43	414	290
1440071_at	Magi1	1.43	293	205
1422602_a_at	Wnt5b	1.43	51	36
1422597_at	Mmp15	1.43	364	255
1415854_at	Kitl	1.43	163	114
1455613_at	E130308A19Rik	1.43	293	205
1453745_at	2700038G22Rik	1.43	230	161
1436190_at	Zfp618	1.43	301	211
1417947_at	Pcna	1.43	11401	7988
1416492_at	Ccne1	1.43	296	207
1446769_at	Ttc39c	1.43	125	88
1442744_at	Rbm39	1.43	157	110
1429619_a_at	8430406I07Rik	1.43	210	147
1416773_at	Wee1	1.43	1557	1092
1438173_x_at	Pmf1	1.43	746	523
1427506_at	Ppil5	1.43	255	179
1417661_at	Rdm1	1.43	427	300
1435644_at	Sh3pxd2b	1.43	1001	702
1425514_at	Pik3r1	1.43	140	98
1449490_at	Mbd4	1.42	280	197
1454734_at	Lef1	1.42	696	489
1436460_at	Tmem194	1.42	135	95
1443999_at	1443999_at	1.42	87	61
1456634_at	9830001H06Rik	1.42	170	120
1452161_at	Tiparp	1.42	295	207
1444018_at	B930098A02Rik	1.42	98	69
1428522_at	Ttf2	1.42	363	255
1442087_at	H3f3a	1.42	349	246
1455355_at	G2e3	1.42	196	138
1457534_at	1457534_at	1.42	73	51
1425271_at	Psmc3ip	1.42	875	617
1427180_at	Slc27a3	1.42	198	139
1447279_at	E130308A19Rik	1.42	79	55
1427147_at	F730047E07Rik	1.42	488	344
1452464_a_at	Metapl1	1.42	364	256
1417910_at	Ccna2	1.42	2112	1489
1419716_a_at	Pou2f1	1.42	260	183
1435771_at	Plcb4	1.42	436	307
1435220_s_at	Cdc42se2	1.42	2859	2016
1430750_at	Dhfr	1.42	111	79
1418703_at	Rbms1	1.42	158	111
1447483_s_at	Snhg7	1.42	174	123
1435417_at	AI464131	1.42	101	71
1431349_at	Hnrnpab	1.42	108	76

1435181_at	Lin54	1.42	546	385
1453639_s_at	Ccdc163	1.42	79	56
1417921_at	2610029G23Rik	1.41	1579	1116
1417120_at	Miip	1.41	443	313
1427529_at	Fzd9	1.41	367	259
1422719_s_at	Nup50	1.41	264	187
1422809_at	Rims2	1.41	274	194
1426002_a_at	Cdc7	1.41	1006	712
1445642_at	Lemd1	1.41	162	115
1425654_a_at	Lima1	1.41	358	254
1452222_at	Utrn	1.41	151	107
1438339_at	Fancd2	1.41	114	80
1416165_at	Rab31	1.41	1382	980
1436845_at	Axin2	1.41	490	348
1428440_at	Slc25a12	1.41	1012	718
1429270_a_at	Syce2	1.41	2253	1598
1454952_s_at	Ncapd3	1.41	702	498
1440935_at	1440935_at	1.41	87	62
1424768_at	Cald1	1.41	257	183
1437162_at	1437162_at	1.41	185	132
1451884_a_at	Lsm2	1.41	751	534
1458878_at	Yes1	1.41	56	40
1417976_at	Ada	1.41	150	106
1425331_at	Zfp106	1.41	288	205
1418380_at	Terf1	1.41	376	267
1455760_at	Slc9a5	1.41	173	123
1436816_at	Nup133	1.41	810	576
1427496_at	Cep152	1.41	149	106

Down-regulated probe sets (866)

1422838_at	Kcnu1	0.71	137	191
1442175_at	C030027H14Rik	0.71	322	451
1455672_s_at	Cplx2	0.71	1053	1474
1449507_a_at	Cd47	0.71	869	1217
1426869_at	Boc	0.71	288	403
1435192_at	Sox3	0.71	948	1329
1449014_at	Lactb	0.71	296	414
1455697_at	1455697_at	0.71	338	474
1435460_at	Prkg2	0.71	52	73
1436297_a_at	Grina	0.71	793	1112
1434921_at	Nr2e1	0.71	341	478
1444451_at	Pappa2	0.71	102	143

1439031_at	Jph4	0.71	955	1340
1450852_s_at	F2r	0.71	1808	2536
1424989_at	Orai1	0.71	64	90
1416156_at	Vcl	0.71	309	433
1438720_at	9330159F19Rik	0.71	495	695
1417524_at	Cnih2	0.71	647	908
1417746_at	Cplx1	0.71	492	690
1435310_at	Syn3	0.71	92	129
1429901_at	Nkain2	0.71	306	430
1435187_at	1435187_at	0.71	550	774
1456322_at	Gas1	0.71	91	128
1434301_at	Fam84b	0.71	481	677
1445597_s_at	Pla2g16	0.71	90	127
1435695_a_at	Ggct	0.71	211	297
1424734_at	Rasgrf1	0.71	71	101
1456946_at	Sh3rf3	0.71	186	261
1435549_at	Trpm4	0.71	116	163
1455733_at	Taok3	0.71	314	442
1452016_at	Alox5ap	0.71	151	212
1430252_at	3110027N22Rik	0.71	133	187
1427442_a_at	App	0.71	5007	7051
1441223_at	March4	0.71	423	595
1460538_at	Cdh10	0.71	58	82
1418895_at	Skap2	0.71	90	127
1457276_at	Sik2	0.71	141	199
1455600_at	Rps3	0.71	607	857
1425510_at	Mark1	0.71	443	626
1416315_at	Abhd4	0.71	287	405
1445438_at	Ddhd1	0.71	61	87
1442347_at	Lrp8	0.71	1050	1483
1426562_a_at	Olfm1	0.71	713	1008
1426301_at	Alcam	0.71	1123	1588
1420925_at	Tub	0.71	646	913
1436733_at	E130309F12Rik	0.71	1301	1842
1424050_s_at	Fgfr1	0.71	783	1108
1458470_at	ENSMUSG00000087143	0.71	100	142
1440181_at	Gm1568	0.71	840	1190
1435297_at	Gjd2	0.71	92	131
1455567_at	Cdk12	0.71	411	583
1433781_a_at	Cldn12	0.71	414	587
1456389_at	Zeb2	0.71	863	1223
1457254_x_at	Tmem229b	0.70	579	821
1427522_at	Arhgap20	0.70	124	175
1416361_a_at	Dync1i1	0.70	961	1364

1426934_at	Nhs1	0.70	535	760
1428749_at	Dmxl2	0.70	849	1206
1455762_at	Kidins220	0.70	137	194
1452779_at	Ube2q1	0.70	2287	3249
1429625_at	2900054C01Rik	0.70	187	266
1425563_s_at	Pcdh10	0.70	90	128
1453304_s_at	Ly6e	0.70	610	867
1416632_at	LOC677317	0.70	236	336
1423376_a_at	Dok4	0.70	314	446
1435230_at	Ankrd12	0.70	326	464
1434757_at	Cbfa2t2	0.70	1187	1690
1445549_at	1445549_at	0.70	103	147
1435120_at	1435120_at	0.70	91	130
1434895_s_at	Ppp1r13b	0.70	216	307
1434374_at	Fam168a	0.70	1221	1739
1420824_at	Sema4d	0.70	328	467
1422626_at	Mmp16	0.70	194	277
1423277_at	Ptprk	0.70	170	242
1436672_at	Grk5	0.70	45	65
1422117_s_at	Khdrbs2	0.70	187	267
1423287_at	Cbln1	0.70	203	290
1434070_at	Jag1	0.70	160	228
1429308_at	Prdm16	0.70	39	56
1449850_at	Scube1	0.70	149	214
1449987_at	Alk	0.70	108	154
1450928_at	LOC100045546	0.70	3010	4305
1455321_at	Ddh1	0.70	211	302
1421840_at	Abca1	0.70	329	471
1454454_at	Elavl2	0.70	596	853
1448721_at	D1Ertd622e	0.70	261	374
1428347_at	Cyfip2	0.70	904	1294
1435038_s_at	Aak1	0.70	278	399
1422945_a_at	Kif5c	0.70	1661	2380
1426696_at	Lrpap1	0.70	494	709
1435537_at	Ptprd	0.70	344	494
1443058_at	Macrod2	0.70	41	59
1429965_at	Lonrf2	0.70	412	592
1417424_at	Ier3ip1	0.70	1052	1512
1437421_at	6330509M05Rik	0.70	48	69
1447763_at	1447763_at	0.70	51	74
1418311_at	Fn3k	0.70	53	76
1453614_a_at	Nfe2l3	0.70	43	61
1418047_at	Neurod6	0.70	5120	7363
1457729_at	1457729_at	0.70	60	86

1420459_at	Ripply3	0.69	37	54
1456637_at	Lrrtm2	0.69	37	53
1434641_x_at	Sez6l2	0.69	967	1392
1437168_at	Sfrs13b	0.69	65	94
1437751_at	Ppargc1a	0.69	69	100
1434260_at	Fchsd2	0.69	1244	1793
1417029_a_at	Trim2	0.69	78	112
1435940_at	Dclk1	0.69	1308	1886
1424246_a_at	Tes	0.69	261	377
1416382_at	Ctsc	0.69	101	146
1429013_at	Mtap7d2	0.69	243	350
1435296_at	Adra2c	0.69	46	66
1435222_at	Foxp1	0.69	900	1299
1432269_a_at	Sh3kbp1	0.69	158	228
1426514_at	Chst15	0.69	218	314
1458625_at	1458625_at	0.69	48	69
1420618_at	Cpeb4	0.69	1454	2098
1419392_at	Pclo	0.69	108	156
1452358_at	Rai2	0.69	74	107
1451628_a_at	Ank3	0.69	897	1296
1433945_at	Fam189a1	0.69	100	145
1418847_at	Arg2	0.69	120	174
1427470_s_at	Napb	0.69	140	203
1422641_at	Dok5	0.69	87	126
1434581_at	2410066E13Rik	0.69	1507	2180
1434283_at	LOC100044968	0.69	144	208
1455554_at	A830039N20Rik	0.69	85	123
1439786_at	Gab2	0.69	97	140
1457046_s_at	C77370	0.69	87	126
1451415_at	1810011O10Rik	0.69	140	203
1420621_a_at	App	0.69	1618	2345
1436455_at	Asph	0.69	89	129
1426300_at	Alcam	0.69	683	990
1416702_at	Serpini1	0.69	499	724
1421028_a_at	Mef2c	0.69	359	521
1420799_at	Ntsr1	0.69	126	183
1419184_a_at	Fhl2	0.69	95	138
1434672_at	Gpr22	0.69	145	211
1455213_at	Tmsb15b1-Tmsb15b2	0.69	1770	2569
1417574_at	Cxcl12	0.69	36	52
1455695_at	St8sia1	0.69	811	1179
1429463_at	Prcaa2	0.69	166	240
1430526_a_at	Smarca2	0.69	906	1316
1424976_at	Rhov	0.69	62	91

1455028_at	Mapt	0.69	1925	2797
1421349_x_at	Cend1	0.69	154	224
1437977_at	Sgtb	0.69	925	1345
1426332_a_at	Cldn3	0.69	49	71
1417293_at	Hs6st1	0.69	330	481
1445815_at	Fzd8	0.69	206	300
1440962_at	Slc8a3	0.69	400	582
1426972_at	Sec24d	0.69	231	336
1429134_at	Hivep3	0.69	159	231
1426466_s_at	Rps6kl1	0.69	77	112
1423862_at	Plekhf2	0.69	108	158
1446321_at	B230208B08Rik	0.69	75	109
1416824_at	B230118H07Rik	0.69	733	1069
1449411_at	Dscam	0.69	252	367
1434736_at	Hlf	0.69	74	108
1439022_at	Phactr1	0.69	312	456
1454782_at	Bai3	0.68	713	1041
1416452_at	Oat	0.68	986	1439
1431403_a_at	Mtap7d2	0.68	132	192
1451177_at	Dnajb4	0.68	314	459
1438134_at	Pcdh10	0.68	196	286
1416114_at	Sparcl1	0.68	581	850
1421096_at	Trpc1	0.68	157	229
1425094_a_at	Lhx6	0.68	329	482
1421844_at	Il1rap	0.68	72	105
1435964_a_at	Taok3	0.68	370	541
1434819_at	St6gal2	0.68	345	505
1454784_at	Hs3st2	0.68	95	139
1454715_at	Ralyl	0.68	410	600
1448551_a_at	Trim2	0.68	747	1094
1457289_at	Nr2e1	0.68	285	418
1436609_a_at	Lrpap1	0.68	1270	1861
1453027_at	Dlgap1	0.68	144	211
1425846_a_at	Caln1	0.68	49	72
1436628_at	Ulk4	0.68	106	155
1448664_a_at	Speg	0.68	60	89
1429402_at	Glt8d2	0.68	65	95
1440161_at	Mmp16	0.68	242	355
1428187_at	Cd47	0.68	1067	1567
1426530_a_at	Klh15	0.68	1191	1750
1438603_x_at	Masp1	0.68	164	241
1424534_at	Mmd2	0.68	652	959
1418003_at	1190002H23Rik	0.68	563	829
1439894_at	A730056I06Rik	0.68	65	96

1424248_at	Arpp21	0.68	63	92
1420973_at	Arid5b	0.68	60	89
1433596_at	Dnajc6	0.68	712	1050
1451529_at	Sgtb	0.68	382	563
1416023_at	Fabp3	0.68	292	431
1434115_at	Cdh13	0.68	950	1401
1450381_a_at	Bcl6	0.68	51	75
1456261_at	Sh3kbp1	0.68	109	161
1428205_x_at	Gabbrb2	0.68	142	210
1459860_x_at	Trim2	0.68	3406	5029
1453771_at	Gulp1	0.68	136	201
1439934_at	Slc30a10	0.68	235	347
1455030_at	Ptprr	0.68	50	74
1452841_at	Pgm2l1	0.68	306	453
1452514_a_at	Kit	0.68	512	758
1438431_at	Abcd2	0.68	166	246
1429105_at	Dlgap1	0.68	142	210
1432432_a_at	LOC100044883	0.67	343	509
1437920_at	Epha5	0.67	1032	1531
1456856_at	Ppfia2	0.67	239	355
1419200_at	Fxyd7	0.67	42	62
1429052_at	Ptprd	0.67	862	1280
1419829_a_at	Gab2	0.67	563	836
1434802_s_at	Ntf3	0.67	51	76
1425181_at	Sgip1	0.67	323	479
1433582_at	1190002N15Rik	0.67	213	317
1456954_at	Kcna6	0.67	108	160
1439259_x_at	Abhd4	0.67	1029	1532
1416406_at	Pea15a	0.67	1478	2202
1419748_at	Abcd2	0.67	199	297
1457743_at	1457743_at	0.67	78	117
1436729_at	Afap1	0.67	1535	2288
1449630_s_at	Mark1	0.67	925	1379
1455272_at	Grm5	0.67	130	194
1452148_at	Lrpap1	0.67	513	765
1426110_a_at	Lpar1	0.67	45	68
1453365_at	Rabgap1l	0.67	65	97
1433476_at	C78339	0.67	2949	4411
1456812_at	Abcd2	0.67	173	260
1456336_at	Csrnp3	0.67	52	78
1449472_at	Gpr12	0.67	141	212
1428265_at	Ppp2r1b	0.67	1729	2591
1451507_at	Mef2c	0.66	186	281
1423551_at	Cdh13	0.66	715	1077

1456220_at	Fbxl7	0.66	56	85
1421604_a_at	Klf3	0.66	121	183
1437811_x_at	1437811_x_at	0.66	1070	1612
1455266_at	Kif5c	0.66	3011	4539
1422130_at	Nptx1	0.66	63	95
1426413_at	Neurod1	0.66	1944	2934
1431046_at	Ppfia3	0.66	245	370
1457198_at	Nrp1	0.66	70	106
1453084_s_at	Col22a1	0.66	33	50
1419489_at	Fam19a5	0.66	237	359
1433977_at	Hs3st3b1	0.66	52	78
1436076_at	Dlgap1	0.66	216	326
1422890_at	Pcdh18	0.66	102	154
1440534_at	Gm10001	0.66	68	103
1441625_at	Rimbp2	0.66	125	190
1448669_at	Dkk3	0.66	89	134
1451809_s_at	Rwdd3	0.66	328	498
1444690_at	Epha5	0.66	1182	1791
1454745_at	Arhgap29	0.66	138	209
1440273_at	1440273_at	0.66	150	227
1440132_s_at	Prkar1b	0.66	526	798
1435305_at	Ntrk2	0.66	177	269
1445275_at	Fam190a	0.66	347	526
1424039_at	Tmem66	0.66	1367	2074
1452872_at	Ank3	0.66	329	499
1452878_at	Prkce	0.66	740	1125
1438088_at	1438088_at	0.66	237	360
1426850_a_at	Map2k6	0.66	639	972
1460249_at	Lnx2	0.66	394	602
1454832_at	Phactr1	0.66	677	1033
1433475_a_at	C78339	0.66	3401	5190
1429464_at	Prkaa2	0.66	64	98
1437964_at	Nxph2	0.65	126	192
1443989_at	Trim9	0.65	46	70
1419490_at	Fam19a5	0.65	377	577
1437680_x_at	Glrx2	0.65	625	955
1437467_at	Alcam	0.65	794	1214
1433939_at	Aff3	0.65	1496	2288
1416828_at	Snap25	0.65	1069	1635
1447825_x_at	Pcdh8	0.65	1413	2161
1456527_at	Hecw1	0.65	513	786
1449154_at	Col11a1	0.65	89	137
1452092_at	Chst15	0.65	462	709
1419673_at	Spock1	0.65	143	219

1430286_s_at	Gm14057	0.65	357	548
1435311_s_at	Syn3	0.65	197	303
1436450_at	D11Bwg0517e	0.65	2547	3911
1437160_at	Nlgn1	0.65	203	311
1447735_x_at	A2bp1	0.65	71	110
1425710_a_at	Homer1	0.65	71	110
1417312_at	Dkk3	0.65	72	110
1424400_a_at	Aldh1l1	0.65	89	137
1434651_a_at	Cldn3	0.65	99	152
1437197_at	Sorbs2	0.65	1424	2189
1438407_at	Dsel	0.65	213	327
1460576_at	Exoc6	0.65	347	533
1428204_at	Gabbrb2	0.65	154	236
1421477_at	Cplx2	0.65	1231	1895
1443694_at	Rgs20	0.65	431	664
1437604_x_at	Apcdd1	0.65	384	593
1444486_at	Klh15	0.65	74	115
1428377_at	Btbd11	0.65	216	334
1423420_at	Adrb1	0.65	83	128
1455535_at	Sox5	0.65	1150	1779
1437284_at	Fzd1	0.65	1382	2140
1422642_at	Cdc42ep3	0.65	416	645
1453261_at	2610035D17Rik	0.64	246	381
1457724_at	Ctsl	0.64	37	58
1424695_at	2010011I20Rik	0.64	548	852
1417028_a_at	Trim2	0.64	3124	4856
1426720_at	Apbb2	0.64	40	63
1419978_s_at	D10Ert610e	0.64	1231	1917
1451313_a_at	1110067D22Rik	0.64	1001	1559
1445202_at	1445202_at	0.64	63	98
1454666_at	LOC100046855	0.64	839	1309
1434112_at	LOC100048050	0.64	1208	1885
1417027_at	Trim2	0.64	2341	3654
1434111_at	LOC100048050	0.64	1677	2618
1438654_x_at	Mmd2	0.64	743	1161
1419554_at	Cd47	0.64	652	1019
1435894_at	C030014L02	0.64	80	125
1460623_at	Skap2	0.64	73	114
1420563_at	Gria3	0.64	213	333
1423557_at	Ifngr2	0.64	1042	1632
1435772_at	Kif21b	0.64	3178	4976
1443485_at	Epha7	0.64	291	456
1458766_at	1458766_at	0.64	55	86
1440745_at	Prdm16	0.64	54	85

1451755_a_at	Apobec1	0.64	69	109
1419672_at	Spock1	0.64	353	554
1439333_at	Kcnv1	0.64	143	224
1434429_at	Syt16	0.64	270	425
1434384_at	Nrip1	0.64	381	600
1441087_at	2810011L19Rik	0.63	86	136
1416753_at	Prkar1b	0.63	522	823
1446399_at	Cdh10	0.63	57	91
1424852_at	Mef2c	0.63	877	1383
1439622_at	Rassf4	0.63	106	167
1456119_at	Grm5	0.63	84	132
1456606_a_at	Chst11	0.63	283	447
1453055_at	Sema6d	0.63	2289	3626
1426799_at	Rab8b	0.63	2211	3502
1453006_at	Fgfbp3	0.63	904	1432
1419382_a_at	Dhrs4	0.63	298	472
1438658_a_at	S1pr3	0.63	176	279
1429348_at	Sema3c	0.63	817	1297
1433782_at	Cldn12	0.63	123	195
1418469_at	Nrip1	0.63	201	320
1449089_at	Nrip1	0.63	322	511
1433711_s_at	LOC100047324	0.63	928	1474
1437750_at	Tmem158	0.63	34	55
1455455_at	Glt28d2	0.63	39	62
1438751_at	Slc30a10	0.63	170	270
1436216_s_at	Inf2	0.63	214	341
1417400_at	Rai14	0.63	1388	2209
1436340_at	6430704M03Rik	0.63	331	527
1421027_a_at	Mef2c	0.63	1041	1657
1457318_at	A330008L17Rik	0.63	76	121
1434025_at	1434025_at	0.63	33	53
1442725_at	1442725_at	0.63	141	224
1457270_at	Gas7	0.63	250	399
1439990_at	1439990_at	0.63	211	336
1429896_at	5830408B19Rik	0.63	44	69
1418086_at	Ppp1r14a	0.63	349	558
1434422_at	1700066M21Rik	0.63	617	986
1419078_at	Nin	0.62	388	621
1426733_at	Itpk1	0.62	986	1577
1434671_at	B230337E12Rik	0.62	1264	2024
1437675_at	Slc8a1	0.62	99	158
1438841_s_at	Arg2	0.62	45	72
1438667_at	5730410E15Rik	0.62	928	1488
1420964_at	Enc1	0.62	125	200

1417428_at	Gng3	0.62	1465	2351
1426719_at	Apbb2	0.62	385	617
1436650_at	Filip1	0.62	50	81
1455845_at	Wscd1	0.62	333	535
1450930_at	Hpcal	0.62	193	310
1423500_a_at	Sox5	0.62	614	987
1434285_at	Frmd4a	0.62	1753	2819
1435047_at	Rab3c	0.62	1134	1824
1426412_at	Neurod1	0.62	2039	3280
1435551_at	Fhod3	0.62	659	1060
1428173_at	Eml2	0.62	235	378
1423478_at	Prkcb	0.62	129	208
1436912_at	Cacnb4	0.62	211	340
1434211_at	Sh3bgrl2	0.62	179	289
1453103_at	Ablim1	0.62	179	289
1456060_at	Maf	0.62	478	771
1454699_at	LOC100047324	0.62	357	575
1435714_x_at	Il17d	0.62	98	158
1417416_at	Kcna1	0.62	206	333
1433590_at	Herc3	0.62	247	400
1448443_at	Serpini1	0.62	1496	2423
1451450_at	2010011I20Rik	0.62	1150	1863
1460619_at	Mfsd9	0.62	51	82
1417051_at	Pcdh8	0.62	1234	2001
1438620_x_at	Sfrp1	0.62	195	317
1433988_s_at	C230098O21Rik	0.62	1004	1630
1432189_a_at	Sox5	0.62	605	983
1455298_at	1455298_at	0.62	234	381
1434423_at	Gulp1	0.61	137	223
1428142_at	Etv5	0.61	293	477
1419147_at	Rec8	0.61	150	244
1454708_at	Ablim1	0.61	280	455
1419033_at	2610018G03Rik	0.61	62	101
1440133_x_at	Prkar1b	0.61	207	338
1448250_at	9030425E11Rik	0.61	839	1367
1442019_at	1442019_at	0.61	200	326
1439830_at	Map3k5	0.61	76	124
1455516_at	Csrnp3	0.61	712	1163
1456475_s_at	Prkar2b	0.61	1630	2660
1458622_at	Ntrk2	0.61	340	556
1440870_at	Prdm16	0.61	447	730
1450027_at	Sdc3	0.61	750	1226
1434539_at	Lrrn3	0.61	494	808
1427308_at	Dab1	0.61	658	1078

1438931_s_at	LOC100047324	0.61	630	1033
1417374_at	Tuba4a	0.61	181	297
1434051_s_at	Hspa12a	0.61	355	582
1421958_at	L1cam	0.61	35	57
1417279_at	Itpr1	0.61	96	158
1428718_at	Scrn1	0.61	133	218
1449056_at	E330009J07Rik	0.61	3498	5750
1443036_at	Zfp804a	0.61	146	240
1419028_at	Arpp21	0.61	207	341
1423668_at	Zdhhc14	0.61	92	152
1440153_at	1440153_at	0.61	173	284
1420818_at	Sla	0.61	54	89
1452298_a_at	Myo5b	0.61	50	82
1433894_at	Jazf1	0.61	157	259
1417962_s_at	Ghr	0.61	58	96
1420892_at	Wnt7b	0.61	881	1453
1457215_at	Gm13111	0.61	54	90
1427974_s_at	Cacna1d	0.60	59	97
1416934_at	Mtm1	0.60	37	61
1427280_at	Scn2a1	0.60	136	226
1440084_at	1440084_at	0.60	518	858
1434766_at	Prcaa2	0.60	188	312
1430667_at	Pcdh10	0.60	85	141
1450435_at	L1cam	0.60	2102	3490
1428717_at	Scrn1	0.60	803	1333
1439500_at	Scrn1	0.60	2095	3478
1422998_a_at	Glrx2	0.60	1950	3241
1437466_at	Alcam	0.60	1039	1727
1453004_at	Slc22a23	0.60	295	491
1434414_at	Foxred2	0.60	198	329
1424694_at	2010011I20Rik	0.60	825	1373
1430112_at	Wdr66	0.60	52	86
1454939_at	1454939_at	0.60	594	990
1418925_at	Celsr1	0.60	457	762
1452399_at	Rgs6	0.60	49	81
1455085_at	1700086L19Rik	0.60	105	175
1429857_at	2900092D14Rik	0.60	705	1178
1417872_at	Fhl1	0.60	993	1658
1421100_a_at	Dab1	0.60	240	401
1434109_at	Sh3bgrl2	0.60	271	453
1440192_at	Ttc39b	0.60	122	205
1437679_a_at	Glrx2	0.60	1452	2433
1448251_at	9030425E11Rik	0.60	1183	1984
1425822_a_at	Dtx1	0.60	875	1468

1438602_s_at	Masp1	0.60	1145	1921
1443187_at	Rspo3	0.60	96	162
1444452_at	D930002L09Rik	0.60	31	52
1455346_at	Masp1	0.60	622	1046
1420965_a_at	Enc1	0.59	6826	11477
1441693_at	Adamts3	0.59	495	833
1436338_at	1436338_at	0.59	314	528
1416594_at	Sfrp1	0.59	804	1354
1456533_at	Dpy19l1	0.59	643	1082
1456116_at	Ctnnd2	0.59	708	1193
1423150_at	Scg5	0.59	1509	2546
1452249_at	Prickle1	0.59	258	436
1459838_s_at	Btbd11	0.59	361	610
1431890_a_at	Milt3	0.59	839	1419
1421175_at	Myt1l	0.59	799	1350
1437574_at	Adamts18	0.59	212	358
1433581_at	1190002N15Rik	0.59	262	444
1452342_at	Apbb2	0.59	411	696
1454048_a_at	4931408A02Rik	0.59	60	101
1451991_at	Epha7	0.59	254	432
1439904_at	Fstl5	0.59	444	753
1435337_at	Tshz3	0.59	421	715
1434470_at	Syt13	0.59	31	53
1418666_at	Ptx3	0.59	302	514
1457587_at	Kcnq5	0.59	76	129
1435402_at	Gramd1b	0.59	73	124
1460406_at	Pls1	0.59	110	187
1431322_at	Igsf3	0.59	198	337
1418995_at	Neurod2	0.59	2948	5017
1426501_a_at	Tifa	0.59	76	129
1460049_s_at	1500015O10Rik	0.59	45	76
1451559_a_at	Dhrs4	0.59	602	1026
1441357_at	Kirrel3	0.59	70	119
1423707_at	Tmem50b	0.59	1197	2040
1428579_at	Fmnl2	0.59	2403	4098
1450831_at	LOC100046032	0.59	662	1131
1427307_a_at	Dab1	0.59	916	1564
1437312_at	Bmpr1b	0.58	149	255
1416855_at	Gas1	0.58	3948	6765
1436829_at	Trim67	0.58	328	563
1440707_at	Dmrt3	0.58	189	324
1460569_x_at	Cldn3	0.58	63	108
1430030_at	5330426P16Rik	0.58	413	709
1433989_at	Slc6a11	0.58	41	70

1418690_at	Ptprz1	0.58	317	544
1452398_at	Plce1	0.58	236	407
1450061_at	Enc1	0.58	3474	5980
1449581_at	Emid1	0.58	192	330
1427005_at	Plk2	0.58	779	1341
1428571_at	Col9a1	0.58	64	111
1450181_at	Cux2	0.58	256	442
1416342_at	Tnc	0.58	227	391
1440827_x_at	Sox5	0.58	335	579
1452426_x_at	1452426_x_at	0.58	80	138
1457361_at	Zfp804a	0.58	75	130
1458403_at	Tnik	0.58	62	107
1455636_at	Lsamp	0.58	88	153
1453622_s_at	Milt3	0.58	369	639
1417672_at	Slc4a10	0.58	85	148
1422053_at	Inhba	0.58	59	103
1438619_x_at	Zdhhc14	0.58	386	671
1457734_at	1457734_at	0.58	201	349
1441371_at	Plxna4	0.58	404	702
1434904_at	Hivep2	0.58	316	550
1423861_at	Plekhf2	0.57	108	188
1437650_at	C730026J16	0.57	182	317
1452728_at	Kirrel3	0.57	251	437
1429918_at	Arhgap20	0.57	60	106
1440711_at	C630001G18Rik	0.57	38	66
1425574_at	Epha3	0.57	149	261
1420938_at	Hs6st2	0.57	91	159
1438975_x_at	Zdhhc14	0.57	322	565
1417394_at	Klf4	0.57	90	158
1439959_at	Fgf11	0.57	137	241
1423025_a_at	Schip1	0.57	1423	2505
1450977_s_at	Ndrg1	0.57	174	306
1422473_at	Pde4b	0.57	125	221
1454729_at	LOC100045503	0.57	659	1161
1455208_at	Pex19	0.57	130	230
1457137_at	1457137_at	0.57	83	147
1428203_at	Gabrb2	0.57	183	324
1457840_at	Plxna4	0.56	75	133
1425985_s_at	Masp1	0.56	757	1343
1430579_at	Tnik	0.56	107	190
1429738_at	Myt1l	0.56	637	1132
1437787_at	Lrrtm2	0.56	88	157
1430629_at	Slc16a14	0.56	102	182
1416711_at	Tbr1	0.56	1411	2511

1429205_at	Milt3	0.56	1118	1993
1423630_at	Cygb	0.56	124	222
1455436_at	Diras2	0.56	138	247
1438624_x_at	Hs3st2	0.56	110	197
1434877_at	Nptx1	0.56	179	320
1460607_at	Igsf11	0.56	132	237
1455925_at	Prdm8	0.56	1002	1794
1437230_at	Kcna1	0.56	55	99
1426880_at	Etl4	0.56	355	637
1429887_at	Nos1	0.56	353	633
1422068_at	LOC100045707	0.56	166	299
1452009_at	Ttc39b	0.56	105	189
1444086_at	Nckap5	0.56	456	819
1459210_at	Tmem108	0.56	201	362
1436026_at	Zfp703	0.56	885	1593
1450700_at	Cdc42ep3	0.55	389	701
1435595_at	1810011O10Rik	0.55	93	168
1459941_at	Clvs1	0.55	54	98
1416371_at	Apod	0.55	197	355
1434273_at	Fam174b	0.55	163	295
1415845_at	Syt4	0.55	834	1511
1422725_at	Mak	0.55	51	93
1424186_at	Ccdc80	0.55	149	270
1431422_a_at	Dusp14	0.55	337	613
1435411_at	Neurod2	0.55	1518	2763
1434881_s_at	Kctd12	0.55	506	922
1436444_at	6030405A18Rik	0.55	87	158
1452473_at	Prr15	0.55	37	68
1458416_at	A330048O09Rik	0.55	140	255
1438664_at	Prkar2b	0.55	1071	1951
1434325_x_at	Prkar1b	0.55	1066	1943
1448598_at	Mmp17	0.55	313	574
1427427_at	Ryr3	0.55	65	119
1460390_at	Sorl1	0.55	34	62
1434590_at	Bend6	0.55	631	1157
1437614_x_at	Zdhhc14	0.54	333	611
1421255_a_at	Cabp1	0.54	48	88
1415844_at	Syt4	0.54	354	653
1435578_s_at	Dab1	0.54	1024	1890
1423278_at	Ptpk	0.54	266	491
1460419_a_at	Prkcb	0.54	424	783
1451506_at	Mef2c	0.54	503	929
1452730_at	Rps4y2	0.54	279	515
1434891_at	Ptgfrn	0.54	537	993

1460411_s_at	Pkdcc	0.54	437	807
1440910_at	C77370	0.54	399	738
1426712_at	Slc6a15	0.54	289	536
1434062_at	Rabgap1l	0.54	1145	2122
1417795_at	Chl1	0.54	229	424
1442206_at	Mdga2	0.54	98	183
1435577_at	Dab1	0.54	1202	2230
1460203_at	Itpr1	0.54	209	387
1460073_at	1460073_at	0.54	42	78
1451701_x_at	Cldn3	0.54	88	164
1442370_at	1442370_at	0.54	99	184
1436646_at	1436646_at	0.54	51	95
1429841_at	Megf10	0.53	339	633
1453777_a_at	Ndst3	0.53	47	88
1449666_at	Atrnl1	0.53	67	126
1426282_at	Ntm	0.53	220	414
1455785_at	Kcna1	0.53	173	326
1419584_at	Ttc28	0.53	2780	5230
1438269_at	Zbtb38	0.53	48	91
1455489_at	Lrrtm2	0.53	126	236
1429685_at	Gabbrb2	0.53	297	560
1455290_at	Znrf2	0.53	155	291
1418984_at	Inadl	0.53	62	117
1436010_at	Lrrc16b	0.53	413	778
1458802_at	Hivep3	0.53	235	444
1426621_a_at	Ppp2r2b	0.53	1610	3049
1454742_at	Rasgef1b	0.53	684	1297
1422592_at	Ctnnd2	0.53	1599	3032
1434016_at	Znrf2	0.53	1573	2986
1455607_at	Rspo3	0.53	590	1120
1423613_at	Ssfa2	0.53	147	280
1456491_at	Rbm24	0.53	32	61
1439661_at	Slc16a14	0.52	187	358
1451331_at	Ppp1r1b	0.52	176	336
1437442_at	Pcdh7	0.52	135	258
1435166_at	Cntn2	0.52	583	1119
1421340_at	Map3k5	0.52	27	53
1438511_a_at	1190002H23Rik	0.52	376	723
1433759_at	Dpy19l1	0.52	2747	5283
1434595_at	Trim9	0.52	318	611
1434728_at	Gria3	0.52	217	417
1455258_at	Kcnc2	0.52	56	107
1435190_at	Chl1	0.52	1816	3501
1455426_at	Epha3	0.52	1341	2587

1429678_at	5730508B09Rik	0.52	339	655
1458492_x_at	Ntm	0.52	391	756
1429274_at	Lypd6b	0.52	62	121
1441603_at	Sstr3	0.52	29	56
1437385_at	Ccbe1	0.52	70	136
1440201_at	Slc8a1	0.52	47	90
1443273_at	1443273_at	0.51	88	171
1442917_at	Gm11627	0.51	316	614
1448494_at	Gas1	0.51	1232	2401
1456214_at	Pcdh7	0.51	110	214
1455292_x_at	Rsl1	0.51	61	120
1436483_at	Myt1l	0.51	770	1509
1450047_at	Hs6st2	0.51	1020	2000
1434441_at	1110018J18Rik	0.51	94	184
1422256_at	Sstr2	0.51	539	1063
1442039_at	Tox	0.51	242	478
1452008_at	Ttc39b	0.51	231	456
1452065_at	Vstm2a	0.51	68	134
1420388_at	Prss12	0.50	77	153
1427306_at	Ryr1	0.50	64	127
1428136_at	Sfrp1	0.50	1522	3037
1448139_at	Mlc1	0.50	100	200
1455256_at	Tnik	0.50	1136	2271
1436916_at	Tmem108	0.50	420	841
1453008_at	Trnp1	0.50	408	817
1435456_at	Ttc28	0.50	1691	3391
1424897_at	Gpr85	0.50	752	1508
1439496_at	Ston1	0.50	257	518
1444026_at	AI593442	0.50	97	196
1439725_at	Ptprt	0.50	106	213
1454622_at	Slc38a5	0.50	82	166
1425483_at	Tox	0.50	95	193
1449520_at	Ttc28	0.49	1235	2501
1442791_x_at	6720407P12Rik	0.49	86	175
1444080_at	Nav2	0.49	40	82
1424525_at	Grp	0.49	28	56
1454886_x_at	Trim9	0.49	174	354
1456392_at	Negr1	0.49	310	632
1431045_at	Fam49a	0.49	128	261
1424896_at	Gpr85	0.49	574	1171
1437558_at	B130021B11Rik	0.49	74	150
1426389_at	Camk1d	0.49	67	137
1434375_at	Fam168a	0.49	1339	2738
1418610_at	Slc17a6	0.49	252	517

1455048_at	Igsf3	0.49	822	1687
1439808_at	Ipcef1	0.49	42	86
1437618_x_at	Gpr85	0.48	1261	2603
1437872_at	Napepld	0.48	71	146
1438483_at	Nos1	0.48	165	341
1434687_at	C730026J16	0.48	80	165
1446990_at	Nfia	0.48	1302	2694
1457148_at	Csmd2	0.48	100	208
1422474_at	Pde4b	0.48	240	499
1434639_at	Klhl29	0.48	323	672
1426283_at	Ntm	0.48	360	749
1425575_at	Epha3	0.48	581	1212
1458967_at	1458967_at	0.48	56	116
1421017_at	Nrg3	0.48	117	245
1433571_at	Serinc5	0.48	111	233
1457088_at	Pldn	0.48	50	106
1450976_at	Ndrg1	0.48	228	479
1433815_at	Jakmip1	0.47	102	216
1434779_at	Cbln2	0.47	71	150
1427281_at	Scn2a1	0.47	41	86
1434017_at	Znrf2	0.47	634	1346
1455620_at	Hs3st4	0.47	461	982
1455049_at	Igsf3	0.47	344	733
1457066_at	Abcc8	0.47	34	71
1452050_at	Camk1d	0.47	143	306
1433906_at	Clvs1	0.47	495	1058
1425484_at	Tox	0.47	136	291
1448977_at	Tcfap2c	0.47	126	270
1454838_s_at	Pkdcc	0.47	444	952
1439862_at	Rorb	0.47	164	352
1418983_at	Inadl	0.47	58	124
1435321_at	Limch1	0.47	992	2133
1433701_at	Mpped1	0.46	900	1950
1438294_at	Atxn1	0.46	75	163
1450174_at	Ptprt	0.46	40	88
1435229_at	Gramd1b	0.46	97	212
1435933_at	Scn2a1	0.46	173	379
1455080_at	Ppp1r16b	0.46	343	751
1419922_s_at	Atrnl1	0.46	616	1350
1435246_at	Paqr8	0.46	103	226
1456684_at	Tmem74	0.45	497	1093
1458624_at	Rbm24	0.45	43	95
1429987_at	9930013L23Rik	0.45	64	142
1417701_at	Ppp1r14c	0.45	195	431

1422018_at	Hivep2	0.45	190	422
1435165_at	Cntn2	0.45	1426	3169
1420760_s_at	Ndrg1	0.45	414	925
1456138_at	Lypd6	0.45	59	132
1454822_x_at	Apcdd1	0.45	835	1868
1449865_at	Sema3a	0.45	38	85
1437671_x_at	Prss23	0.45	54	121
1426910_at	Pawr	0.45	190	427
1428379_at	Slc17a6	0.44	628	1418
1439807_at	Tmem74	0.44	43	96
1417133_at	Pmp22	0.44	80	180
1444735_at	1444735_at	0.44	125	284
1440206_at	A930024E05Rik	0.44	341	774
1457052_at	Kcng1	0.44	187	426
1454997_at	Msrb3	0.44	75	171
1435106_at	Limch1	0.44	556	1272
1418383_at	Apcdd1	0.44	156	357
1436139_at	1436139_at	0.44	28	63
1458421_at	Kcnq3	0.44	74	171
1459900_at	C79468	0.43	265	611
1455291_s_at	Znrf2	0.43	355	821
1456064_at	AI504432	0.43	284	662
1442257_at	1442257_at	0.43	56	130
1456962_at	Cntn2	0.43	257	601
1453478_at	Pou3f2	0.43	222	520
1417520_at	Nfe2l3	0.43	183	430
1428184_at	3110035E14Rik	0.43	165	387
1418147_at	Tcfap2c	0.42	204	480
1438306_at	Rnf180	0.42	670	1578
1445767_at	Ptprd	0.42	169	398
1441317_x_at	Jakmip1	0.42	896	2121
1418382_at	Apcdd1	0.42	441	1043
1434249_s_at	Trim9	0.42	46	109
1447100_s_at	5730508B09Rik	0.42	199	473
1423413_at	Ndrg1	0.42	187	445
1421101_a_at	Ldb2	0.42	453	1081
1460038_at	LOC100045707	0.42	564	1353
1421180_at	Lix1	0.42	314	755
1417373_a_at	Tuba4a	0.41	336	812
1447813_x_at	Sla	0.41	101	246
1449070_x_at	Apcdd1	0.41	838	2039
1421937_at	Dapp1	0.41	31	75
1420416_at	Sema3a	0.41	286	698
1454720_at	Apba3	0.41	29	72

1447500_at	Cux2	0.41	489	1200
1426341_at	Slc1a3	0.41	50	122
1434759_at	Lrrtm3	0.40	21	52
1434083_a_at	Elmod1	0.40	700	1741
1444468_at	Paqr8	0.40	120	298
1418314_a_at	A2bp1	0.40	740	1848
1434052_at	Al593442	0.40	42	107
1426063_a_at	Gem	0.40	24	61
1425092_at	Cdh10	0.40	227	574
1456174_x_at	Ndrg1	0.40	441	1114
1455799_at	Rorb	0.40	130	330
1455161_at	Al504432	0.39	604	1530
1428958_at	Paqr8	0.39	157	398
1442021_at	Gnal	0.39	446	1134
1434760_at	Lrrtm3	0.39	55	139
1437904_at	Rbm45	0.39	1105	2826
1424454_at	Tmem87a	0.39	130	336
1439957_at	Gnal	0.39	240	621
1435895_at	Lsamp	0.39	214	555
1452114_s_at	Igfbp5	0.38	231	601
1456495_s_at	Osbpl6	0.38	47	122
1429027_at	Snord123	0.38	221	575
1449848_at	Gna14	0.38	27	71
1454806_at	Fam49a	0.38	1785	4664
1455358_at	A2bp1	0.38	591	1547
1433776_at	Lhfp	0.38	228	602
1435957_at	B830032F12	0.38	585	1549
1438989_s_at	B130021B11Rik	0.38	124	330
1421818_at	Bcl6	0.37	141	375
1435605_at	Actr3b	0.37	186	497
1428074_at	Tmem158	0.37	249	665
1420819_at	Sla	0.37	409	1095
1450910_at	Cap2	0.37	119	320
1434171_at	Zfp874	0.37	30	81
1443749_x_at	Slc1a3	0.37	192	516
1423852_at	Shisa2	0.37	283	762
1439557_s_at	Ldb2	0.37	499	1345
1455765_a_at	Abcc8	0.37	141	381
1438217_at	A2bp1	0.37	278	755
1436392_s_at	Tcfap2c	0.37	251	682
1434069_at	Prex1	0.37	348	948
1455262_at	Thsd4	0.36	75	206
1448943_at	Nrp1	0.36	907	2504
1448944_at	Nrp1	0.36	431	1193

1429833_at	Ly6g6e	0.36	86	239
1418084_at	Nrp1	0.36	557	1566
1424299_at	Oma1	0.35	183	519
1457881_at	Osbpl6	0.35	38	109
1456786_at	Ldb2	0.35	136	390
1423851_a_at	Shisa2	0.35	213	609
1423450_a_at	Hs3st1	0.35	400	1150
1448606_at	Lpar1	0.35	196	564
1456543_at	Prokr1	0.35	51	148
1455365_at	Cdh8	0.34	41	120
1422052_at	Cdh8	0.34	57	168
1417143_at	Lpar1	0.34	132	391
1445894_at	1445894_at	0.34	32	94
1422605_at	Ppp1r1a	0.34	482	1438
1456180_at	Rbm24	0.33	100	298
1452031_at	Slc1a3	0.33	187	561
1422851_at	Hmga2	0.33	105	315
1422839_at	Neurog2	0.33	1688	5119
1454969_at	Lypd6	0.33	190	582
1439870_at	A330008L17Rik	0.32	18	56
1435172_at	Eomes	0.32	1289	3984
1435981_at	Nav2	0.32	143	442
1426340_at	Slc1a3	0.32	163	508
1450780_s_at	Hmga2	0.32	130	407
1451461_a_at	Aldoc	0.32	2048	6419
1426258_at	Sorl1	0.31	225	716
1426001_at	Eomes	0.31	1399	4507
1454752_at	Rbm24	0.31	250	813
1455056_at	Lmo7	0.31	95	311
1428393_at	Nrn1	0.31	554	1808
1456397_at	Cdh4	0.30	461	1542
1449422_at	Cdh4	0.30	496	1676
1423222_at	Cap2	0.30	88	297
1460187_at	Sfrp1	0.29	141	488
1452077_at	Ddx3y	0.29	166	577
1426439_at	Ddx3y	0.28	78	278
1424903_at	Kdm5d	0.27	121	441
1457843_at	Lypd6	0.27	24	88
1426438_at	Ddx3y	0.27	245	913
1450781_at	Hmga2	0.26	64	246
1425952_a_at	Gcg	0.25	48	190
1432088_at	Veph1	0.25	39	157
1437422_at	Sema5a	0.25	164	662
1453003_at	Sorl1	0.24	47	191

1434776_at	Sema5a	0.24	79	333
1449420_at	Pde1b	0.23	273	1206
1428114_at	Slc14a1	0.21	14	69
1431491_at	9430087N24Rik	0.20	43	212
1440484_at	Unc5d	0.20	124	620
1427017_at	Satb2	0.20	437	2224
1440990_at	Kif26b	0.20	93	474
1438428_at	Jph1	0.18	26	148
1448823_at	Cxcl12	0.18	118	671
1425443_at	Tcfap2d	0.17	15	88
1438531_at	A730054J21Rik	0.17	104	619
1425452_s_at	Fam84a	0.16	232	1408
1436694_s_at	Neurod4	0.16	30	184
1438551_at	Neurog1	0.16	46	295
1453245_at	9130024F11Rik	0.16	111	709
1418054_at	Neurod4	0.10	11	103
1441579_at	Dmrt1	0.08	15	193
1418310_a_at	Rlbp1	0.02	22	1445

Table S6. Overlap of significantly altered probe sets between Pax6^{Leca4} and Pax6^{Leca2} cortices

Probe_set	Gene symbol or ID	Ratio Pax6 Leca2 vs. WT (94)	Ratio Pax6 Leca4 vs. WT (416)	Ratio Pax6 Sey vs. WT (1898)	Pax6 Chip binding sites (Qing Xie, unpublished)
17 probe sets					
1418310_a_at	Rlbp1	0.12	0.46	0.02	cortex
1428114_at	Slc14a1	0.25	0.12	0.21	
1449848_at	Gna14	0.26	0.55	0.38	
1438551_at	Neurog1	0.38	2.53	0.16	cortex
1455056_at	Lmo7	0.39	0.47	0.31	
1452114_s_at	Igfbp5	0.41	0.64	0.38	
1421937_at	Dapp1	0.49	0.50	0.41	
1453465_x_at	Gm14057	0.50	0.42		
1424186_at	Ccdc80	0.51	0.41	0.55	cortex
1450990_at	Gpc3	0.53	0.54		
1421999_at	Tshr	0.59	0.60		
1420500_at	Dnajc1	0.63	1.49		
1423478_at	Prkcb	0.71	0.43	0.62	
1421836_at	Mtap7	0.71	0.62		
1428990_at	2310047K21Rik	1.74	1.77		
1454772_at	Snrnp200	2.25	2.43		
1438571_at	Bub1	2.53	1.86	2.19	

**Table S7. Comparison of significantly altered probe sets between Pax6^{Leca4}.
Pax6^{Leca2} cortices and Pax6 ChIP data**

Probe_set	Gene symbol or ID	Ratio Pax6 Leca2 vs. WT	Ratio Pax6 Leca4 vs. WT	Ratio Pax6 Sey vs. WT	Pax6 Chip binding sites (Qing Xie, unpublished)
3 probe sets Pax6^{Leca4} / Pax6^{Leca2} /Pax6^{Sey} / Pax6 ChIP signal					
1438551_at	Neurog1	0.38	2.53	0.16	cortex
1424186_at	Ccdc80	0.51	0.41	0.55	cortex
1418310_a_at	Rlbp1	0.12	0.46	0.02	cortex
23 probe sets Pax6^{Leca4} / Pax6^{Sey} / Pax6 ChIP signal					
1457843_at	Lypd6	0.57	0.27		lens
1422052_at	Cdh8	0.43	0.34		lens
1455365_at	Cdh8	0.43	0.34		lens
1417133_at	Pmp22	0.6	0.44		cortex, lens
1456138_at	Lypd6	0.61	0.45		lens
1450047_at	Hs6st2	0.6	0.51		cortex, lens
1420938_at	Hs6st2	0.53	0.57		cortex, lens
1455636_at	Lsamp	0.56	0.58		cortex
1416342_at	Tnc	0.4	0.58		cortex
1450181_at	Cux2	0.65	0.58		cortex
1450930_at	Hpca	0.63	0.62		cortex
1420981_a_at	Lmo4	1.41	1.43		lens
1429284_at	Mobkl2b	1.76	1.47		lens
1449167_at	Epb4.1I4a	1.43	1.57		lens
1419573_a_at	Lgals1	3.84	1.57		cortex, lens, pancreas
1455439_a_at	Lgals1	3.96	1.58		cortex, lens, pancreas
1442542_at	Eya4	5.03	1.67		lens
1425669_at	Mobkl2b	1.41	1.84		lens
1451119_a_at	Fbln1	1.53	2.17		cortex
1436791_at	Wnt5a	1.93	2.31		lens
1451191_at	Crabp2	2.23	3.4		cortex
1437442_at	Pcdh7	1.43	0.52		cortex
1453006_at	Fgfbp3	2.47	0.63		cortex
16 probe sets Pax6^{Leca2} / Pax6^{Sey} / Pax6 ChIP signal					
1418054_at	Neurod4	0.28		0.1	cortex
1436694_s_at	Neurod4	0.36		0.16	cortex
1420459_at	Ripply3	0.59		0.69	lens
1433782_at	Cldn12	0.67		0.63	cortex, pancreas
1417872_at	Fhl1	0.67		0.6	cortex
1435449_at	Bcl2l11	1.56		1.95	lens

1456006_at	Bcl2I11	1.61	1.79	lens
1456005_a_at	Bcl2I11	1.67	1.88	lens
1439854_at	Hrk	1.8	2	cortex
1452526_a_at	Pax6	1.81	1.52	cortex
1439627_at	Zic1	1.87	2.73	pancreas
1438737_at	Zic3	1.9	2.83	lens
1419271_at	Pax6	1.9	1.48	cortex
1438194_at	Slc1a2	2.66	1.61	cortex
1423422_at	Asb4	3.19	7.94	cortex
1433919_at	Asb4	3.54	12.29	cortex

3 + 23 + 16 = 42 probe sets overlap

42 / total overlap 182 probe sets (see Venn diagram Fig. 6F) = **23%**

3 probe sets (labeled in violet) regulated in different directions

39 / 42 regulated in the same direction = **93%**

Table S8. Comparison of significantly altered probe sets between Pax6^{Leca4} cortices and Pax6 ChIP data

Probe_set	Gene symbol or ID	Ratio Pax6 Leca4 vs. WT	Pax6 Chip binding sites (Qing Xie, unpublished)
1434369_a_at	Cryab	8.89	cortex
1460412_at	Fbln7	7.47	lens
1416455_a_at	Cryab	5.62	cortex
1416953_at	Ctgf	5.41	lens
1442542_at	Eya4	5.03	lens
1445897_s_at	Ifi35	5	lens
1455439_a_at	Lgals1	3.96	cortex, lens, pancreas
1419573_a_at	Lgals1	3.84	cortex, lens, pancreas
1456665_at	Eya4	3.7	lens
1439795_at	Gpr64	3.27	lens
1438551_at	Neurog1	2.53	cortex
1453006_at	Fgfbp3	2.47	cortex
1419215_at	Aox4	2.28	cortex
1451191_at	Crabp2	2.23	cortex
1417090_at	Rcn1	2.2	pancreas, cortex
1440374_at	Pde1c	2.14	cortex
1415897_a_at	Mgst1	2.08	pancreas
1443998_at	Rassf2	2.06	cortex
1448392_at	Sparc	1.99	cortex
1436791_at	Wnt5a	1.93	lens
1441499_at	Grid1	1.91	cortex
1454985_at	Ambra1	1.85	lens
1416589_at	Sparc	1.82	cortex
1424617_at	Ifi35	1.81	lens
1429284_at	Mobkl2b	1.76	lens
1437930_at	Glt25d2	1.74	lens
1420919_at	Sgk3	1.72	pancreas, lens
1459151_x_at	Ifi35	1.71	lens
1454728_s_at	Atp8a1	1.67	cortex
1435828_at	Maf	1.67	lens
1452217_at	Ahnak	1.66	cortex
1454984_at	Lifr	1.65	pancreas
1447849_s_at	Maf	1.64	lens
1433827_at	Atp8a1	1.62	cortex
1420918_at	Sgk3	1.56	pancreas, lens
1417694_at	Gab1	1.56	pancreas
1449314_at	Zfpm2	1.55	lens
1451119_a_at	Fbln1	1.53	cortex
1456060_at	Maf	1.51	lens
1449933_a_at	Tsen15	1.48	cortex

1417693_a_at	Gab1	1.46	pancreas
1451693_a_at	Fgf12	1.46	cortex
1450036_at	Sgk3	1.44	pancreas, lens
1450716_at	Adamts1	1.44	lens
1427369_at	Nlrp6	1.44	cortex
1419093_at	Tdo2	1.44	pancreas
1455182_at	Kif1b	1.43	pancreas, lens
1423258_at	Syt9	1.43	cortex
1437442_at	Pcdh7	1.43	cortex
1433501_at	Ctso	1.43	cortex
1449167_at	Epb4.1l4a	1.43	lens
1433643_at	Cacna2d1	1.43	lens
1417130_s_at	Angptl4	1.42	cortex
1434775_at	Pard3	1.41	lens
1417667_a_at	Pter	1.41	pancreas
1420981_a_at	Lmo4	1.41	lens
1425669_at	Mobkl2b	1.41	lens
1427535_s_at	Obsl1	0.7	cortex
1421262_at	Lipg	0.7	lens
1456759_at	Lrrc4c	0.69	cortex
1450188_s_at	Lipg	0.69	lens
1439248_at	Rmi1	0.69	cortex
1441690_at	Cdh8	0.68	lens
1418495_at	Zc3h8	0.67	cortex
1420838_at	Ntrk2	0.67	lens
1457836_at	Mfsd11	0.67	pancreas
1418153_at	Lama1	0.67	lens
1440770_at	Bcl2	0.67	cortex, lens
1450181_at	Cux2	0.65	cortex
1458023_at	Gpkow	0.64	cortex
1421970_a_at	Gria2	0.64	cortex
1450930_at	Hpca	0.63	cortex
1456901_at	Adamts20	0.63	lens
1450047_at	Hs6st2	0.6	cortex, lens
1417133_at	Pmp22	0.6	cortex, lens
1435494_s_at	Dsp	0.6	lens
1450512_at	Ntn4	0.6	lens
1454969_at	Lypd6	0.59	lens
1425833_a_at	Hpca	0.59	cortex
1457843_at	Lypd6	0.57	lens
1455636_at	Lsamp	0.56	cortex
1431057_a_at	Prss23	0.56	cortex
1453596_at	Id2	0.56	pancreas, lens
1422573_at	Ampd3	0.54	cortex
1415824_at	Scd2	0.53	pancreas
1448754_at	Rbp1	0.53	lens
1420938_at	Hs6st2	0.53	cortex, lens

1435196_at	Ntrk2	0.53	lens
1448842_at	Cdo1	0.48	cortex
1438842_at	Mtch2	0.46	cortex, lens
1418310_a_at	Rlbp1	0.46	cortex
1449859_at	Golt1b	0.44	cortex, lens
1455365_at	Cdh8	0.43	lens
1422052_at	Cdh8	0.43	lens
1424186_at	Ccdc80	0.41	cortex
1416342_at	Tnc	0.4	cortex
1439794_at	Ntn4	0.39	lens
1450992_a_at	Meis1	0.24	cortex

98 probe sets overlap between Pax6^{Leca4} array data and Pax6 ChIP data

98 / total 416 probe sets = **24%** overlap

Table S9. Comparison of significantly altered probe sets between Pax6^{Leca2} cortices and Pax6 ChIP data

Probe_set	Gene symbol or ID	Ratio Pax6 Leca2 vs. WT	Pax6 Chip binding sites (Qing Xie, unpublished)
1433919_at	Asb4	3.54	cortex
1423422_at	Asb4	3.19	cortex
1438194_at	Slc1a2	2.66	cortex
1419271_at	Pax6	1.9	cortex
1438737_at	Zic3	1.9	lens
1439627_at	Zic1	1.87	pancreas
1452526_a_at	Pax6	1.81	cortex
1439854_at	Hrk	1.8	cortex
1456005_a_at	Bcl2l11	1.67	lens
1456006_at	Bcl2l11	1.61	lens
1435449_at	Bcl2l11	1.56	lens
1447628_x_at	Mrps5	1.5	lens
1430798_x_at	Mrpl15	1.46	pancreas
1418172_at	Hebp1	0.7	lens
1442312_at	Tbl1xr1	0.69	cortex, lens
1423259_at	Id4	0.68	cortex
1417872_at	Fhl1	0.67	cortex
1433782_at	Cldn12	0.67	cortex, pancreas
1421365_at	Fst	0.66	cortex
1420459_at	Ripply3	0.59	lens
1423260_at	Id4	0.58	cortex
1424186_at	Ccdc80	0.51	cortex
1436694_s_at	Neurod4	0.36	cortex
1418054_at	Neurod4	0.28	cortex
1418310_a_at	Rlbp1	0.12	cortex

25 probe sets overlap between Pax6^{Leca2} array data and Pax6 ChIP data
25 / total 94 probe sets = **27%** overlap